# Molecular Mechanisms of Notochord Vacuole Formation and Their Role in Zebrafish Development

by

Kathryn Leigh Ellis

Department of Cell Biology
Duke University

Date:_____

Approved:

_____
Michel Bagnat, Advisor

_____
Kenneth Poss, Chair

_____
Christopher Nicchitta

_____
Jun Chen

_____
Raphael Valdivia

Dissertation submitted in partial fulfillment of the requirements for the degree of Doctor of Philosophy in the Department of Cell Biology in the Graduate School of Duke University

2014

# ABSTRACT

Molecular Mechanisms of Notochord Vacuole Formation

and Their Role in Zebrafish Development

by

Kathryn Leigh Ellis

Department of Cell Biology
Duke University

Date:_____

Approved:

_____
Michel Bagnat, Advisor

_____
Kenneth Poss, Chair

_____
Christopher Nicchitta

_____
Jun Chen

_____
Raphael Valdivia

An abstract of a dissertation submitted in partial
fulfillment of the requirements for the degree
of Doctor of Philosophy in the Department of
Cell Biology in the Graduate School of
Duke University

2014

## Abstract

The notochord plays critical structural and signaling roles during vertebrate development. At the center of the vertebrate notochord is a large fluid-filled organelle, the notochord vacuole. While these highly conserved intracellular structures have been described for decades, little is known about the molecular mechanisms involved in their biogenesis and maintenance. Here we show that zebrafish notochord vacuoles are specialized lysosome-related organelles whose formation and maintenance requires late endosomal trafficking regulated by the vacuole-specific Rab32a, and $H^+$-ATPase-dependent acidification. We establish that notochord vacuoles are required for body axis elongation during embryonic development and identify a novel role for notochord vacuoles in spine morphogenesis. Disruption of notochord vacuoles results in juveniles with spine kinks that are similar to those found in congenital scoliosis (CS) in humans. Thus, the vertebrate notochord plays important structural roles beyond early development. Using forward genetics, reverse genetics, live imaging techniques and genetic manipulations we are using the zebrafish as a powerful model to understand mechanisms underlying congenital scoliosis (CS).

## Dedication

I would like to dedicate my dissertation to Oliver, for instant comfort and for never tiring of listening to the ups and downs of a graduate career in science.

# Contents

# List of Figures

# List of Abbreviations

IVD = intervertebral disc

NP = nucleus pulposus

ss = somite stage

hpf = hours post fertilization

dpf = days post fertilization

GAG = glycosaminoglycan

ECM = extracellular matrix

Shh = Sonic hedgehog

DN = dominant-negative

LRO = lysosome-related organelle

ER = endoplasmic reticulum

TGN = *trans* Golgi network

GAP = GTP-hydrolysis activating proteins

GDI = guanine-nucleotide dissociation inhibitor

GEF = guanine-nucleotide exchange factor

VPS = vacuole protein sorting

HOPS = homotypic fusion and protein sorting

CORVET = class c core vacuole/endosome-tethering

WPB = Weibel – Palade body

LG = lytic granule

AP = adaptor protein

BLOC = biogenesis of lysosome-related organelles complex

Lamp = lysosome-associated membrane protein

NTR = nitroreductase

Mtz = metronidazole

SNP = single nucleotide polymorphism

CS = congenital scoliosis

## Acknowledgements

I would like to thank my advisor, Michel Bagnat, for his mentorship and for pushing me to accomplish so much during my time in his lab. I would like to thank my lab for guidance and helpful discussions. I especially thank Jennifer Bagwell for being both an invaluable resource in the lab and a great friend out of the lab. I would like to acknowledge my thesis committee, especially Chris Nicchitta, for valuable suggestions, discussions, and guidance. I thank the team in the Zebrafish Facility at Duke for their care and expertise.

I would like to thank Brent Hoffman for the many helpful discussions. I thank Didier Stainier for the *dwarf* mutant. I also thank Koichi Kawakami, Brian Link, Ryan Thummel, Jeff Gross, John Rawls, and Sarah Kucenas for fish lines.

I would like to thank my friends in the DSCB program at Duke, especially Christina Pham and Chris Pirozzi, for keeping me sane during graduate school. I also thank my friends outside of Duke, especially Kaitlin Stock, for their support, understanding, and for reminding me how to be social. I thank John Cosgriff for feigning interest in my science and for being my biggest cheerleader. And finally, I thank my family for their unwavering support throughout my many years of school. I would be lost without you all.

# 1. Introduction

The acquisition of a notochord is an important event in evolutionary history as it marks the beginning of our phylum, chordata. In vertebrates the notochord arises from the dorsal organizer, also known as the embryonic shield in zebrafish, and is critical for proper vertebrate development (Saude et al., 2000; Shih and Fraser, 1996). The notochord is an important midline structure that serves both patterning and structural roles during the early gastrula period. In non-vertebrate chordates and in lower vertebrates, such as lampreys and primitive fish, the notochord persists throughout life and is crucial for locomotion. In most vertebrates it is a more transient structure that is largely replaced during bone formation by vertebrae and contributes to the center of the intervertebral discs (IVDs), the nucleus pulposus (NP) (Choi et al., 2012; McCann et al., 2012). The notochord in zebrafish is comprised of two cell layers, an outer epithelial-like layer and an inner core of vacuolated cells, and is present throughout spine formation (Figure 1). Notochord vacuoles have been described in nearly every embryonic vertebrate studied from fish to amphibians, birds, and mammals (Bancroft and Bellairs, 1976; Leeson and Leeson, 1958; Waddington, 1962). In these species the vacuoles are maintained in the cells of the NP where they can persist well beyond skeletal maturity (Hunter et al., 2004; Meachim and Cornah, 1970).

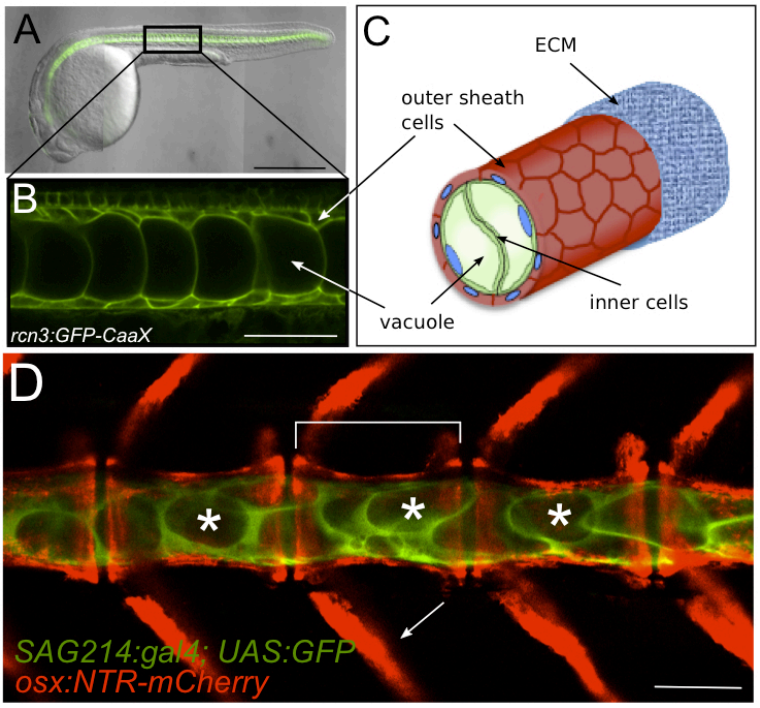


**Figure 1. The zebrafish notochord is comprised of two cell layers and persists throughout spine development.**

(A) 24 hpf transgenic embryo expressing membrane GFP in the notochord. *Tg(rcn3:GFP-CaaX).* (B) Live confocal image of 24 hpf transgenic GFP-CaaX embryo illustrating orientation of fish for all live imaging done in this work. Anterior is left, posterior is right, dorsal is top, and ventral is bottom. (C) Cartoon of a zebrafish notochord depicting outer and inner cell layers and the inner cell vacuoles. The entire notochord is encased in a thick ECM. (D) 16 dpf transgenic fish expressing GFP in the notochord inner vacuolated cells and osteoblasts labeled with RFP; *Gt(SAGFF214A:gal4); Tg(UAS:GFP); Tg(osx:NTR-mCherry).* Bracket labels vertebral centra. Arrow indicates vertebral arch. Asterisks indicate notochord vacuoles. The notochord persists and still retains its vacuoles throughout the process of spine morphogenesis. (A) scale bar = 500 μm. (B) scale bar = 50 μm. (D) scale bar = 100 μm.

Because notochord-derived vacuolated cells are present postnatally in mammalian IVDs, understanding how these structures develop could provide valuable insight into understanding their maintenance and degeneration in the adult. Degenerative disc disease is common among the aging population and the field of regenerative medicine targeting IVDs is rapidly growing (Richardson et al., 2010; Urban and Roberts, 2003). Zebrafish provide a powerful model system in which to study notochord development as embryos are optically clear, they are a genetically tractable system, they are amenable to reverse and forward genetics, and notochord defects are easy to identify in large clutches as they typically produce shortened or curved body axes.

### *1.A. Notochords: the rise of phylum Chordata*

There is debate as to when phylum chordata arose, but primitive chordates are seen in the fossil record as early as the Cambrian explosion, over 540 million years ago. The characteristics of a chordate include: a notochord, a dorsal hollow nerve chord, pharyngeal slits, an endostyle, and a post-anal tail. Phylum chordata can be split into three sub phyla, cephalochordates such as amphioxus, Urochordates such as the sea squirt, and Vertebrates (Kent and Carr, 2001).

While the notochord performs similar functions of providing the structural support necessary for locomotion across all members of chordata, the notochord structure varies greatly. In cephalochordates, like amphioxus, the notochord is comprised of parallel notochord plates with a gel-like liquid between the plates

(Bocina and Saraga-Babic, 2006). The notochord of the urochordate, *Ciona intestinalis,* has recently been proposed as a new model for understanding lumen formation during tubulogenesis (Denker and Jiang, 2012). The notochord in *Ciona* begins as convergent extension movements create a rod of stacked cells at the midline of the embryo. Then the cells elongate along the anterior-posterior axis and generate apical and basal polarity. Extracellular lumens form between cells at the apical domain and this apical domain expands as fluid enlarges the lumens. Finally, cells rearrange and migrate to allow for the lumens to fuse, generating a tube comprised of many cells with a single central lumen. In vertebrates, the notochords do not undergo tubulogenesis, but instead are comprised of cells containing fluid-filled intercellular vacuoles.

Regardless of the anatomical differences, common among all chordates is the presence of a fluid-filled structure within the notochord and a fibrous sheath surrounding the notochord (Kent and Carr, 2001). Highlighting the importance of these components for proper notochord function.

## *1.B. The notochord patterns the early vertebrate embryo*

Centrally located in the vertebrate embryo during the development, the notochord is well positioned to act as a source of developmental signals to pattern surrounding tissues. Indeed, the notochord has roles in patterning all three germ layers: the ectoderm, mesoderm and endoderm (Cleaver and Krieg, 2001).

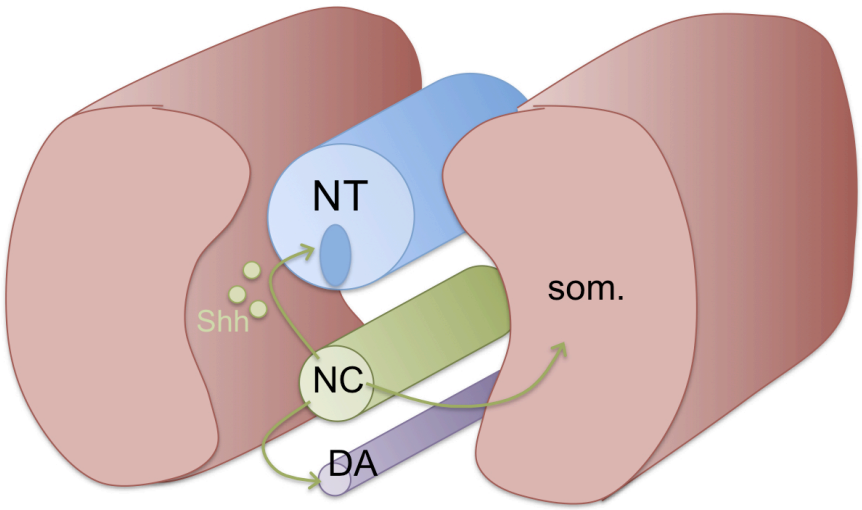


**Figure 2. The notochord patterns surrounding tissues during early development**

The notochord (NC) secretes sonic hedgehog (Shh) to pattern the ventral fates of the neural tube (NT), induce sclerotome fate in the surrounding somites (som), and pattern the dorsal aorta (DA).

The notochord signals to the ectoderm to pattern the ventral portion of the neural tube. The notochord secretes sonic hedgehog (Shh), which induces the floor plate and ventral motor neuron cell fate in the neural tube while simultaneously suppressing dorsal cell fates (Yamada et al., 1993) (Figure 2). In classical chick experiments, ectopic notochord or Shh secreting cells placed near the lateral surface of the neural tube are sufficient to induce a second set of floor plate cells and motor neurons (Placzek et al., 1990).

The notochord signals to the mesoderm in order to pattern the somites, cardiac field, dorsal aorta, and help establish left-right asymmetry. The notochord secretes Shh to pattern surrounding paraxial mesoderm inducing sclerotome fate in the somites (Fan and Tessier-Lavigne, 1994) (Figure 2). The anterior most portion of the notochord corresponds to the posterior limit of cells specified for cardiac fate. In notochord ablation experiments, removing the anterior portion of the notochord led to a posterior expansion of the cardiac field. Therefore, the notochord restricts the cardiac field by suppressing heart cell fate (Goldstein and Fishman, 1998). The notochord also patterns the dorsal aorta, a major blood vessel lying ventral to the notochord (Figure 2). In zebrafish mutants that lack chordamesoderm and therefore notochords, like *no tail (ntl)* and *floating head (flh)*, the dorsal aorta fails to develop. This structure can be rescued by transplantation of wild-type notochord cells into *flh* mutants (Fouquet et al., 1997; Sumoy et al., 1997). Lastly, there is evidence that the notochord plays a role in

establishing left-right asymmetry of the body axis. When the notochord is experimentally ablated in *Xenopus*, or in zebrafish mutants lacking notochords, lateral plate mesoderm markers that are typically expressed asymmetrically (*nodal* and *lefty*) become randomized or are expressed bilaterally (Danos and Yost, 1996; Lohr et al., 1997).

The notochord also signals to the endoderm to pattern the foregut and pancreas. In vertebrates, the notochord is physically in contact with the foregut endoderm for much of early development before becoming an independent structure. Improper resolution of the notochord from the dorsal foregut endoderm leads to mispatterning of the pharynx, trachea, esophagus, and stomach (Qi and Beasley, 1999). The notochord has also been shown to be important for patterning the dorsal bud of the pancreas. In chick, when the notochord is removed early the dorsal bud of the pancreas fails to express both endocrine and exocrine markers while the ventral bud remains unperturbed (Kim et al., 1997).

## *1.C. Zebrafish notochord anatomy*

In zebrafish, the notochord is one of the earliest distinguishable features in the embryo. It forms as chordamesoderm cells undergo convergent extension at the midline creating a rod of stacked cells with a characteristic “stack of coins” appearance (Glickman et al., 2003; Sepich et al., 2005). Around the 15-somite stage (15 ss) or 16.5 hours post fertilization (hpf) this stack of cells differentiates into two distinct cell populations: the outer sheath layer and an inner layer of vacuolated cells (Figure 3). During this process outer sheath cells leave the

midline and divide to surround and enclose the inner vacuolated cells in an epithelial-like manner (Dale and Topczewski, 2011). Simultaneously the inner cells inflate their large fluid-filled intracellular vacuoles. The outer sheath cells differentiate in a notch-dependent manner (Yamamoto et al., 2010). Yamamoto and others showed that when the notch intracellular domain (NICD) is over expressed, the notochord cells differentiate into outer sheath cells at the expense of inner vacuolated cells. At the 30 ss, or 24 hpf, the two cell layers have fully differentiated (Figure 3). The inner cells have fully inflated vacuoles that occupy the majority of the volume of the inner cells with diameters of up to 40 μm. The sheath cells secrete a thick extracellular basement membrane rich in glycosaminoglycans (GAGs) and collagens that surrounds the entire notochord.

The outer sheath cells have previously been referred to as chordoblasts and the inner vacuolated cells as chordocytes (Grotmol et al., 2003). I will use the terminology sheath cells to refer to the outer cells and vacuolated cells to refer to the inner cells as the term “chordoblast” implies an immature cell population and there is not yet convincing evidence that the sheath cells give rise to vacuolated cells.

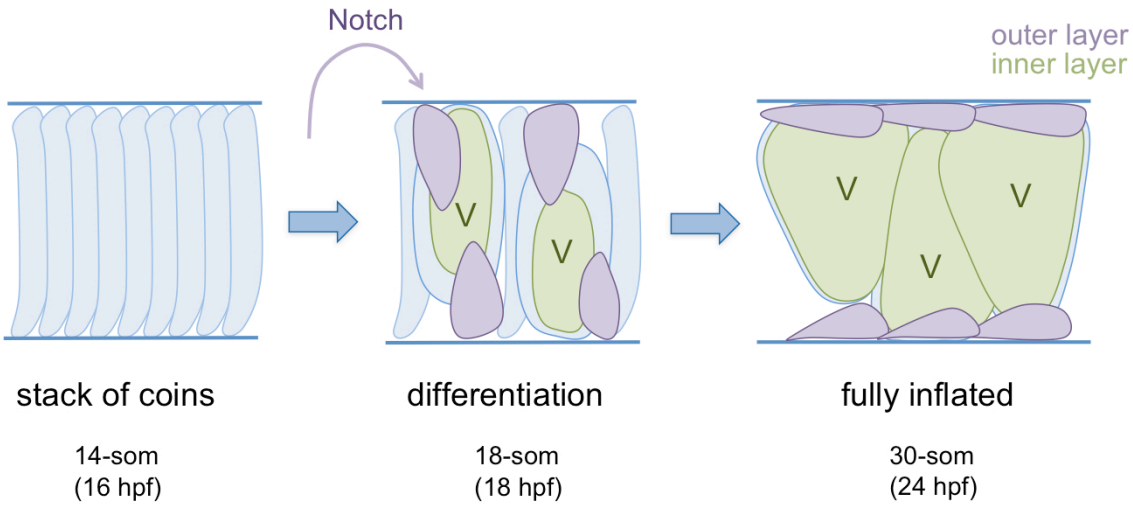


**Figure 3. Notochord cell layers differentiate through Notch signaling**

The notochord begins as a single row of cells with a “stack of coins” appearance. Around the 18 somite stage the outer cells differentiate in a notch-dependent manner. The outer cells leave the midline and spread out to surround the inner cells creating an epithelial-like sheath. Simultaneously, the inner cells start to inflate their intracellular vacuoles. At the 30 somite stage, or 24 hpf, the outer cells surround the inner vacuolated cells entirely and the vacuoles are fully inflated.

Along the length of the anterior-posterior axis of the notochord, inner vacuolated cells are organized into two rows. When viewed dorsally, the two rows of inner vacuolated cells are aligned such that two vacuoles are not exactly side-by-side, but are slightly offset, with one row being more anterior than the other. The same structure viewed laterally is seen as a single layer of vacuolated cells. This arrangement seen in cross-section shows two vacuolated cells that occupy nearly the entire ~80 μm diameter of the notochord (Figure 4).

Nixon and others showed that the notochord of zebrafish contains the most caveolae out of any other tissue studied (Nixon et al., 2007). Caveolae are specialized invaginations in the plasma membrane that are rich in cholesterol and sphingolipids and are one source of clathrin-independent endocytosis (Parton and del Pozo, 2013). Morpholino knockdown of caveolin-1 in zebrafish results in embryos with curved body axis and smaller notochord vacuoles (Nixon et al., 2007). Therefore, these structures may play a role in vacuole biogenesis by being a source of membrane to the growing vacuole while simultaneously delivering cargo to the lumen of the vacuole. Alternatively, these structures have been proposed to be a reservoir of extra membrane that when stretched can relieve cell membrane tension (Mayor, 2011). Thus, the caveolae may line the inner cell plasma membrane in order to accommodate the growing intracellular vacuole.

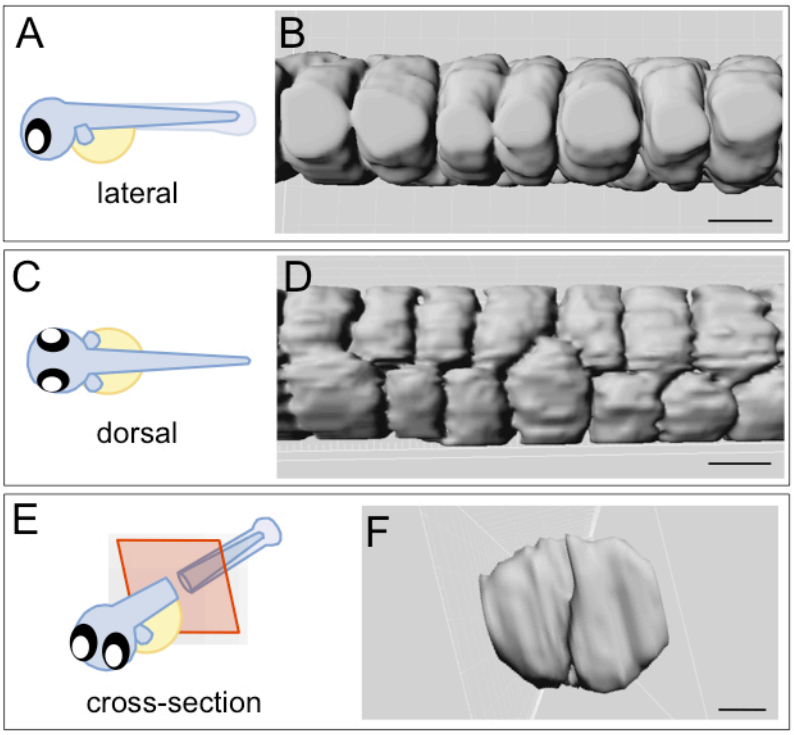


**Figure 4. Zebrafish notochord vacuoles are arranged into two rows**

Imaris software was used to generate a 3-D model of vacuolated cells using a transgenic line that expresses GFP in the cytosol of the inner vacuolated cells, *Gt(Gal4FF)nksagff214a; Tg(UAS:GFP). (*A, C, E) Cartoons depicting orientation of the embryo for the following panels. (B, D, F) 3-D rendering of vacuolated cells. Scale bars = 30μm.

Recently, Tong and others identified a novel type of intermediate filament, termed chordostatin, which is necessary for maintaining cellular architecture in the inner vacuolated cells of the notochord. Larvae mutant for chordostatin have smaller vacuolated cells in distinct regions of the notochord. Smaller vacuolated cells were suggested to be the result of damage to the notochord from the force of swimming, as anesthetized mutants who could not swim did not develop these defects. This group showed that the damaged vacuolated cells were able to recover over time, rescuing differences in body length. They also showed mitotically active cells in regions of the notochord following damage. They suggest that the outer cells are dividing to replace the inner vacuolated cells disrupted from physical force (Tong et al., 2013). This work discovered a novel type of intermediate filament that is necessary for inner cells to develop proper vacuoles. However, proper lineage tracing experiments need to be done in order to determine in outer sheath cells divide after differentiation and can give rise to new inner vacuolated cells.

### *1.D. Intracellular trafficking*

The majority of proteins begin synthesis in the cytosol yet many perform their functions in specific organelles. Proteins arrive at their final destinations through the use of sorting signals found on nascent proteins that act like zip codes to direct the proteins to their proper locations (Martoglio and Dobberstein, 1998; Walter and Johnson, 1994). Cells use several mechanisms to move proteins between different compartments within the cell: gated transport,

transmembrane transport, and vesicular transport. For the bulk of my work I will be discussing vesicular transport as the means by which cargo and membrane are trafficking to the notochord vacuole (Figure 5).

### 1.D.1. Biosynthetic sorting and trafficking

Newly synthesized proteins traverse the biosynthetic pathway through the endoplasmic reticulum (ER) and the Golgi. The ER membrane is the site of production of all the transmembrane proteins and lipids for the ER, Golgi, lysosomes, endosomes, secretory vesicles, and the plasma membrane. Proteins destined for any of these locations are translocated from the cytosol to the lumen of the ER through the use of a signal sequence (Johnson and van Waes, 1999). Once in the ER lumen the protein will fold and assemble or, if it posses multiple start and stop transfer signals, the protein will be threaded through the ER membrane multiple times generating a multipass transmembrane protein (von Heijne, 1995). In the ER most proteins are glycosylated by the addition of common N-linked oligosaccharides that mark the state of protein folding (Parodi, 2000). Mature fully folded proteins are then sent via COPII-coated vesicles to the Golgi apparatus (Barlowe et al., 1994) (Figure 5).

In the Golgi the oligosaccharide chains are further processed and O-linked oligosaccharides are added. Once the protein arrives to the *trans* Golgi network (TGN), receptors and adaptors recognize specific sorting signals and further sort proteins so that they can be trafficked to their final destinations (Rothman and Wieland, 1996). Mechanisms for sorting from the TGN to lysosomes have been

well studied and characterized, especially sorting via the mannose 6-phosphate receptor and tyrosine-based sorting motifs. Here, I will briefly describe the tyrosine-based mechanisms of sorting from the TGN to lysosomes as this mechanism or a similar one may be used in sorting to the notochord vacuole.

For many lysosomal membrane proteins, sorting is accomplished through the use of the tyrosine-based sorting motif YXXØ, where Y is a tyrosine residue, X can be any amino acid but tends to be hydrophilic, and Ø is any large hydrophobic amino acid. This sorting motif can be found in other instances of intracellular sorting, but its location in the peptide dictates the type of sorting. When the tyrosine-based motif is used for lysosomal sorting it is found 6 – 9 residues from the transmembrane domain on the C-terminal side. This sorting motif is recognized on the cytosolic side of the TGN by the adaptor protein (AP) complexes AP-1 and AP-2 (Bonifacino and Traub, 2003). These complexes ensure that cargo with a lysosomal sorting signal is sorted into vesicles en route to lysosomes.

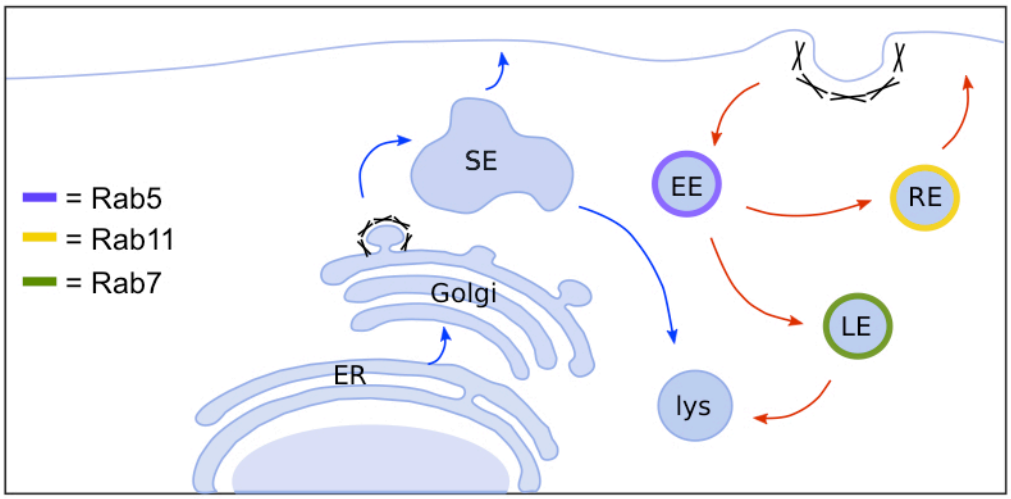


**Figure 5. Intracellular trafficking routes**

Cartoon depicting intracellular vesicular trafficking routes. Red arrows indicate endocytic traffic and blue arrows indicate biosynthetic traffic. Clathrin coats are depicted as X's and form at vesicles leaving the plasma membrane and TGN. The Rab GTPases Rab5, Rab11, and Rab7 regulate traffic at the early endosome, recycling endosome, and late endosome, respectively. EE=early endosome, RE=recycling endosome, LE=late endosome, SE=sorting endosome, lys=lysosome.

### 1.D.2. Endocytic trafficking and Rab GTPases

Many extracellular molecules that cells must utilize cannot pass through the plasma membrane passively and instead must actively be internalized via endocytosis. The endocytic pathway is composed of membrane-bound vesicles that shuttle membrane and cargo within the cell (Figure 5). The cytosolic surface of these vesicles, or endosomes, contains specific markers that confer endosomal identity and serve as a guidance cue during vesicular transport while the luminal surfaces are all topologically equivalent.

Several types of protein coats can surround vesicles where they function to recruit specific cargo into the vesicle and to deform the membrane into a spherical shape. COPII coats are found on vesicles leaving the ER, COPI coats are found on vesicles from the Golgi and on early endosomes, and clathrin coats can be seen on vesicles from the Golgi and the plasma membrane (Schekman and Orci, 1996). The scission protein, dynamin, pinches off vesicles exiting a membrane and the coat proteins quickly fall off afterwards (Hinshaw and Schmid, 1995).

Vesicular trafficking is mediated by SNARE proteins and targeting Rab GTPases. Rabs are small monomeric GTPases that work together with other proteins to regulate the initial docking and tethering of vesicles to their target membranes. SNARE proteins then ensure specificity between transport vesicles and their target membrane. The two components of the SNARE proteins the t-SNARE, found on the target membrane, and the v-SNARE, found on the vesicle

membrane, bring the vesicle and membrane into close proximity and possibly catalyze the fusion of the two membranes (Chavrier and Goud, 1999; Pelham, 2001).

Rab proteins act as molecular switches in order to perform their functions of regulating vesicular traffic. Rabs catalyze protein fusion in vesicle docking and tethering steps in their GTP-bound, active state. Rab-specific GTP-hydrolysis activating proteins (GAPs) convert the Rab to a GDP-bound, inactive form. The cytosolic protein guanine-nucleotide dissociation inhibitor (GDI) then retrieves Rab proteins from fusion target membranes and recycles them back to their original membrane. The cycle starts again when a Rab-specific guanine-nucleotide exchange factor (GEF) converts the Rab back to its active GTP-bound state (Novick and Zerial, 1997; Pfeffer, 1994). The Rab-specific GAPs and GEFs ensure proper temporal control of the active form of Rab proteins.

The Rabs that have been best characterized function most prominently in endocytic trafficking. These Rabs are Rab5, which functions at the early endosome, Rab7 at the late endosome, and Rab11 at the recycling endosome (Figure 5). Endosomal studies often employ the use of dominant-negative versions of Rab proteins in order to probe their functions. Dominant-negative (DN) Rabs are mutated at conserved residues that result in binding sites with reduced GTP affinity. This keeps the Rab in its inactive GDP-bound state, thereby preventing the Rab from interacting with its downstream effectors (Grosshans et al., 2006).

### 1.D.3. Acidification and vesicular trafficking

Each type of endosome performs a specific function along the endosomal pathway. In order to accomplish this, early endosomes must look distinct from recycling endosomes or late endosomes in terms of the proteins found on the cytosolic surface as well as their luminal content. This is a major feat for the cell to accomplish given that endosomes are constantly shuttling cargo and membrane along the pathway yet preserving their own protein composition.

One way that endosomes maintain their distinct identity is by varying the luminal pH. Acidity typically increases as molecules traverse the biosynthetic pathway. The ER has a pH of ~7.2, the Golgi has a pH of ~6.4, early endosomes have a pH of 6.3 – 5.5, late endosomes have a pH less than 5.5, and finally lysosomes can have a pH as low as 4.6 (Kornfeld and Mellman, 1989; Wu et al., 2000). The proteins that function at each step of the endosomal pathway perform optimally only at the pH that is specific to their organelle. At increased pH, receptors lose affinities for their ligands, proteins undergo conformational changes, and enzymes no longer function (Mellman et al., 1986). In this way, proteins are partitioned along the endosomal pathway and only function at discrete places. This way acidic hydrolases only work in late endosomes and lysosomes and not prematurely in the Golgi.

Intracellular compartments are acidified by the vacuolar-type-$H^+$-ATPase (hereinafter V-ATPase). The V-ATPase is comprised of two multi-subunit complexes, the $V_1$ complex which hydrolyzes ATP, and the $V_0$ complex which in

turn uses this energy to pump protons across the membrane. The role of acidification in vesicular trafficking has been well studied *in vitro* and *in vivo* through the use of the pharmacological inhibitor, bafilomycin, which specifically inhibits V-ATPase activity (Bowman et al., 1988). In murine liver cells or human epithelial cells, treated with bafilomycin, the pH of lysosomes goes from an acidic 5.1 up to 6.3. In these cells, the lysosomal dye acridine orange or endocytosed cargo such as dextrans do not accumulate in lysosomes (Yoshimori et al., 1991). Thus, acidification is important for proper sorting and trafficking within the cell.

## *1.E. Other vacuoles*

Most plant and fungal cells and some animal cells have fluid-filled vacuoles that are related to lysosomes but can perform a wide array of functions depending on their specific cell type. Here I will briefly describe the function and biogenesis of two well-characterized vacuoles, the plant tonoplast and the yeast vacuole, since several molecular mechanisms are conserved and also used for zebrafish notochord vacuole biogenesis.

### 1.E.1. The plant vacuole

There are two major types of plant vacuoles, or tonoplasts, each performing distinct functions for the cell (Etxeberria et al., 2012; Marty, 1999). Lytic vacuoles act as lysosomes to degrade proteins and recycle the amino acids. Storage vacuoles are the main reservoir of metabolites but have been shown to carry out many functions for the cell including, regulating cell turgor pressure and osmolarity through the transport of osmotically active solutes

across the vacuole membrane (Mimura et al., 2003), defense strategies (Hara-Nishimura and Hatsugai, 2011), and metabolite synthesis such as fructan (Darwen and John, 1989) and nicotine (Kajikawa et al., 2011). Recent proteomics studies have revealed that there are at least 90 tonoplast transporters in *Arabidopsis* that mediate the transport of molecules across the vacuole membrane (Jaquinod et al., 2007).

The plant vacuole is formed through the transport of solutes via both the endocytic and biosynthetic routes. Unlike the endosomal system that has been well characterized in mammalian cells, plant cells have only two major endosomal compartments: The TGN and late endosomes. The plant TGN and TGN-derived compartments act as early endosomes or recycling endosomes (Dettmer et al., 2006; Lam et al., 2007). Cargo that is internalized from the plasma membrane is sent directly to the TGN where it is then sorted to the vacuole (Hanton et al., 2007; Otegui et al., 2006) or back to the cell surface (Toyooka et al., 2009). The TGN is also the major site of sorting for biosynthetic cargo coming from the Golgi (Kang et al., 2011; Viotti et al., 2010). Late endosomes, also known as pre-vacuolar compartments, sort proteins to be degraded to the vacuole (Reyes et al., 2011).

The ESCRT complex and retromer complex are the two major protein complexes that function in plant vacuole biogenesis and are conserved across the animal and plant kingdoms. The ESCRT complex sorts ubiquitin-tagged proteins internalized via endocytosis to the degradative pathway (Hicke and

Dunn, 2003; Lauwers et al., 2009). The retromer complex serves to retrieve biosynthetic receptors and transmembrane proteins back from the TGN (Niemes et al., 2010).

### 1.E.2. The yeast vacuole

The vacuole in yeast is a large organelle that serves several functions for the cell including, pH regulation, osmoregulation, protein degradation, and amino acid storage (Latterich and Watson, 1991; Martinez-Munoz and Kane, 2008; Takeshige et al., 1992; Wiemken and Durr, 1974). Because this structure performs several roles for the cell, it receives membrane and cargo from various sources in order to obtain its full repertoire of necessary vacuole proteins. The yeast vacuole receives cargo via endocytosis and functions like the mammalian lysosome at the end of the endocytic pathway. Vacuoles in yeast also receive cargo through biosynthetic trafficking (Bryant and Stevens, 1998). Soluble cargo require a sorting signal to be trafficked to the vacuole (Wilcox et al., 1992), while integral membrane proteins go to the vacuole by default and need a signal to be sorted away from the vacuole (Roberts et al., 1992).

Intracellular protein trafficking in yeast is mediated by the vacuole protein sorting (VPS) class of proteins. VPS proteins come in several different classes based on mutant vacuole morphology (Raymond et al., 1992). Importantly, VPS Class E genes function to mediate sorting and trafficking of endocytic cargo to the vacuole (Piper et al., 1995; Rieder et al., 1996) and VPS Class C genes function to mediate sorting and trafficking of post-Golgi cargo to the vacuole

(Peterson and Emr, 2001; Sato et al., 2000). VPS Class C is composed of a core of four proteins, Vps11, Vps16, Vps18, and Vps33. This core of proteins can interact with two accessory subunits, Vps39 that functions as a GEF for Rab7 (Wurmser et al., 2000) and Vps41 that acts as an effector for Rab7 (Brett et al., 2008), to form the homotypic fusion and sorting (HOPS) complex. The VPS HOPS complex is found at the yeast vacuole where it regulates all membrane and cargo trafficking. The VPS Class C core can also interact with two additional subunits, Vps3 and Vps8, to form the Class C core vacuole/endosome-tethering (CORVET) complex that is found to interact with the early endosome regulator Rab5 (Peplowska et al., 2007). Together, the HOPS and CORVET complexes mediate the sorting and trafficking of all cargo to late endosomes and lysosomes (Nickerson et al., 2009).

Another way that yeast vacuoles receive cargo is through cytoplasm-to-vacuole targeting (CVT). In CVT, cytosolic components are sequestered possibly through a receptor-mediated process into a double membrane compartment synthesized *de novo* in the cytosol, which then merges with the vacuole (Klionsky et al., 1992). This process is reminiscent of autophagosome formation in mammalian cells. (Scott et al., 1996) A final mechanism through which yeast vacuoles obtain membrane and cargo is through the inheritance of vacuolar components from the mother cell during cell division (Weisman, 2006).

## *1.F. Lysosome-related organelles*

We have characterized the notochord vacuole as a novel lysosome-related organelle (LRO). Here, I will briefly describe the biogenesis, maturation, and function of some well-characterized LROs as similar mechanisms are used during notochord vacuole biogenesis and maintenance.

LROs are specialized structures that share many characteristics with lysosomes and perform specific functions for the cell type in which they are found (Raposo et al., 2007). The most well characterized and studied LROs are the pigment producing melanosomes found in melanocytes, Weibel – Palade bodies (WPBs) found in endothelial cells that regulate hemostasis (blood clotting) and inflammation, α granules found in platelets that also regulate hemostasis, and lytic granules (LGs) found in natural killer cells or cytotoxic T lymphocytes which function in the immune response.

Because LROs perform such a wide array of functions, it follows that the morphology of LROs also varies greatly. Despite this, all LROs must undergo similar biogenesis and maturation processes. LRO precursors obtain specific cargo and create luminal environments tailored to carry out their specialized functions. Various LRO precursors have different origins within the cell. Melanosomes come from compartments with characteristics of early endosomes (Hurbain et al., 2008), WPBs are derived from specialized regions of the TGN (Michaux et al., 2006), platelet α granules are late endosomal in origin (van Nispen tot Pannerden et al., 2010), and LGs are modified lysosomes (Peters et

al., 1991). After receiving initial cargo, LRO precursors undergo maturation where they acquire important transmembrane proteins through membrane trafficking. Once an LRO is mature it can then recruit effector proteins that are essential for the function of the organelle (Marks et al., 2013).

There are several protein complexes that have proven to be critical for LRO formation and maturation. They are: AP-3, vacuolar protein sorting (VPS) Class C, biogenesis of lysosome-related organelles complex (BLOC) -1, BLOC-2, and BLOC-3. Mutations in members of these complexes comprise the heterogeneous genetic disorder known as Hermansky-Pudlak syndrome (Wei and Li, 2013). The small Rab GTPases Rab32 and Rab38 through the use of effector proteins have been shown to regulate cargo delivery to LROs such as melanosomes (Wasmeier et al., 2006), platelet dense granules (Ambrosio et al., 2012), and lamellar bodies (Zhang et al., 2011). These complexes and Rab proteins are crucial for proper protein sorting and membrane trafficking required for LRO maturation and function.

## *1.G. Vertebral column development*

Because my work in notochord vacuole formation led to the discovery that vacuole defects cause spine morphogenesis defects, I will briefly describe what is known about spine development in mammals and the teleost linage of fish. The ancestral vertebral column in vertebrates consisted of a persistent notochord without vertebral centra and mineralized arches formed and attached directly to the notochord sheath (Arratia et al., 2001). Vertebral centra, or vertebral bodies,

arose independently several times during vertebrate evolution. Because these structures are not homologous, their formation differs across vertebrate groups.

### 1.G.1. In mammals

In mammals the vertebrae are first formed as a cartilage mold that will become ossified by bone matrix producing cells, osteoblasts. During ossification the type II collagen present in the cartilage precursor is replaced by type I collagen, the primary collagen present in bone matrix (Wang et al., 2013). This process of using a cartilage intermediate before forming true bone is known as endochondral ossification.

As vertebrae form, the underlying notochord becomes sequestered to the intervertebral regions. There, notochord cells contribute to the center of the intervertebral disc (IVD), the nucleus pulposus (NP), which is surrounded by a fibrous outer layer, the annulus fibrosis (McCann et al., 2012). In nearly every embryonic vertebrate species examined histologically, the notochord-derived NP cells still contain their fluid filled vacuoles (Hunter et al., 2004). Surprisingly, in many species these vacuolated cells will persist well past the age of skeletal maturity, implying a sustained role for the fluid-filled vacuoles well past embryonic development. Ultimately, the IVDs are prone to degenerate in long-lived species, largely because the ends of the vertebrae seal off with cartilage endplates depriving the NP encased in its fibrous layer of oxygen and nutrients (Bibby and Urban, 2004).

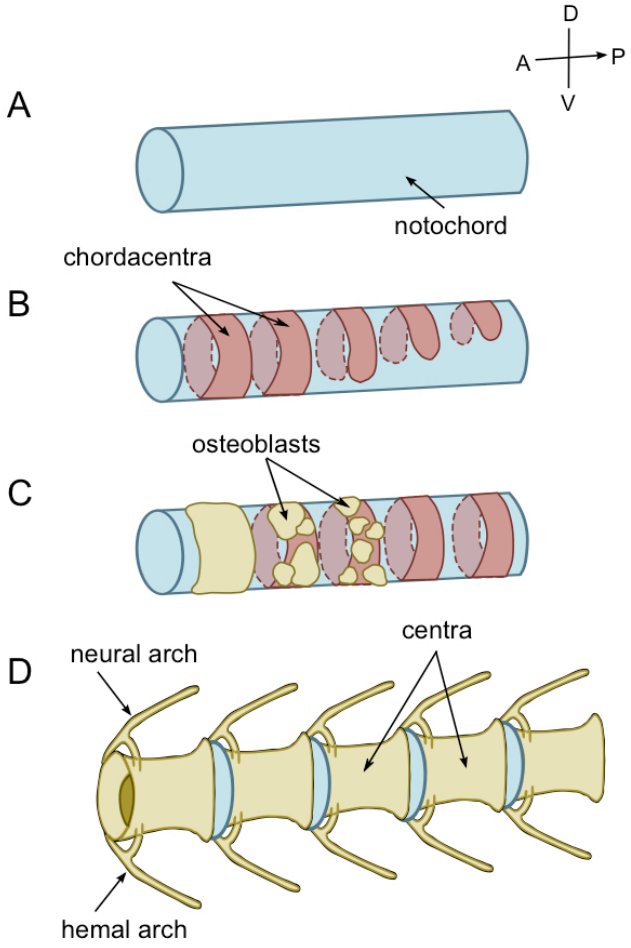


**Figure 6. Fish vertebral development**

(A) The notochord is fully differentiated and has been serving as a hydrostatic skeleton for the larvae for weeks prior to spine formation. The vertebral column develops in an anterior to posterior gradient. (B) Regions of the notochord ECM mineralize, forming bands perpendicular to the long axis of the notochord. These bands, termed chordacentra, lie on top of the notochord outer sheath cells and form in the absence of osteoblasts. (C) Osteoblasts differentiate from surrounding sclerotome and migrate down to the notochord. They land on the notochord in regions with underlying chordacentra and begin to deposit bone matrix in a segmented fashion. (D) Vertebrae mature as the bony centra grow laterally and concentrically. Neural and hemal arches form surrounding the neural tube and dorsal aorta, respectively. The notochord persists and is continuous as a solid rod underneath the centra and between individual vertebrae. dorsal is up, ventral is down, anterior is left, and posterior is right.

### 1.G.2. In teleost fish

In bony fishes the vertebrae do not use a cartilage intermediate and instead undergo direct mineralization, or intramembranous ossification. This process of vertebrae ossification occurs in two steps: formation of a chordacentrum followed by formation of the vertebra (Figure 6).

To form the chordacentra the thick extracellular matrix (ECM) surrounding the notochord mineralizes in discrete bands that run perpendicular to the long axis of the notochord. Mineralization occurs as hydroxyapatite crystals form in the collagen matrix in the regions where the collagen fibrils run parallel to one another, forming rings around the notochord (Wang et al., 2013). In salmon, chordacentra formation begins at the ventral midline and proceeds dorsally until a complete ring is made (Grotmol et al., 2003). In medaka and zebrafish, however, this process begins at the dorsal midline and proceeds ventrally (Inohaya et al., 2007). The entire process of chordacentra formation happens in the absence of osteoblasts (Figure 6).

After chordacentra formation, osteoblasts differentiate from sclerotome in the surrounding somites and migrate to the notochord. The osteoblasts migrate to specified regions of the notochord where they begin to lay down bone matrix on top of the chordacentra and the notochord ECM sheath (Grotmol et al., 2003). The bone matrix deposited by the osteoblasts is rich in type I collagen and is subsequently mineralized. Vertebrae in fish have neural and hemal arches protruding off of the dorsal and ventral sides respectively (Figure 6). The arches

serve to protect delicate structures like the neural tube enclosed by the neural arch and the dorsal aorta enclosed by the hemal arch. The arches are sclerotome-derived and form through the condensation of mesenchyme between somite segments (Grotmol et al., 2003).

While type I and type II collagens are the best characterized collagens that function during bone formation, recent studies in zebrafish have also implicated collagen type VIII and collagen type XXVII as being important. When type XXVII collagens (*col27a1a* and *col27a1b)* were knocked down independently using anti-sense oligonucleotide morpholinos, the resulting embryos displayed abnormal notochord ECM sheath morphology and juveniles developed kinks in their spines (Christiansen et al., 2009). Similarly, mutants for type VIII collagen (*col8a1a*) display severe kinking in their notochords as embryos, which leads to scoliosis of the spine and vertebral fusions in juveniles (Gray et al., 2014). The skeletal defects seen in these collagen mutants or morphants likely reflects an inability of the notochord to act as a rigid scaffold for the deposited bone matrix during spine formation. Instabilities in the notochord ECM sheath could lead to buckling of the notochord during vacuole inflation which would generate a curved scaffold instead of a straight one for vertebral growth.

Retinoic acid is known to be important for its roles in helping to pattern the embryo along its anterior-posterior axis during development. It has also recently been shown to be an important regulator of vertebrae formation in zebrafish. When embryos are exposed to exogenous retinoic acid, or in embryos mutant for

the enzyme that degrades retinoic acid, *cyp26b1*, the vertebrae develop fused to one another (Spoorendonk et al., 2008). Spoorendonk and others showed that cyp26b1 is expressed in sclerotome-derived osteoblasts and that *cyp26b1* mutants have the same number of osteoblasts as wildtype siblings, the osteoblasts are simply over-active. They hypothesize that there needs to be a sharp contrast in levels of retinoic acid in adjacent segments of cells along the length of the notochord in order for proper osteoblast activity to generate the segmented pattern of vertebrae and intervertebral discs.

# 2. Materials and methods

## Fish Stocks

Zebrafish stocks were maintained at 28°C and bred as previously described (Westerfield, 2000). A list of zebrafish lines used for this work can be found in Table 1.

## Plasmid Construction

All constructs for transgenic fish were generated using the Tol2kit gateway cloning system using the p5E-MCS, p5E-hsp70l, pME-MCS, pME-EGFP-CaaX, p3E-polyA, pDestTol2pA2 and pDestTol2CG2 vectors (Kwan et al., 2007). The p5E-4xUAS vector was a kind gift from Mary Goll (Akitake et al., 2011). The 1 kb *rcn3* promoter fragment was amplified from genomic DNA using primers with KpnI and HindIII restriction sites: rcn3_KpnI_forward=GGTACCAACATGACCACGTCAGACCA and rcn3_HindIII_reverse=AAGCTTAAGTGTCCCCAGAAAGAGCA. pME-Dyn1-K44A-GFP was generated from Addgene plasmid 22197, pEGFP-N1-human Dynamin1aa-K44A (Lee and De Camilli, 2002). pME-Dyn2-K44A-GFP was generated from pEGFP-NI-rat Dynamin2aa-K44A (Cook et al., 1994). Rab7b (NM_001002178) was amplified from cDNA using primers with BamHI and NotI restriction sites: rab7b_BamHI_forward=GGATCCATGGCTTCCCGTAAAAAGGTCCTCC and rab7b_NotI_reverse=GCGGCCGCTCAGCAGCTGCAGCCTTCACCGTTA. Rab38b was amplified from cDNA using primers with BamHI and NotI restriction

sites:

rab38b_BamHI_forward=GGATCCATGCATAACAATCAGAAGGAGCATTTGTAT and

rab38b_NotI_reverse=GCGGCCGCTCAAGGTTTGAAGCAAGCGGAACAAGT.

Rab32a was amplified from cDNA using primers with BglII and NotI restriction sites: rab32a_BglII_forward=AGATCTATGGCAGGCGGGTCCGTGTCGG and rab32a_NotI_reverse=GCGGCCGCCTAGCAGCAACCTGACTTGCTCTC.

Dominant negative Rab7b, Rab32a, and Rab38b were made using QuikChange II |XL site-directed mutagenesis kit (Agilent). Lamp2 was amplified from cDNA using primers with EcoRI and BamHI restriction sites: lamp2_EcoRI_forward=GAATTCATGGCTGTCCGCGGTTTTCTGCCTC and lamp2_BamHI_reverse=GGATCCCAGTGTCTGATATCCAACATAGGTTCGTCG . pME-Lamp1-RFP was generated from rat Lamp1-RFP (Sherer et al., 2003).

**Microscopy**

Time-lapse imaging of notochord development, whole-mount live imaging, and fixed section imaging were performed on a Leica SP5 confocal microscope with 10x/0.40 HC PL APO air objective, 20x/0.70 HC PL APO oil objective, and 40x/1.25-0.75 HCX PL APO oil objective (all Leica) and Leica Application Suite software. Whole-mount live imaging was also performed on a Zeiss 780 inverted confocal microscope with 20x/0.8 Dry Plan-Apochromat DIC objective and 40x/1.4 Oil Plan-Apochromat objective (all Zeiss) and Zen software. Dissected notochord cells were imaged using a Zeiss 710 inverted confocal microscope

with 63x/1.40 Oil Plan-Apochromat objective (Zeiss) and Zen software. Whole-mount live imaging was also performed on a Zeiss Axio Imager.M1 microscope with 10x/0.3 EC Plan-NeoFluar objective and 20x/0.8 Plan-Apochromat objective (all Zeiss), a Zeiss AxioCamMRm camera, and AxioVision software. Whole-mount live imaging for body length measurements and before calcein dye was performed on a Zeiss Setero Discovery.V20 microscope with 1.0x Achromat S FWD 63mm objective (Zeiss), a Zeiss AxioCamHRc camera, and AxioVision software. Where necessary, images were minimally post-processed in ImageJ software for overall brightness and contrast or to realign channels in order to correct for drift that occurs during live imaging.

**Immunohistochemistry**

For cross-sections, zebrafish embryos were anesthetized in tricaine solution (Sigma), fixed in 4% PFA overnight, washed several times in PBS, embedded in 4% low melt agarose (GeneMate) and sectioned using a vibratome (Leica VT 1000S) as previously described (Bagnat et al., 2010). Alexa-568 phalloidin (Invitrogen) was used at 1:500 and sections were mounted on glass slides with Vectashield mounting media containing DAPI (Vector Laboratories). A mouse monoclonal antibody against keratan sulfate (Developmental Studies Hybridoma Bank. Univ. of Iowa) was used at 1:100 and detected with Alexa Fluor 488 goat anti-mouse antibody (Molecular Probes) at 1:300.

**Pharmacological treatments**

Brefeldin A (Sigma) was prepared as a 20 mg/mL stock solution in DMSO and used at 5 µg/mL in egg water. Bafilomycin (Sigma) was prepared as a 2 mM stock solution in DMSO and used on fish at 500 nM in egg water and on dissected notochords at 1 µM in L-15 culture media. Rapamycin (Santa Cruz) was prepared as a 10 mM stock solution in DMSO and used at 400 nM in egg water. 3-methyladenine (Tocris) was prepared as a 100 mM stock in water and used at a range of concentrations from 5 mM to 20 mM. Ciliobrevin was prepared as a 2.5 mg/mL stock solution in DMSO and used at 25 µM in egg water. Metronidozole was used at a concentration of 10 mM in egg water.

**Live imaging**

The vital dye GFP Counterstain BODIPY TR Methyl Ester (Molecular Probes) was used for most live imaging. Briefly, embryos were soaked in 2% Methyl Ester Dye (MED) for 30 min. – 1 hr. depending on age, rinsed in egg water, mounted on a glass slide in egg water, and imaged immediately. Spines were labeled with the vital dye calcein (Sigma). Fish were incubated in a solution of 0.2% calcein in water for 10 min. as previously described (Du et al., 2001), rinsed in fish water, allowed to rest for 10 min. at room temp before mounting in fish water on a slide for imaging. All live imaging was performed at room temperature.

**Heat shock**

Embryos in egg water were transferred to 50mL conical tubes and submerged in a 39°C water bath for 30 min. to induce *hsp70l* expression.

**Dissected notochord assays**

Notochords were dissected from fish by incubating embryos in 0.25% trypsin (Gibco) for 5 – 20 min. depending on age. The cell suspension was passed through a 70 μm cell strainer, and the contents retained in strainer were cultured in L-15 media without phenol red (Gibco) containing 10% fetal bovine serum. For endocytosis assays, FM4-64 dye (Molecular Probes) was prepared as a 4mM stock solution in water and was co-cultured with notochord cells at a final concentration of 4 μM. Dextran Alexa Fluor 568 10,000 MW (Molecular Probes) was prepared as a 5 mg/mL stock and co-culted with notochord cells at a final concentration of 100 μg/mL. LysoTracker Red DND-99 (Molecular Probes) comes as a 1 mM stock solution in DMSO and was co-cultured with notochord cells at a final concentration of 1 μM. Notochord cells were imaged in L-15 culture media described above in 35mm glass bottom microwell dishes at room temperature.

**Body length measurements**

Fish were mounted in 2% methylcellulose for whole-mount imaging and then recovered. Body length was measured from the tip of the nose to the tip of the tail using ImageJ software.

**Western blot**

HEK 293AD cells were transfected with pcDNA3-s-RFP or pcDNA3-s-GFP-GAG using Lipofectamine 2000 (Invitrogen). Cells were allowed to secrete into media for 3 days and then supernatants were collected. Samples were spun

for 5 min. at 1.5k to pellet any cellular debris and the supernatant was removed. Laemmli sample buffer was added to supernatant and cells and boiled for 5 min. and samples were loaded into SDS-PAGE gels. Secreted-RFP was detected with rabbit polyclonal anti-DS red antibody (Clonetech) at 1:1000 and Secreted-GFP-GAG was detected with rabbit polyclonal anti-GFP antibody (Anaspec).

**Alcian Blue**

Glycosaminoglycans were labeled with Alcian blue as previously described (Neuhauss et al., 1996). Briefly, embryos were fixed in 4% PFA overnight and washed several times in PBS. Embryos were bleached in 30% hydrogen peroxide until the eyes were translucent. Embryos were rinsed in PBS and transferred to Alcian blue solution overnight (70% EtOH, 1% HCl, 0.1% Alcian blue). Embryos were cleared in acidic ethanol (70% EtOH, 5% HCl) until clear.

**Alizarin Red**

Bone was labeled using Alizarin Red. Briefly, fish were fixed in 80% EtOH for at least 2 hours at room temperature. Viscera and skin were removed completely using forceps. Samples were fixed in 4% PFA overnight at 4°C and then washed well in PBS. Samples were bleached in equal parts 5% $H_2O_2$ and 1% KOH until the eyes became clear, about an hour. Samples were dehydrated using an EtOH series: 25%, 50%, 75%, 90% EtOH for 5 minutes each. Samples were stained with 0.1% Alizarin red in 96% EtOH overnight at room temperature. Samples were washed well in distilled water until water ran clear. Tissues were

cleared of unbound alizarin red using 1% KOH, replaced every day, until muscles are clear and bone is easily visible.

**TUNEL assay**

Tissue was embedded and sectioned as described above. TUNEL assay was performed using TACS 2 TdT-Fluor In Situ Apoptosis Detection Kit according to the manufacturers protocol. Instead of slide chambers, solutions were placed directly on sections on slides. Briefly, sections were incubated in PBS for 10 minutes. Sections were incubated in ProK solution for 15 minutes and then washed twice with distilled water. Sections were incubated with 1x TdT Labeling Buffer for 5 min. Sections were then incubated with Reaction Mix using Mn as the cation and placed in a humidity chamber for 1 hour at 37°C. Nuclease and Nuclease Buffer was added to positive control sections. Sections were incubated in Stop Buffer for 5 min and then washed well with distilled water. Sections were incubated in Strep-Fluor solution for 20 minutes in the dark and then washed well with distilled water. Finally, sections were incubated with permeabilizing solution containing phaloidin568 at 1:500 before imaging.

**NTR and Mtz. cell ablation**

Embryos injected with cyb5r2:mCherry-NTR were treated with Mtz. at 11 dpf to ablate notochord cells. Fish were incubated in 10 mM Mtz. and kept in the dark for 24 hours at 28 °C. Embryos were washed well, placed in fresh egg water, and allowed to recover for 24 hours before imaging.

# 3. Biogenesis of the notochord vacuole

While notochord vacuoles have been described physically for decades (Waddington, 1962), the sorting and trafficking requirements for their formation were previously unknown. Here I will describe how we elucidated the cellular and molecular mechanisms involved in notochord vacuole inflation and maintenance.

## *3.A. Introduction*

The zebrafish notochord is comprised of two cell layers, an outer epithelial-like sheath, and an inner layer of cells containing one large vacuole each that occupies the majority of the cell volume. To elucidate how notochord vacuoles are formed we generated various transgenic zebrafish lines to drive notochord-specific or inner cell-specific expression of various transgenes. To drive expression in both outer and inner cell populations we isolated a ~1 kb regulatory sequence from the *rcn3* gene. This promoter sequence is active in the notochord before vacuole formation, beginning at 6 ss (~12 hpf). For inner cell-specific expression we used a gal4 enhancer trap line (SAGFF214A) that is active after vacuole formation at 26 ss (~22 hpf).

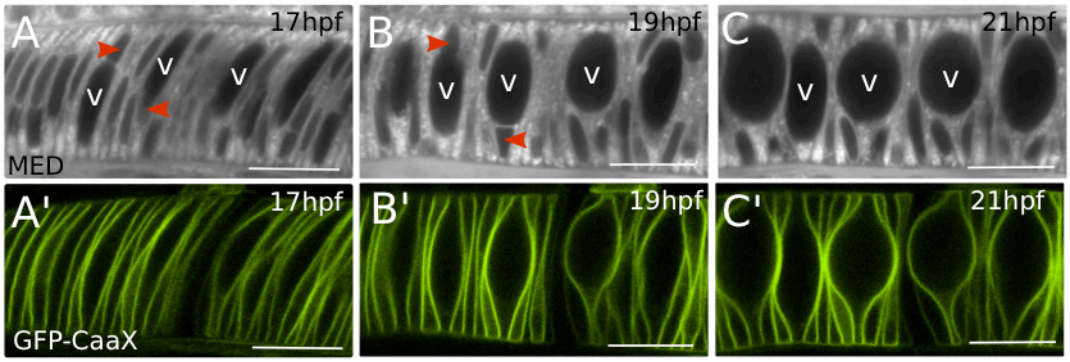


**Figure 7. Notochord vacuoles inflate rapidy during development**

(A-C') Wildtype notochord vacuole inflation was visualized with the vital dye BODIPY TR Methyl Ester Dye (MED) using live confocal time-lapse imaging of GFP-CaaX transgenic embryos; *Tg(rcn3:gal4); Tg(UAS:GFP-CaaX).* The vacuoles inflate rapidly over a short developmental period. The plasma membranes of the inner cells deform greatly as the intracellular vacuoles expand. (A-C) MED. (A'-C') Notochord-specific membrane GFP. v labels vacuole and red arrowheads label nuclei. Scale bars = 50 μm.

To determine the time course of notochord vacuole formation we first performed live, time-lapse imaging of vacuole expansion in wild-type (WT) embryos (Figure 7). All live imaging in this work was performed in the same orientation at approximately the same position along the anterior-posterior axis. Transgenic membrane GFP (GFP-CaaX) embryos were incubated in the vital dye BODIPY TR Methyl Ester Dye (MED) to visualize internal membranes. We observed that over the course of 4 hours (from 17 to 21 hpf) notochord vacuoles expand their volume dramatically, changing the shape of the prospective inner cells from disc-shaped rods to large spheroids. Concurrently, outer cells migrate to the periphery to form an epithelial-like sheath surrounding the inner cells.

## *3.B. Results*

There are several trafficking routes that could contribute membrane and cargo to the growing vacuole. Vacuoles could receive contributions from endocytic trafficking via early endosomes, biosynthetic trafficking through the ER and Golgi complex, or both. Alternatively, the vacuole could form *de novo* in the cytosol through the sequestration of cytoplasmic components as occurs during autophagosome formation. The experiments performed here were designed to distinguish between the possible trafficking routes involved in vacuole biogenesis.

### 3.B.1. Biosynthetic trafficking is required for the rapid inflation of the notochord vacuoles

In order to determine if biosynthetic trafficking contributes to the growing vacuole membrane, embryos were treated with brefeldin A (BFA), an inhibitor of ER to Golgi transport (Figure 8). Notochord-specific GFP-CaaX embryos were treated before vacuole formation for a duration of 5 hours from 16 ss until 25 ss with either 5µg/mL BFA or DMSO. While vacuole formation initiated and progressed normally in DMSO-treated embryos, the vacuoles failed to inflate or appear fragmented in BFA-treated embryos, indicating that ER to Golgi trafficking is essential for vacuole biogenesis. This role for ER to Golgi transport is consistent with the defects seen in the notochords of COPI and COPII mutant zebrafish (Coutinho et al., 2004; Melville et al., 2011).

The fragmented vacuole phenotype is somewhat surprising. If biosynthetic trafficking is necessary for generating vacuole membrane and supplying cargo, I would expect to see no vacuoles at all after BFA treatment. The fragmented vacuole phenotype looks like a defect in a later trafficking stage. This could be the case, as BFA is known to inhibit the proteins that activate ADP-ribosylation factors (Arfs) (Donaldson et al., 1992; Helms and Rothman, 1992). Arfs are small G proteins that are involved in the sorting of cargo into transport vesicles and aid in formation of protein coats (Schekman and Orci, 1996). By inhibiting activation of Arfs, BFA generates DN GDP-bound Arfs that can then sequester GEFs and prevent endogenous small G proteins from functioning. Furthermore, not all Arfs

are equally sensitive to disruption by BFA. Mammals have three classes of Arf proteins that display varying degrees of sensitivity to BFA (Chardin and McCormick, 1999). Therefore, the Arfs that function early in the secretory route may be more insensitive to BFA and the effects we see are due to a disruption of Arfs that function at the late endosome or pre-vacuolar endosome stage of trafficking.

The effects of BFA on notochord vacuoles also suggests autophagy is not involved in vacuole formation as ER and Golgi stress have been shown to increase autophagosome size and number (Purhonen et al., 1997). To explore this further we generated a transgenic line expressing the autophagosome marker LC3 under the control of the heat shock promoter. To induce autophagy, embryos were treated with 400nM rapamycin or DMSO for 20 hours from 75% epiboly to the 25-somite stage. LC3 expression was induced with a heat shock 3 hours prior to imaging and then embryos were returned to media containing rapamycin for the remaining time of the 20 hours. Live confocal imaging revealed LC3-positive punctae throughout the inner cells but LC3 did not label the vacuole membrane (data not shown). To further test the role of autophagy in vacuole formation, embryos were treated with a range of concentrations of 3-methyladenine, an inhibitor of autophagosome formation, from 5mM to 20mM or DMSO for 10 hours starting at the 10-somite stage ending at 24 hpf.

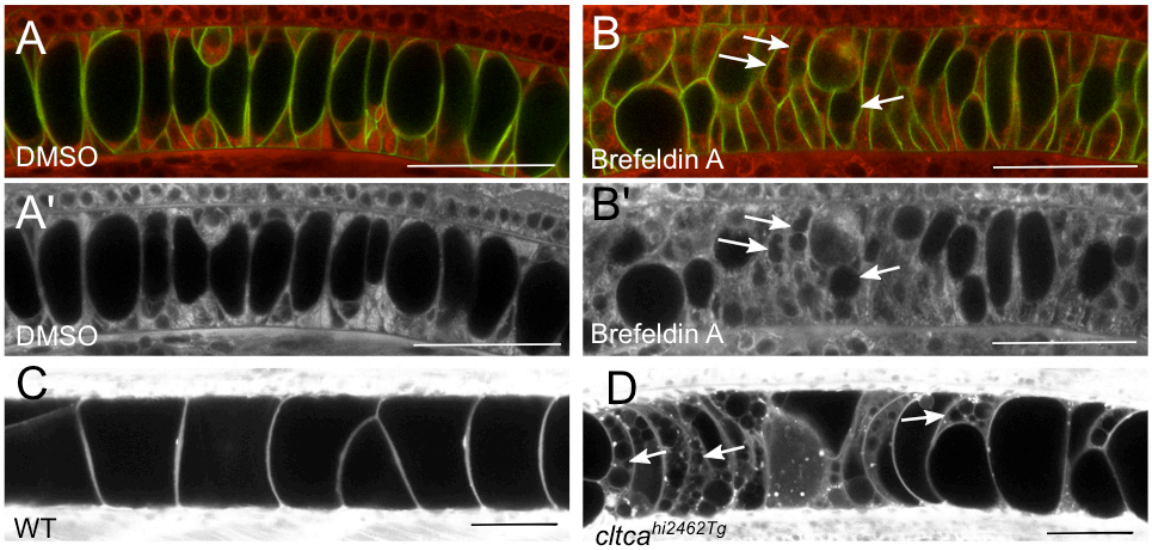


**Figure 8. Biosynthetic trafficking is required for notochord vacuole formation**

(A-B') Live confocal images of embryos treated with either DMSO (A,A') or 5 µg/mL brefeldin A (B,B') at the time of vacuole inflation to inhibit ER to Golgi traffic. Embryos were visualized with notochord-specific membrane GFP and the vital dye, MED. (A,B) MED and membrane-GFP merge. (A',B') MED in grayscale alone. Brefeldin A results in smaller, fragmented vacuoles indicated with arrows. (C,D) Live confocal image of *cltca*$^{hi2462Tg}$ mutant and WT sibling larvae at 4 dpf dyed with MED. Arrows label fragmented or small vacuoles. This data shows that clathrin-dependent biosynthetic trafficking is required for vacuole biosynthesis and maintenance. Scale bars = 50 µm.

No obvious differences in notochord vacuoles were seen at any concentration in the 3-methyladenine treated embryos compared to DMSO controls (data not shown). Taken together these data suggest that the notochord vacuoles do not form *de novo* in the cytosol through an autophagy-like process.

Next, to investigate the potential role of post-Golgi trafficking in vacuole formation we asked whether clathrin coats are required. Clathrin coats are important mediators of coated vesicle formation in post-Golgi trafficking as well as during plasma membrane internalization from the cell surface (Anderson et al., 1977; Deborde et al., 2008). The transgenic line *cltca*$^{hi2462Tg}$ contains a retroviral insertion in the clathrin heavy chain gene, which generates a null mutant allele (Amsterdam et al., 2004). Using live confocal imaging we observed that in clathrin mutants, but not in WT siblings, notochord vacuoles begin to fragment and fall apart around 96 hpf (Figure 8). This phenotype is not apparent until 4 dpf, most likely due to a maternal load of functional protein. This data implicates post-Golgi trafficking in vacuole maintenance.

We next investigated the presence of secreted cargo within the vacuole lumen. We generated secreted versions of GFP and RFP and tested them for secretion *in vitro*. In transgenic embryos expressing secreted GFP in the notochord, no GFP was detected in the lumen of the vacuole (Figure 9). Since bulk secretory cargo is sorted away from the vacuole, our data suggest that a specialized post-Golgi trafficking pathway is required for notochord vacuole biogenesis.

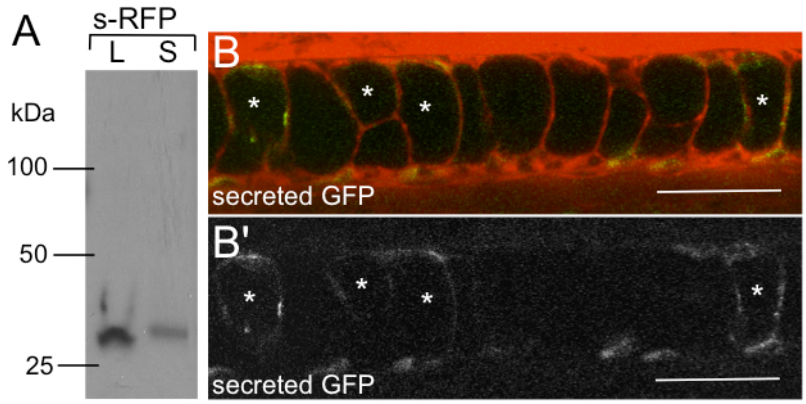


**Figure 9. Bulk secretory cargo is sorted away from the vacuole**

(A) Western blot of HEK293AD cells expressing secreted RFP using an anti-RFP antibody. A GFP-tagged version of the same protein was used for the transgenic fish line. L is cell lysate. S is supernatant showing the protein is secreted from cells *in vitro*. (B, B') Live confocal image of a 24 hpf embryo expressing secreted GFP; *Tg(rcn3:gal4); Tg(UAS:s-GFP),* visualized with MED (B) and grayscale GFP alone (B'). No GFP is detected in the lumen of the vacuoles. This data suggests that vacuole cargo requires specific sorting to the vacuole. Scale bars = 50 μm.

Traditionally, it has been assumed that notochord vacuoles contain glycosaminoglycans (GAGs) and that these highly negatively-charged molecules might drive vacuole expansion by attracting cations and water (Waddington, 1962). In order to determine if GAGs are present in zebrafish notochord vacuoles we generated a secreted GFP that contains a short sequence tag of 10 amino acids (EDEASGIGPE) that is a known GAG attachment site in the proteoglycan decorin (Kobialka et al., 2009) (Figure 10). The GAG-tagged GFP (GAG-GFP) was modified and secreted from cells *in vitro*. In 24 hpf embryos expressing secreted GAG-GFP under the control of the *rcn3* promoter, no GAG-GFP was detected in the vacuole lumen, suggesting that GAGs are not trafficked to the vacuole at this stage. We also checked for the presence of GAGs using immuno-histochemistry. Anti-keratan sulfate antibodies labeled the peri-notochordal basement membrane as well as the space between the outer sheath layer and inner cell layer but not the lumen of the vacuole. Next, we stained embryos with the basic dye Alcian blue, which labels acidic polysaccharides and mucopolysaccharides, and did not detect any labeling inside the vacuoles, suggesting that GAGs are not likely to function as osmolytes within the zebrafish notochord vacuole during embryogenesis (Figure 10).

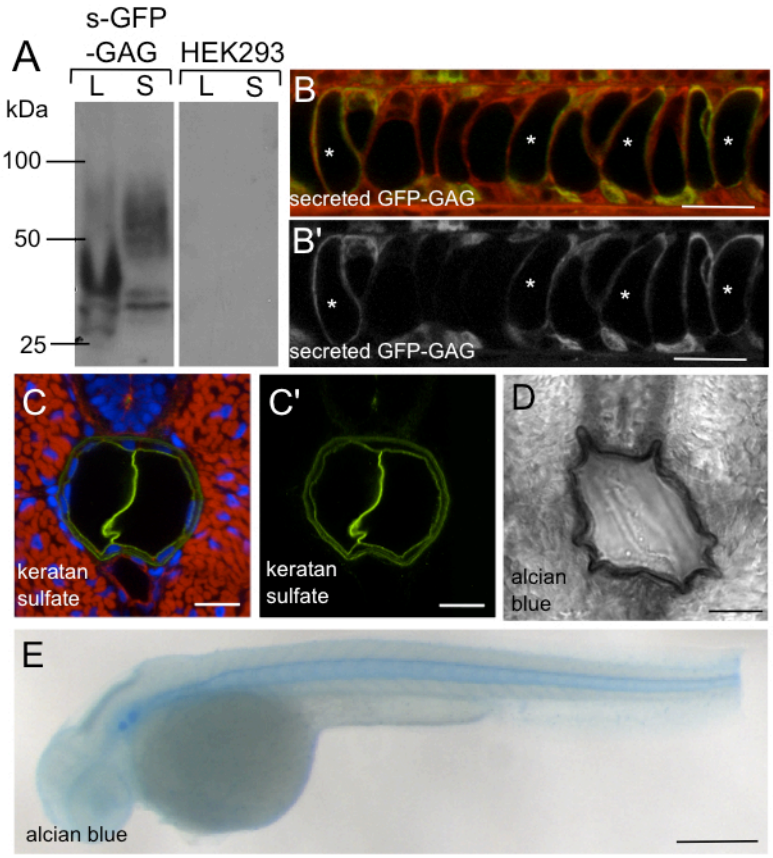


**Figure 10. GAGs are not present in the notochord vacuole**

(A) Western blot of HEK293AD cells expressing secreted GFP-GAG using an anti-GFP antibody. The characteristic smear in the supernatant is indicative of GAG modification. L is cell lystate. S is supernatant showing the construct is secreted from cells *in vitro*. (B, B') Live confocal image of a transgenic 24 hpf embryo expressing GAG-tagged secreted GFP; *Tg(rcn3:gal4); Tg(UAS:s-GFP-GAG)*, visualized with MED (B) and grayscale GFP-GAG alone (B'). (C) Confocal image of a cross-section of a 2 dpf embryo immunostained with an antibody against keratan sulfate in green, phalloidin is in red, and DAPI is in blue. (C') anti-keratan sulfate alone. (E) 2 dpf embryo labeled with Alcian blue reveals staining in developing otoliths and peri-notochordal sheath. (D) Cross section of a 2 dpf Alcian blue stained embryo. Alcian blue labels the peri-notochordal sheath but not the lumen of the vacuoles. No GAGs are detected in the lumen of the vacuoles. This data shows that GAGs are not the osmolyte present in the notochord vacuoles. (B, B') Scale bars = 50 μm. (C-D) Scale bars = 20 μm. (E) Scale bar = 250 μm.

### 3.B.2. Endocytosis is not a major contributor to vacuole formation or maintenance

Because clathrin is involved in vesicle formation at both the Golgi complex and the plasma membrane during endocytosis, we next investigated if endocytosis contributes to the growing vacuole. To determine whether endocytosis is required for vacuole formation we generated dominant-negative (DN) constructs to block Dynamin, a GTPase that plays a major role in endocytosis as well as in Golgi complex exit (Chen et al., 1991; Herskovits et al., 1993; Kreitzer et al., 2000). DN Dynamin constructs were expressed mosaically or induced after notochord differentiation to avoid defects in convergent extension and differentiation of the outer and inner cell types (Kida et al., 2007). UAS:Dyn1-K44A-GFP or UAS:Dyn2-K44A-GFP DNA were injected into *Tg(rcn3:gal4)* embryos at the one-cell stage and embryos were then live imaged at 24 hpf using confocal microscopy (Figure 11). We observed that most inner cells expressing DN Dynamin had fully inflated vacuoles, whereas only 9.6% of expressing cells had fragmented vacuoles (n = 52 cells).

We also tested the requirement of endocytosis for vacuole maintenance by expressing a DN version of the early endosome regulator Rab5c. To drive the expression of DN Rab5c after vacuole formation we crossed the SAG214A driver described above to a *Tg(UAS:mCherry-rab5c-S34N)* line (Clark et al., 2011; Yamamoto et al., 2010). At 2 dpf, when the DN protein had been present in the inner cells for at least 24 hours, transgenic embryos had normal notochords with

fully inflated vacuoles (Figure 11). Of the inner cells expressing DN Rab5c only 2.8% were fragmented at 2 dpf (n = 572 cells), suggesting that early endosome trafficking is not required for vacuole maintenance.

To test more directly the contribution of endocytosis to vacuole formation we used the endocytic tracer FM4-64 to track internalized membranes. Because FM4-64 did not readily label inner notochord cells in intact embryos, we cultured dissected notochords in medium with FM4-64 for 30 minutes and then assessed dye distribution by confocal microscopy (Figure 12). In partially intact notochords, the dye was internalized and transiently co-localized with the early endosomal marker Venus-FYVE (data not shown). However, there was little internalization of the dye and few detectable endosomes in the inner cells after 1 hour, and no FM4-64 was seen on the vacuole membrane. To enhance endocytosis we dissociated notochords further and incubated them with dye for 20 minutes. After washing out un-incorporated dye, we added fresh media and monitored the notochord cells for an additional 40 minutes using confocal microscopy. Under these conditions much more FM4-64 was internalized, yet the dye never labeled the vacuole membrane (Figure 12). Similar experiments were also done with fluorescently-labeled dextran. After incubation for 30 min, dextran-labeled punctae were seen within cells but no dextran was visible inside the vacuole (data not shown). Taken together, these data show that notochord vacuoles do not receive internalized membranes or soluble cargo via endocytosis and that endocytosis does not play a major role in vacuole maintenance.

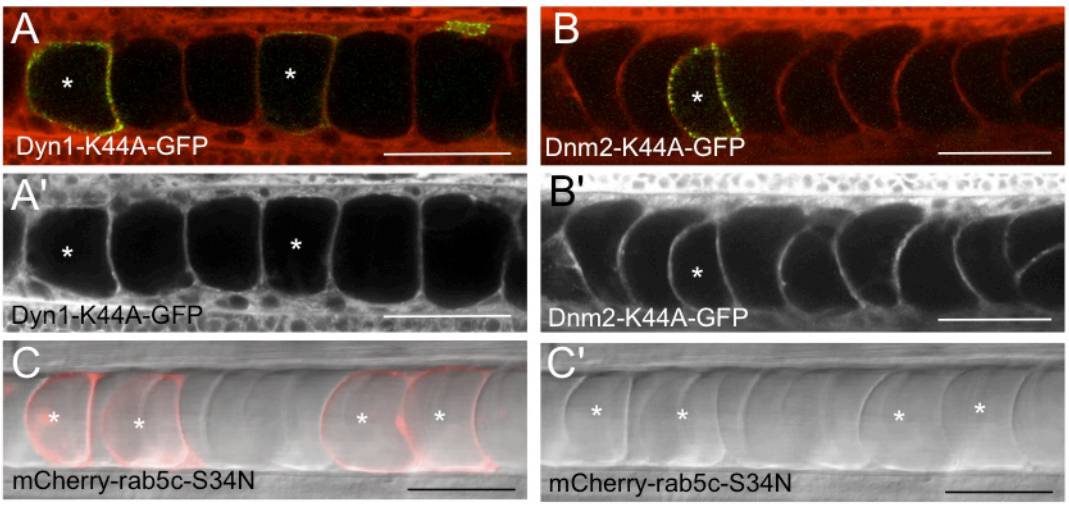


**Figure 11. Endocytosis does not play a major role in vacuole formation**

UAS:Dyn1-K44A-GFP and UAS:Dyn2-K44A-GFP DNA were injected into *Tg(rcn3:gal4)* embryos for mosaic expression of DN dynamin1 or dynamin2. (A) Live confocal image of a 24 hpf embryo mosaically expressing DN Dynamin1-GFP and stained with MED. Asterisks label expressing cells. (A') MED alone. (B) Live confocal image of a 24 hpf embryo mosaically expressing DN Dynamin2-GFP and stained with MED. Asterisks label expressing cells. (B') MED alone. Inner cells expressing DN dynamin early still form fully inflated vacuoles. This data suggests that endocytosis is not required for vacuole formation. (C) Live confocal image of a 48 hpf embryo expressing DN mCherry-Rab5 in the inner cells using the late driver, *Gt(SAGFF214A:gal4); Tg(UAS:mCherry-rab5c-S34N)*. Asterisks label expressing cells. (C') DIC alone. Inner cells expressing DN rab5 late have fully inflated vacuoles. This data suggests that endocytosis does not play a major role in vacuole maintenance. (A-C) Scale bars = 50 μm.

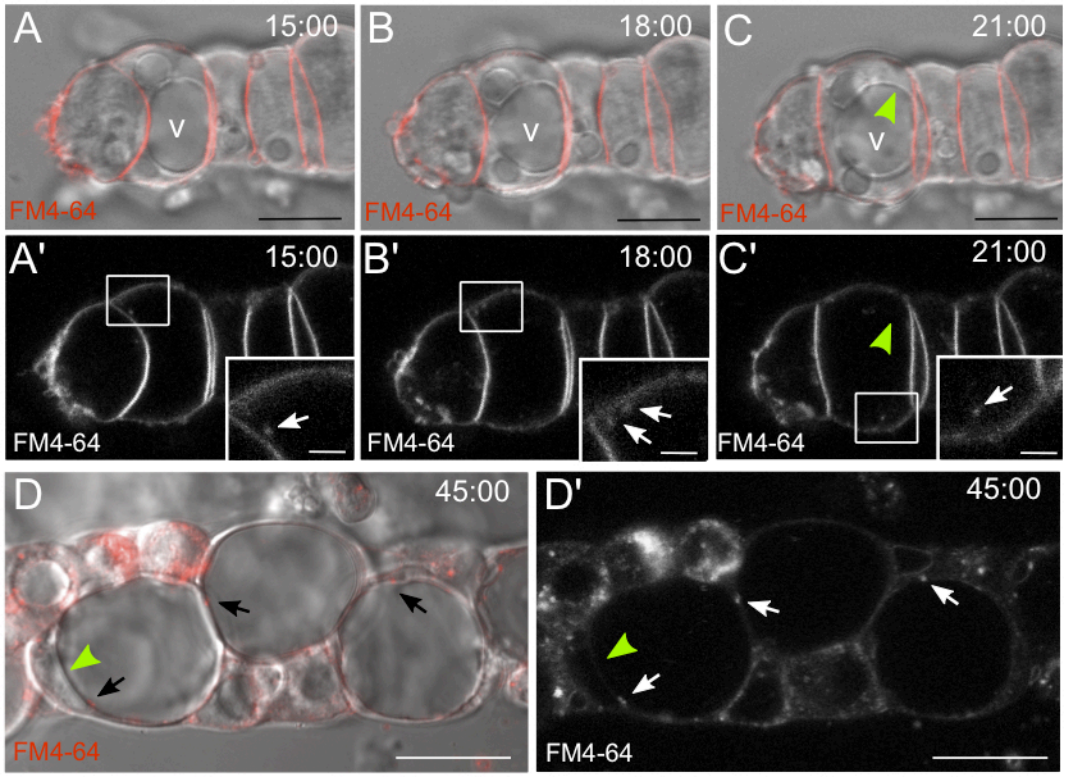


**Figure 12. Endocytic tracers do not label the notochord vacuole**

(A-C') Still images from time-lapse confocal live imaging of dissected notochords cultured with FM4-64. (A-C) Bright field and FM4-64 dye merge and (A'-C') FM4-64 dye in grayscale alone. Arrows indicate FM4-64-labeled endosomes in inner cells, v labels vacuole. After 20 minutes, no FM dye is seen on the vacuole membrane. (D) In further dissociated notochords, cells internalize more dye, but FM dye is still not found on the vacuole membrane. Arrows indicate FM dye labeled endosomes in inner cells and green arrowhead labels vacuole membrane. (D) Bright field and FM dye merge and (D') FM dye in grayscale alone. This data further shows that endocytosis does not contribute membrane or cargo to the vacuole. (A-C) Scale bars = 10 μm. (A'-C' insets) Scale bars = 2 μm. (D) Scale bars = 20 μm.

### 3.B.3. Vacuole inflation requires late endosomal machinery and Rab32a

Clathrin is known to regulate vesicular traffic out of the Golgi complex, and as shown here, is required for vacuole maintenance. To investigate the role of the post-Golgi late endosomal pathway in vacuole formation, we obtained mutant zebrafish with null alleles of genes that function at the late endosome and lysosome, the vacuolar protein sorting genes (VPS). VPS genes were first discovered and characterized in yeast where they function to regulate the trafficking of transport vesicles to the yeast vacuole (Raymond et al., 1992). Zebrafish mutant for *vps11* and *vps18* were shown to have pigmentation defects in the skin and retinal epithelium as well as liver defects (Sadler et al., 2005; Thomas et al., 2011). Using live confocal and DIC imaging we analyzed the notochords of 2 dpf *vps11*$^{wsu1}$ and *vps18*$^{hi2499aTg}$ mutant embryos and found that notochord vacuoles fragment and appear disorganized in these mutants, indicating that the late endosomal pathway is important for vacuole maintenance (Figure 13). To verify that the fragmented vacuole phenotype is not the result of cell death I have performed TUNEL assays and cleaved caspase-3 antibody staining to detect apoptosis. In all of the mutants analyzed thus far, the fragmentation of vacuoles precedes TUNEL signal, caspase-3 signal, and cell death by at least 24 hours (data not shown).

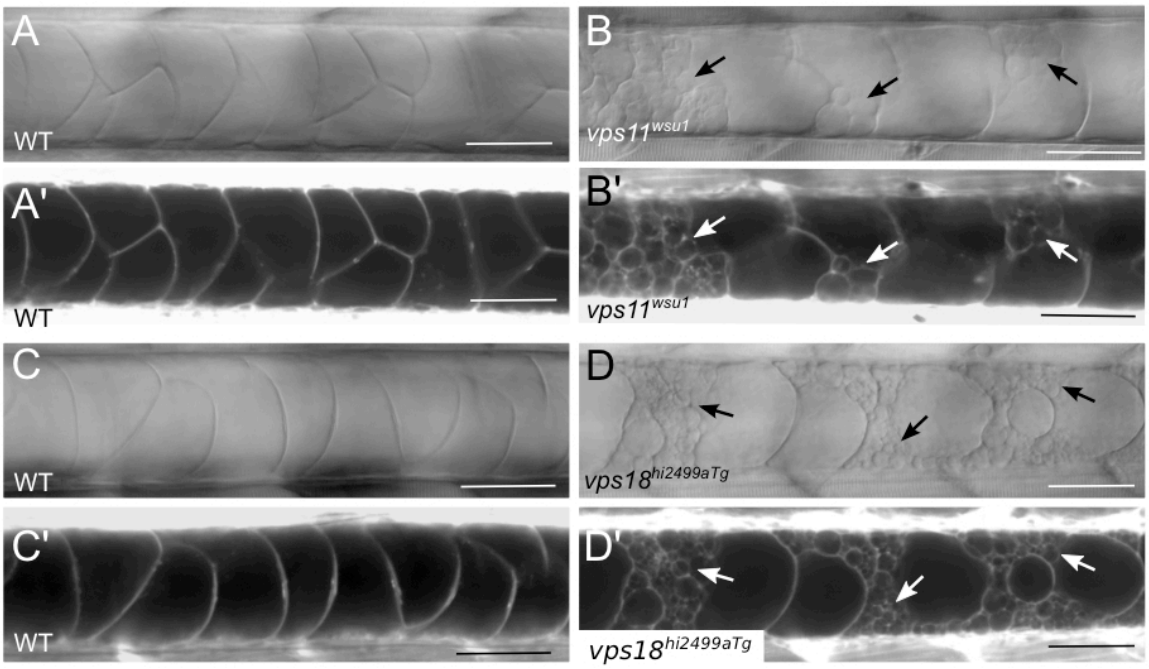


**Figure 13. Vacuole formation requires late endosomal machinery**

(A, A') Live DIC and confocal images of a 3 dpf WT sibling. (B, B') Live DIC and confocal images of a 3 dpf *vps11*$^{wsu1}$ mutant larva dyed with MED. Arrows indicate fragmented vacuoles. (C, C') Live DIC and confocal images of a 3 dpf WT sibling. (D, D') Live DIC and confocal images of a 3 dpf *vps18*$^{hi2499aTg}$ mutant larva dyed with MED. Arrows indicate fragmented vacuoles. This data shows that the late endosomal machinery, specifically the HOPS complex, is essential for vacuole maintenance. Scale bars = 50 μm.

Next, we tested if Rab7, the classical regulator of late endosomes, is important for vacuole formation. To this end we expressed DN mCherry-Rab7a (Clark et al., 2011) under the control of the *rcn3:gal4* driver. Live confocal imaging revealed that inner cells developed vacuoles normally in transgenic embryos expressing DN mCherry-Rab7a in the notochord. As several isoforms of *rab7* exist in zebrafish we also generated and tested the effects of a DN GFP-Rab7b construct. UAS:GFP-rab7b-T22N DNA was injected into *Tg(rcn3:gal4)* embryos at the one-cell stage. At 24 hpf, mosaic expression of DN GFP-Rab7b did not affect vacuole formation in GFP-positive inner cells (Figure 14).

We next investigated whether other Rabs known to function at late endosomes or lysosome-related organelles (LROs) are necessary for vacuole formation. Rab32 and Rab38 have been shown to regulate post-Golgi trafficking to the melanosome (Wasmeier et al., 2006), a LRO, and *in-situ* hybridization reveals that *rab32a* is expressed in the notochord at the time of vacuole inflation (Thisse et al., 2001). Therefore, we expressed DN GFP-Rab38b under the control of the *rcn3* promoter and analyzed the effect in transgenic embryos by live confocal microscopy. At 24 hpf, DN GFP-Rab38b did not cause any defects in vacuole formation. In contrast, expression of DN Rab32a caused fragmentation of vacuoles in 90.6% of the expressing cells (n = 32 cells), indicating that Rab32a functions in vacuole formation (Figure 14).

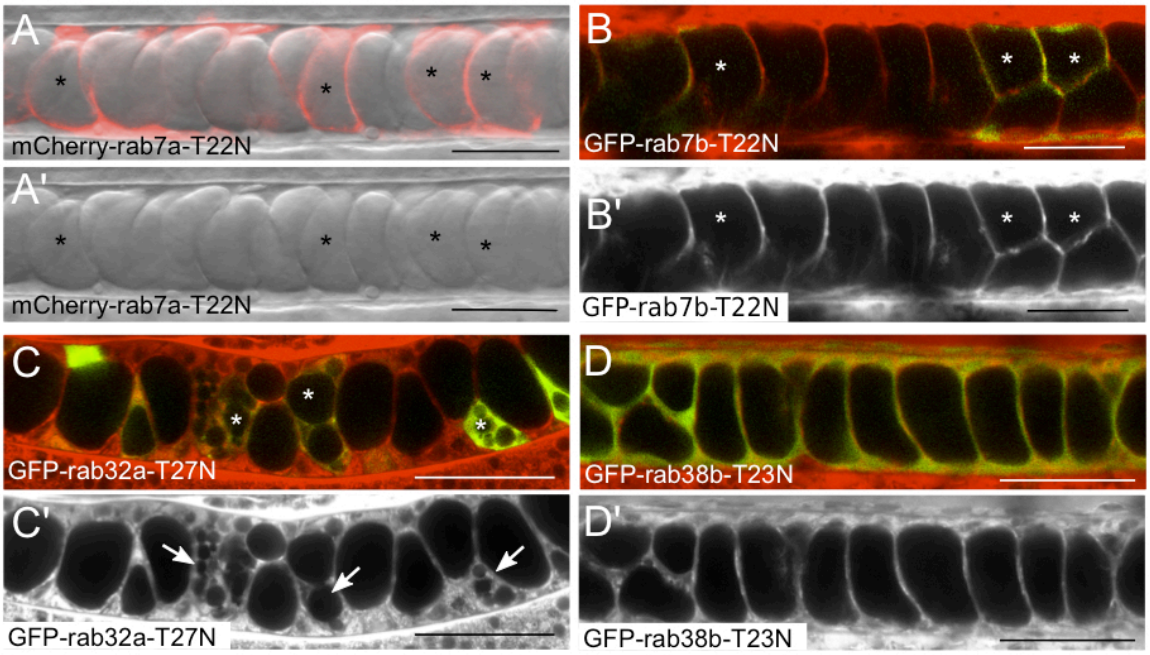


**Figure 14. Notochord vacuole biogenesis requires rab32a**

(A) Live confocal image of a 24 hpf transgenic embryo expressing DN mCherry-Rab7a; *Tg(rcn3:gal4); Tg(UAS:mCherry-rab7a-T22N).* (A') DIC alone. Asterisks label expressing cells. (B) UAS:GFP-rab7b-T22N DNA injected into *Tg(rcn3:gal4)* embryos for mosaic expression of DN GFP-Rab7b. Live confocal image of a 24 hpf embryo with MED and GFP merged. (B') MED in grayscale alone. Asterisks label expressing cells. Inner cells expressing DN rab7 form fully inflated vacuoles. This data suggests that the late endosomal regulator, rab 7, does not function in vacuole biogenesis. (C) UAS:GFP-rab32a-T27N DNA injected into *Tg(rcn3:gal4)* embryos for mosaic DN GFP-Rab32a expression. Live confocal image of a 24 hpf embryo with MED and GFP merged. (C') MED in grayscale alone. Asterisks label expressing cells and arrows indicate fragmented vacuoles. (D) Live confocal image of a 24 hpf transgenic embryo expressing DN GFP-Rab38b in the notochord; *Tg(rcn3:gal4); Tg(UAS:GFP-rab38b-T23N)*. MED and GFP merge. (D') MED in grayscale alone. This data shows that vacuole formation requires regulation from rab32a, but not rab38b. (A – D') Scale bars = 50 μm.

It has been well established that acidity increases within the secretory pathway, from neutral pH in the ER to acidic pH in post-Golgi compartments and lysosomes, and that acidification is required for post-Golgi sorting and trafficking (Mellman, 1992). Since notochord vacuoles use late endosomal machinery and Rab32a, we sought to determine if acidification is necessary for sorting and trafficking to the vacuole. In zebrafish mutant for components of the H+-ATPase complex (Nuckels et al., 2009), which drives acidification of intracellular compartments, we assessed vacuole integrity by MED labeling. In atp6v1e1bhi577aTg, atp6v1fhi1988Tg, and atp6v0cahi1207Tg mutants notochord vacuoles initially formed, but then fragmented by 3 dpf (Figure 15).

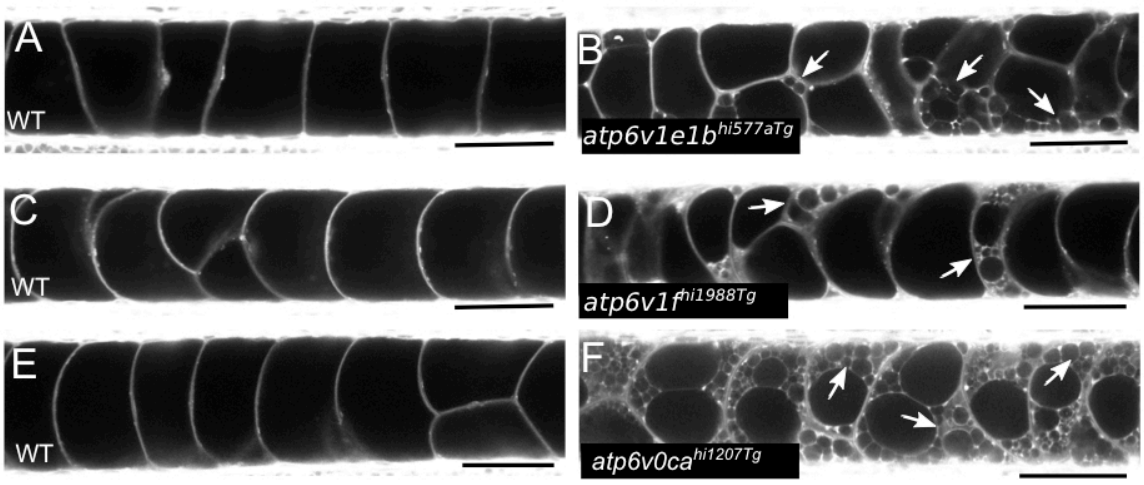


**Figure 15. Vacuole maintenance requires the Vacuolar-H+-ATPase**

(A-F) Live confocal images of a 4 dpf WT sibling (A, C, E) and Vacuolar-H+-ATPase mutant (B, D, F) larvae dyed with MED. (B) $H^+$-ATPase mutant ***atp6v1e1b***$^{hi577aTg}$. (D) $H^+$-ATPase mutant ***atp6v1f***$^{hi1988Tg}$. (F) $H^+$-ATPase mutant ***atp6v0ca***$^{hi1207Tg}$. Arrows indicate fragmented vacuoles. This data illustrates that acidification is required for vacuole maintenance. Scale bars = 50 μm.

In order to test if H+-ATPase function is necessary for vacuole formation, embryos were treated with bafilomycin, a potent inhibitor of vacuolar type H+-ATPases, before vacuole formation. Embryos expressing notochord-specific GFP-CaaX were treated for 4 hours at 15 ss, before the time of vacuole formation, with either 500nM bafilomycin or DMSO, and incubated in MED. Live confocal imaging revealed that vacuole formation was arrested in bafilomycin-treated embryos. We also treated GFP-CaaX embryos after vacuole formation had initiated, from 20 ss until 28 ss, with 500nM bafilomycin or DMSO. Vacuole growth stopped in the bafilomycin-treated embryos, while continuing normally in the DMSO controls, indicating that acidification is necessary for vacuole formation. Taken together, these data show that notochord vacuole formation and maintenance requires late endosomal trafficking regulated by Rab32a and H+-ATPase-dependent acidification (Figure 16).

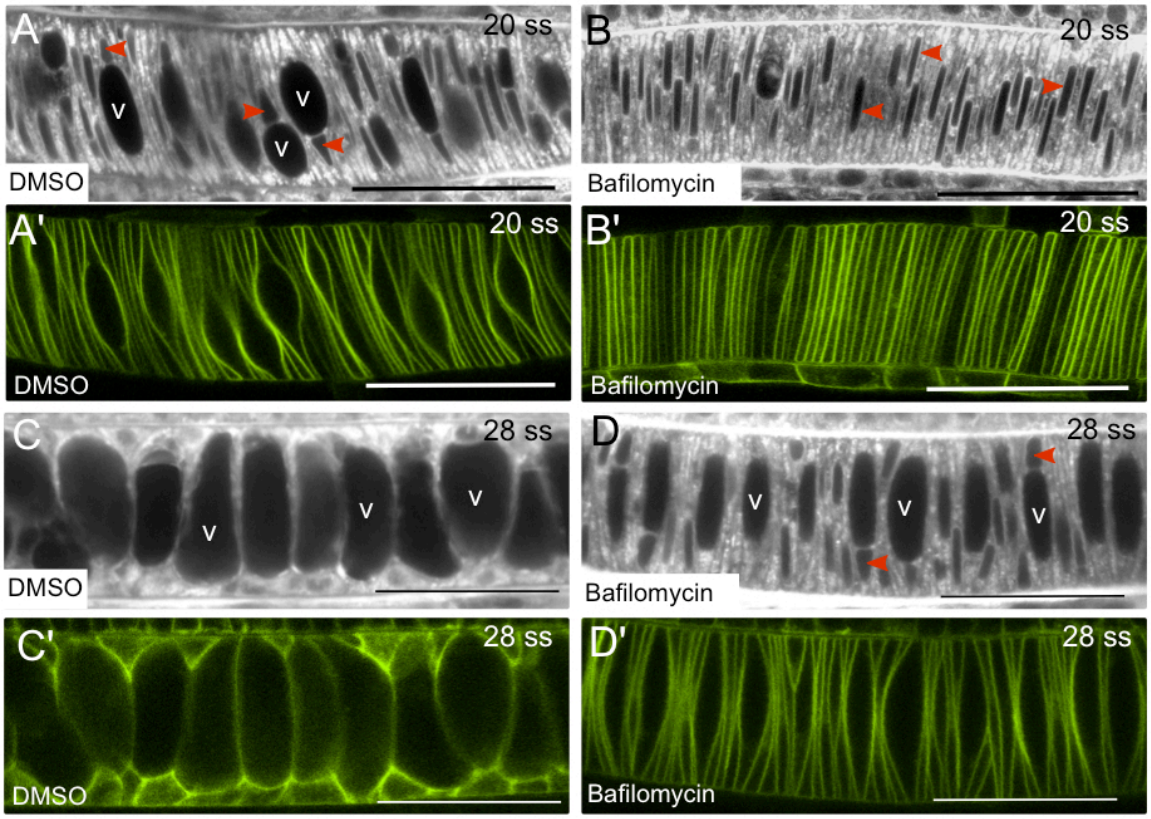


**Figure 16. Acidification is required for notochord vacuole biogenesis**

(A-D') Live confocal images of embryos treated with either DMSO or 500nM Bafilomycin to inhibit acidification for 4 hours before vacuole inflation until the 20-somite stage, visualized with MED (A, B) or membrane GFP (A', B'). Vacuoles fail to initiate inflation when the V-ATPase is inhibited with bafilomycin. Live confocal images of embryos treated with either DMSO or 500nM Bafilomycin for 4 hours, after vacuole formation had begun, until the 28-somite stage, visualized with MED (C, D) or membrane GFP (C', D'). v labels vacuoles inflating in DMSO control and red arrowheads label nuclei. When acidification is inhibited during vacuole inflation, vacuole growth is arrested and they do not expand further. This data shows that V-ATPase-dependent acidification is necessary for vacuole formation. Scale bars = 50 μm.

### 3.B.4. The notochord vacuole is a novel lysosome-related organelle

Because notochord vacuoles use late endosomal and lysosomal machinery as well as Rab32a that is known to traffic to LROs, we investigated whether lysosomal proteins localize to the vacuole (Granger et al., 1990). We generated transgenic fish expressing lysosomal-associated membrane protein 2 (Lamp2) and lysosomal-associated membrane protein 1 (Lamp1) under the control of a heat shock promoter. Through live confocal imaging, we observed Lamp2-GFP-positive lysosomes within the outer and inner cells of the notochord. Interestingly, Lamp1-RFP labeled punctae within the outer and inner cells as well as the vacuole membrane. Embryos expressing both transgenes showed some co-localizing punctae as well as Lamp1-RFP, but not Lamp2-GFP, on the vacuole membrane. This data shows that notochord vacuoles share some characteristics with lysosomes (Figure 17).

In order to test this further, we investigated the subcellular localization of Rab32a. GFP-Rab32a was expressed in transgenic embryos also expressing the vacuole marker Lamp1-RFP in triple transgenic fish – *Tg(rcn3:gal4); Tg(hsp:Lamp1-RFP)*; *Tg(UAS:GFP-rab32a)*. Live confocal imaging at 24 hpf revealed a precise co-localization of GFP-Rab32a with Lamp1-RFP on the vacuole membrane, but not in lysosomes where GFP-Rab32a was absent (Figure 17).

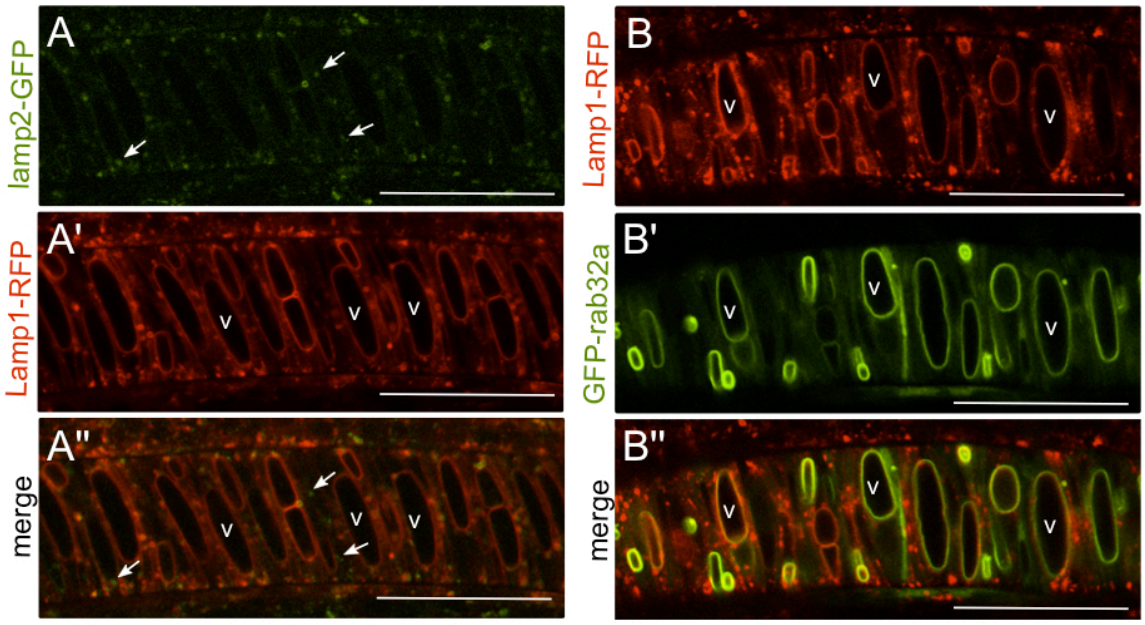


**Figure 17. The notochord vacuole is a unique lysosome-related organelle**

(A, A', A'') Live confocal image of a 20 ss transgenic embryo expressing lamp2-GFP and Lamp1-RFP; *Tg(hsp:lamp2-GFP); Tg(hsp:Lamp1-RFP)*. Lamp expression was induced at 16 ss. Lamp2 labels true lysosomes while Lamp1 labels both lysosomes and the vacuole membrane. (B, B', B'') Live confocal image of a 20 ss transgenic embryo expressing Lamp1-RFP and GFP-Rab32a; *Tg(hsp:Lamp1-RFP); Tg(rcn3:gal4); Tg(UAS:GFP-rab32a)*. Lamp1-RFP expression was induced at 16 ss. Rab32a localizes to the vacuole membrane, further demonstrating its role in vacuole formation and illustrating that notochord vacuoles share characteristics with lysosome-related organelles.

Many specialized cells contain lysosome-related organelles (LROs) that are similar to late endosomes or lysosomes and carry out specific functions. Given our data, we propose that the notochord vacuole is a novel LRO that functions as the main structural component of the notochord. The notochord vacuole, like previously characterized LROs, is a highly specialized post-Golgi structure that requires acidification for its formation, uses the LRO Rab32a, and contains at least one lysosomal membrane protein.

Unlike some LROs, the lumen of the notochord vacuole is not acidic. LysoTracker labeled lysosomes and other internal structures, but not the vacuole lumen in dissected notochords (Figure 18). Nevertheless, vacuoles require acidification for their biogenesis and maintenance. We reasoned that the pH gradient generated by the $H^+$-ATPase might be rapidly dissipated in the vacuole. This could be due to the presence of basic amino acids in the vacuole or, more likely, due to the activity of alkali/$H^+$ exchangers on the vacuole membrane (Casey et al., 2010). Transport of alkali ions into the vacuole lumen would then drive the movement of water, thereby leading to the swelling of the organelle. In this scenario vacuole integrity should be dependent on the activity of the $H^+$-ATPase. To test this hypothesis further, we treated dissected notochords from 20 ss embryos with bafilomycin. In agreement with our working model, confocal imaging revealed that after 2 hours of incubation with bafilomycin, vacuoles begin to fragment (Figure 18).

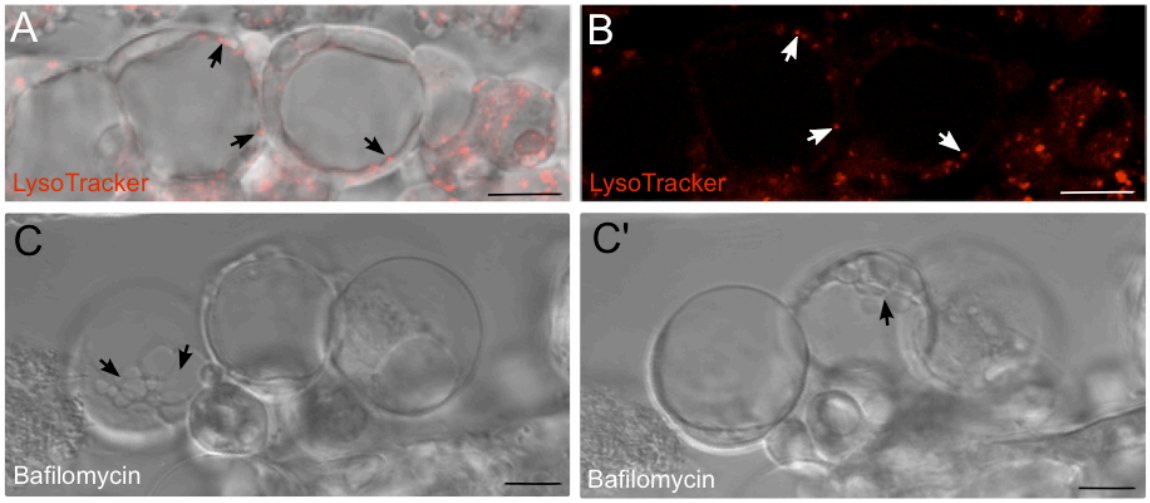


**Figure 18. The lumen of the vacuole is not acidic**

(A) Confocal image of cells from a dissected notochord of a 24 hpf embryo incubated with LysoTracker for 20 minutes. Bright field and LysoTracker merged. (B) LysoTracker alone. LysoTracker labels lysosomes in dissociated cells, but not the lumen of the vacuole. (C,C') Confocal images of cells from a dissected notochord of a 24 hpf embryo incubated with 1μM bafilomycin for 2 hours. Arrows indicate fragmenting vacuoles. The same cells are shown in (C) and (C') in different focal planes to show vacuole fragmentation. These data shows that while acidification is necessary for vacuole formation and maintenance, the vacuole itself is not acidic. Scale bars = 10 μm.

## *3.C. Discussion*

I have shown that notochord vacuole biogenesis requires clathrin-dependent biosynthesis, acidification by the vacuolar-ATPase as well as the vacuole-specific Rab32a. This molecular characterization of vacuole formation has raised several new and interesting questions. Here I will discuss some preliminary data addressing how single vacuoles form and how the notochord vacuoles inflate.

### 3.C.1. Multiple pre-vacuolar compartments coalesce to form a single vacuole per inner cell

Inner vacuolated cells of the zebrafish notochord always possess a single vacuole per cell, yet early during vacuole biogenesis there are many small pre-vacuolar compartments per cell. How do many small compartments come together to give rise to a single vacuole? Vesicles move throughout the cell along cytoskeletal elements like microtubules (Cole and Lippincott-Schwartz, 1995). If the microtubules in inner vacuolated cells are arranged in a radial array, then pre-vacuolar compartments can be trafficked along microtubules using the minus-end directed motor, dynein, to bring the compartments together to allow for their fusion.

In order to visualize the arrangement of pre-vacuolar compartments, transgenic fish expressing the vacuole marker Lamp1-RFP and the primary cilia marker Arl13b-GFP were analyzed at the 15 ss before vacuole inflation. We use Arl13b, a small GTPase localized to primary cilia (Cantagrel et al., 2008), as a

marker to identify the microtubule-organizing center found at the base of primary cilia. Thus, the microtubule-organizing center, the end point for minus-end directed traffic along microtubules, corresponds to the location where pre-vacuolar fusion would occur. Arl13b-GFP positive primary cilia and Lamp1-RFP positive pre-vacuolar compartments both localize along the midline of the notochord. In order to test if these structures are trafficked via dynein, embryos were soaked in media containing 25μM ciliobrevin D, a pharmacological inhibitor of dynein, before vacuole inflation until 24 hpf. Embryos treated with ciliobrevin D failed to form single vacuoles per cell and instead have many small fragmented vacuoles compared to DMSO controls (Figure 19).

This data suggests that dynein-dependent minus-end directed trafficking is important for single vacuole formation. Future studies will work to better understand this process using dominant negative components of the dynein complex to genetically disrupt dynein transport. Future work will also determine the machinery required for the fusion of the pre-vacuolar compartments.

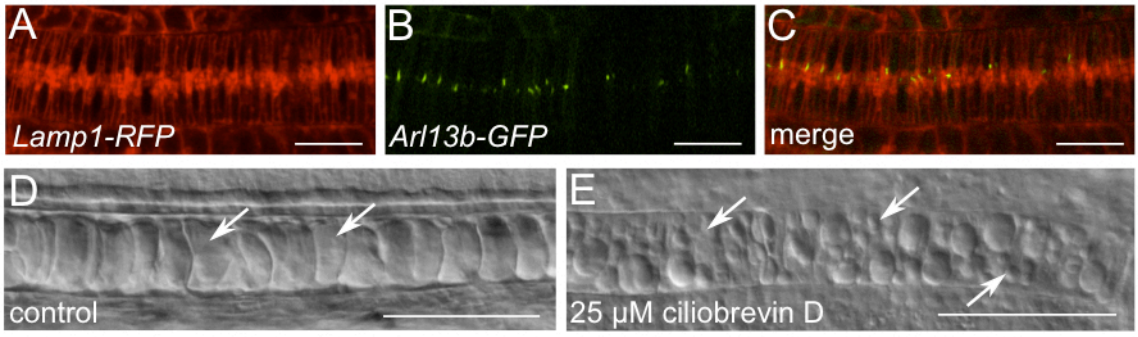


**Figure 19. Prevacuolar compartments coalesce to form a single vacuole**

(A, B, C) Live confocal image of a 15 s.s. transgenic embryo expressing Lamp1-RFP and Arl13b-GFP; *Tg(hsp:lamp1-RFP); Tg(βact:arl13b-GFP).* Pre-vacuolar compartments align at the midline of the notochord and colocalize with the primary cilia marker, Arl13b. (D) Live DIC image of a 24 hpf WT notochord. Asterisks label fully inflated vacuoles. (E) Live DIC image of a 24 hpf embryo treated with 25µM ciliobrevin D, an inhibitor of dynein, beginning at the time of vacuole formation. Asterisks label vacuoles that failed to coalesce properly. This data suggests that pre-vacuolar compartments are trafficked together via dynein to allow for coalescence. (A, B, C) scale bars = 20 µm. (D, E) scale bars = 100 µm.

### 3.C.2. Channels and transporters on the vacuole membrane transport osmolytes to the vacuole lumen

Our findings have raised additional questions about vacuole inflation. One area of interest is to determine the types of channels and transporters found on the vacuole membrane that allow for its rapid inflation. We found that notochord vacuoles are very sensitive to perturbations in the V-$H^+$-ATPase; therefore, it is highly likely that this pump is located on the vacuole membrane and transports protons into the lumen. However, we know that the lumen of the vacuole is not acidic. Thus, there must be a system that removes protons from the lumen of the vacuole at the same rate as the V-$H^+$-ATPase pumps them inside.

A possible candidate for the transporter moving osmolyte into the vacuole is a member of the sodium-dependent neutral amino acid transporter family, Slc38a8b. The Slc38 family of neutral amino acid transporters controls cellular osmolyte balance and therefore plays a role in regulating cell volume (Franchi-Gazzola et al., 2006). This gene is highly expressed specifically in the inner cell population of the notochord based on microarray analysis comparing the transcriptional profile of inner cells to that of the whole notochord, making it a good candidate for a vacuole transporter. Furthermore, *slc38a8b* morpholinos (Shestopalov et al., 2012) blocking translation or splicing injected into one-cell stage embryos produce embryos with smaller notochord vacuoles (Figure 20).

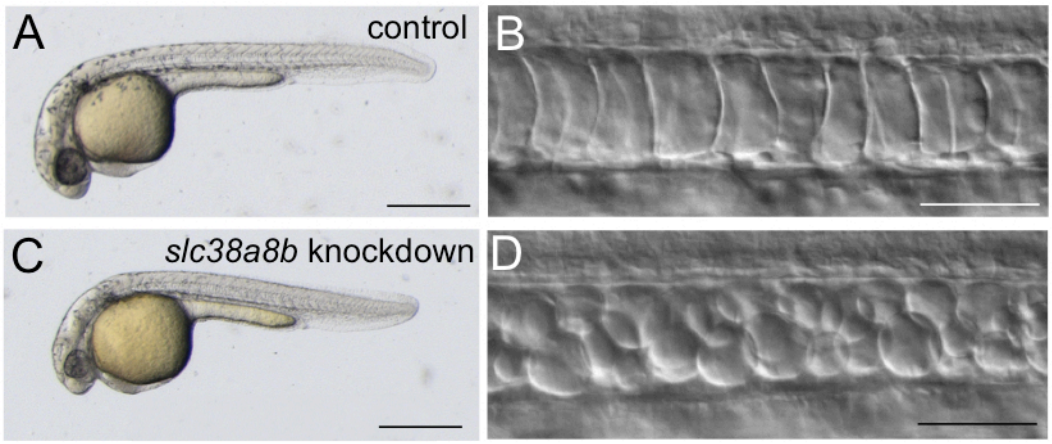


**Figure 20. slc38a8b morphants have smaller notochord vacuoles**

(A) Live whole mount image of a 30 hpf control embryo. (B) Live whole mount DIC image of a 30 hpf control embryo. (C) Live whole mount image of a 30 hpf embryo injected with *slc38a* morpholino at the 1-cell stage. (D) Live whole mount DIC image of a 30 hpf *slc38a8l* MO injected embryo with smaller vacuoles. This data suggests that Slc38a8b is necessary for vacuole inflation. (A, C) Scale bars = 500 μm. (B, D) Scale bars = 50 μm.

Slc38a8b is an orphan member of the Slc38 family of transporters categorized as either the System A subtype or System N subtype, depending on the type of amino acids transported (Mackenzie and Erickson, 2004). If Slc38a8b is a system A type transporter, it would preferentially transport nonpolar neutral amino acids such as alanine, valine, or leucine along with $Na^+$ into the vacuole. In this system, $Na^+/H^+$ exchangers would also be present on the vacuole membrane in order to remove the protons being pumped into the vacuole by the V-ATPase. If Slc38a8b is a system N type transporter, it would preferentially transport neutral amino acids with polar side chains such as asparagine or glutamine along with $Na^+$ into the vacuole and while transporting protons out of the vacuole (Figure 21). These polar amino acids could then function as an osmolyte to attract water into the lumen of the vacuole.

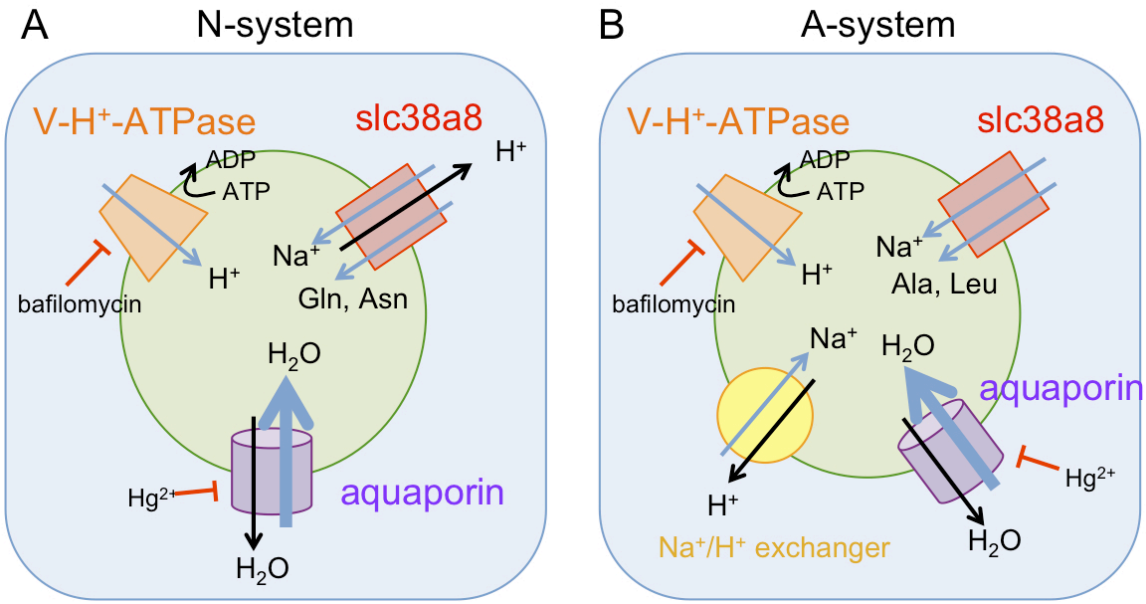


**Figure 21. Possible channels found on the vacuole membrane**

(A) Working model of N-system type transporter on the vacuole membrane. Slc38a8b would transport $Na^+$ and neutral amino acids with polar side chains like Gln and Asn into the vacuole while removing protons from the lumen of the vacuole. (B) Working model of A-system type transporter on the vacuole membrane. Slc38a8b would transport $Na^+$ and non-polar neutral amino acids like Ala and Leu into the vacuole and a $Na^+$ / $H^+$ exchanger would simultaneously remove protons from the lumen of the vacuole.

In order to determine if Slc38a8b is important for notochord vacuole inflation, I generated mutants using TAL effector nucleases (TALENs) (Miller et al., 2011). TALENs are made up of modular DNA-binding domains that can be customized to target nearly any gene in the genome. The DNA-binding domains are fused to the endonuclease Fok1, which generates a double stranded break in the DNA. Through error-prone repair mechanisms the double-stranded break is repaired, often generating frameshifts or introducing stop codons. I have generated two *slc38a8b* mutant alleles, one with a four amino acid change (*slc38a8b*$^{pd1106}$) and one with a seven-nucleotide deletion that generates a frameshift (*slc38a8b*$^{pd1105}$). Initial characterization of the frameshift mutant *slc38a8b*$^{pd1105}$ shows no obvious vacuole phenotype compared to wildtype siblings at 24 hpf. This could be due to the fact that many proteins important for early development are maternally provided to the zygote. Therefore, raising mutant fish to test maternal-zygotic mutants for phenotypes is necessary. Alternatively, the mutant phenotype may not be non-inflated vacuoles, but perhaps vacuoles that inflate less efficiently. Therefore, it will be important to analyze if the kinetics of vacuole inflation are disrupted in mutant embryos.

Future studies will be aimed at identifying the type of amino acids transported by Slc38a8b *in vivo* as well as determining if Slc38a8b is localized to the notochord vacuole membrane and if it plays a role in vacuole inflation. Alternatively, other positively charged small molecules might serve a similar role in order to draw water into the vacuole.

# 4. Post-embryonic roles of the zebrafish notochord

I have shown molecular requirements for notochord vacuole formation, but the structural function of these organelles remained unclear. Studies have suggested the notochord vacuoles are important for embryo elongation but this has not been addressed *in vivo*. Here I will discuss the structural post-embryonic roles for the notochord vacuoles.

## *4.A. Introduction*

Structurally, the notochord acts as a hydrostatic skeleton for the embryo for several weeks before bone formation. This axial support is crucial for locomotion in embryos that develop externally such as fish and amphibians in order to evade predation. The pressure exerted from the inflating notochord vacuoles on the constricting peri-notochordal basement membrane gives this structure its flexural stiffness and mechanical strength (Koehl et al., 2000). Notochords dissected from *Xenopus* embryos are osmotically active structures and undergo drastic shape changes in hypotonic and hypertonic conditions (Adams et al., 1990). Similarly, osmotic activity was also seen in dissociated cells from canine intervertebral discs (Hunter et al., 2007). It has been suggested that the pressure generated within the notochord from the inflating vacuoles acts as a morphogenic force that elongates and straightens the embryo along the anterior-posterior axis. However, this has only been shown *ex vivo* and in modeled notochords and *in vivo* data supporting this model is still lacking.

## *4.B. Results*

Elegant *ex vivo* and modeling experiments suggested that the inflation of notochord vacuoles may drive the straightening and elongation of the vertebrate embryo along the rostral-caudal axis. To directly test the role of notochord vacuoles in embryonic zebrafish axis development we targeted vacuole formation and differentiation of the inner and outer cell layers.

### 4.B.1. Notochord vacuoles elongate the embryo along the anterior-posterior axis

Previous work showed that ubiquitous expression of the notch intracellular domain (NICD) during notochord differentiation causes the notochord to adopt an entirely outer sheath cell fate at the expense of the inner cell fate (Yamamoto et al., 2010). To inhibit vacuolated cell differentiation, we expressed NICD in a notochord-specific manner using the *rcn3:gal4* driver (Scheer and Campos-Ortega, 1999). DIC imaging revealed that the majority of the notochord vacuoles failed to form, with only a few vacuoles detectable in the anterior portion of the notochord, a result consistent with previous work (Latimer and Appel, 2006). The body lengths of these larvae were measured from 1 dpf to 5 dpf and compared to non-expressing siblings (Figure 22). At all time points assessed, NICD-expressing fish were on average 35% shorter than their WT siblings after 1 dpf ($p < 0.0001$ at all time points. $n = 16$ for NICD. $n = 37$ for WT at 5 dpf). Rab5-mediated internalization of the notch receptor is important for proper notch signaling and accumulation of the notch receptor in early endosomes results in

increased notch signaling (Vaccari et al., 2008). We analyzed larvae expressing DN mCherry-Rab5c (Clark et al., 2011) in the notochord before differentiation of inner and outer cell types using the *rcn3* early driver. DN mCherry-Rab5-expressing embryos phenocopied embryos expressing NICD and formed very few vacuoles (Figure 19). At 1-5 dpf, DN mCherry-Rab5c fish were on average 18% shorter than their WT siblings ($p < 0.0001$ at all time points. n = 48 for DN Rab5c. n = 84 for WT at 5 dpf). This defect was only seen when DN mCherry-Rab5c was expressed before differentiation. Expression in the inner cells after differentiation and vacuole formation, using the *SAG214A:gal4* driver, had no effect on vacuole integrity or body axis length (n = 46 for DN Rab5c. n = 49 for WT at 5 dpf) (Figure 22).

We next investigated the role of inner cell vacuoles in body axis elongation in a more vacuole-specific manner using a mosaic approach. As shown above, in notochord cells expressing DN GFP-Rab32a vacuoles were fragmented. Fish expressing DN GFP-Rab32a in a mosaic fashion were on average 8% shorter than their WT siblings ($p < 0.0001$ at all time points. n = 73 for DN Rab32a. n = 84 for WT at 5 dpf) (Figure 22). As a control, larvae expressing DN mCherry-Rab11a in the notochord showed no vacuole formation defect and were not significantly shorter than their siblings (Figure 22). The same was also seen with DN mCherry-Rab7a (data not shown).

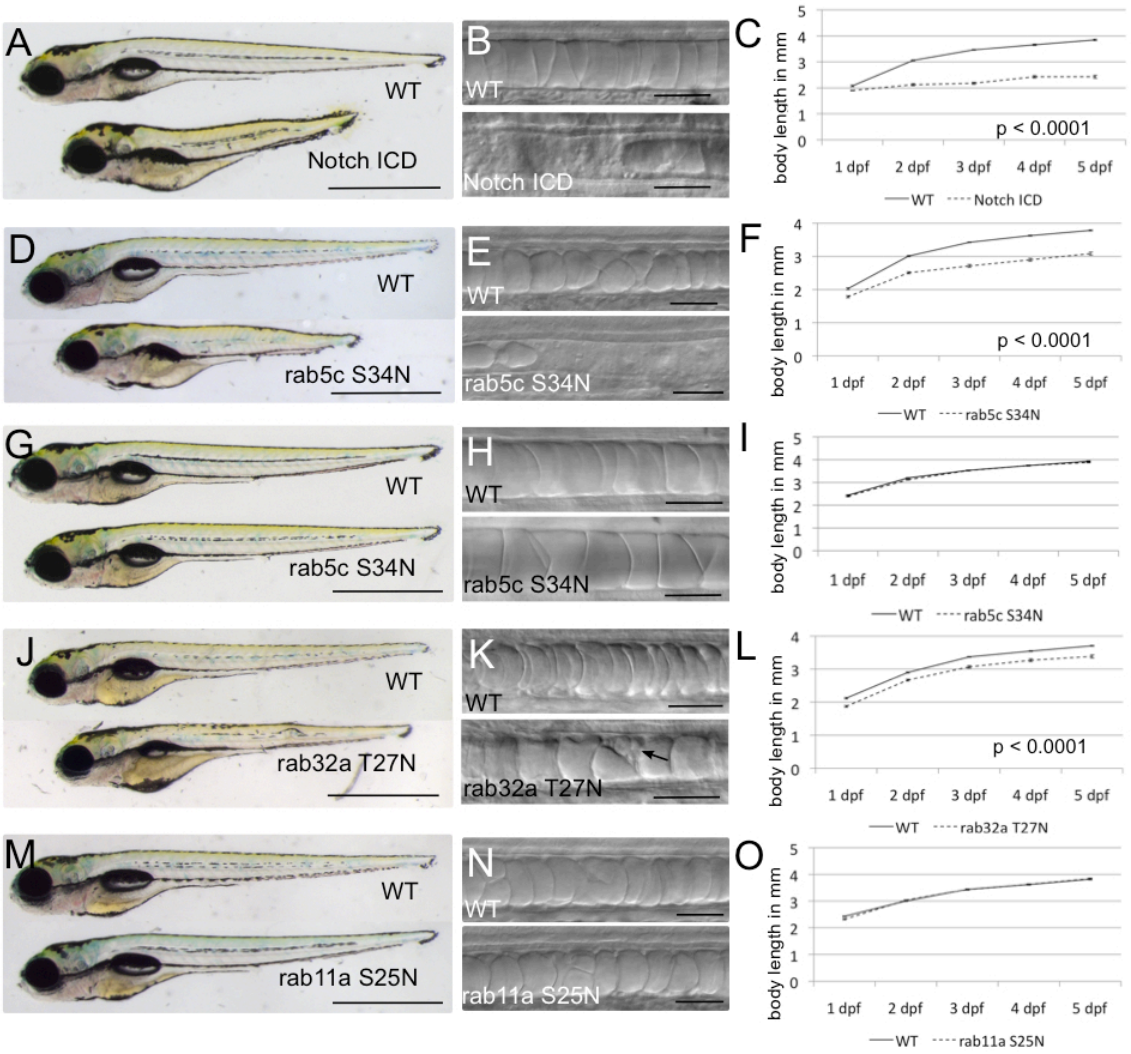


**Figure 22. Notochord vacuoles are required for elongation of the embryonic axis**

Figure 22**. Notochord vacuoles are required for elongation of the embryonic axis**

(A) Whole-mount image of 5 dpf WT larva expressing NICD in the notochord; *Tg(rcn3:gal4); Tg(UAS:myc-Notch1a-intra)*. (B) Live DIC images of notochords in 48 hpf WT and NICD-expressing larvae. (C) Body length in mm from 1 dpf to 5 dpf. $p < 0.0001$ at all time points. n = 16 in NICD. n = 37 for WT at 5dpf. (D) Whole-mount image of 5 dpf WT and DN mCherry-Rab5-expressing larvae from the early *rcn3* promoter; *Tg(rcn3:gal4); Tg(UAS:mCherry-rab5c-S34N)*. (E) Live DIC image of 24 hpf WT and DN mCherry-Rab5 notochords. (F) Body length in mm from 1 dpf to 5 dpf. $p < 0.0001$ at all time points. n = 48 for Rab5cDN. n = 84 for WT at 5 dpf. (G) Whole-mount image of 5 dpf WT and DN mCherry-Rab5-expressing larvae from the late *SAG214* driver; *Gt(SAGFF214A:gal4); Tg(UAS:mCherry-rab5c-S34N)*. (H) Live DIC image of 48 hpf WT and rab5cDN notochords. (I) Body length in mm from 1 dpf to 5 dpf. No significant difference. n = 46 for Rab5cDN. n = 49 for WT at 5 dpf. (J) Whole-mount image of 5 dpf transgenic *Tg(rcn3:gal4)* larvae injected with UAS:GFP-rab32a-T27N DNA for mosaic expression. WT is non-expressing, injected sibling. (K) Live DIC image of 24 hpf WT and DN GFP-Rab32a notochords. Arrows indicate expressing cells with fragmented vacuoles. (L) Body length in mm from 1 dpf to 5 dpf. $p < 0.0001$ at all time points. n = 73 for Rab32aDN. n = 84 for WT at 5 dpf. (M) Whole-mount image of 5 dpf WT and DN mCherry-Rab11a larvae; *Tg(rcn3:gal4); Tg(UAS:mCherry-rab11a-S25N)*. (N) Live DIC image of 24 hpf WT and DN mCherry-Rab11a notochords. (O) Body length in mm from 1 dpf to 5 dpf. No significant difference. n = 54 for Rab11aDN. n = 48 for WT at 5 dpf. These data show that inflated vacuoles elongate the embryo along the anterior-posterior axis. (A, D, G, J, M) Scale bars = 1mm. (B, E, H, K, N) Scale bars = 50 μm. (C, F, I, L, O) Error bars = s.e.m.

Thus, when notochord vacuoles are absent or fragmented the body axis is shorter but straight, with normal body curvature. We conclude that notochord vacuoles are required for elongation of the embryonic body axis but not straightening.

### 4.B.2. Notochord vacuoles are necessary for proper spine morphogenesis

Work in various animal models has shown that notochord cells, including vacuolated cells, become part of the nucleus pulposus within the intervertebral discs as the notochord is replaced by the spine (Walmsley, 1953). We next investigated the role of notochord vacuoles in spine morphogenesis in young juvenile fish. Short larvae without notochord vacuoles were raised for 21 days post fertilization (21dpf), after which spine morphology was analyzed using the vital dye calcein (Du et al., 2001). In juveniles (21 dpf) that expressed DN mCherry-Rab5c before vacuole differentiation, using the *rcn3* promoter, the body axis appeared straight from a lateral view. By contrast, it was dysmorphic when viewed dorsally. Live imaging with calcein revealed that the spine was severely kinked and wavy with mature and fully formed vertebrae (Figure 23). In contrast, juveniles that expressed DN mCherry-Rab5c after differentiation had normal spines. Fish expressing NICD in the notochord fail to inflate their swim bladders and die because they are unable to feed, and therefore could not be analyzed for spine morphogenesis.

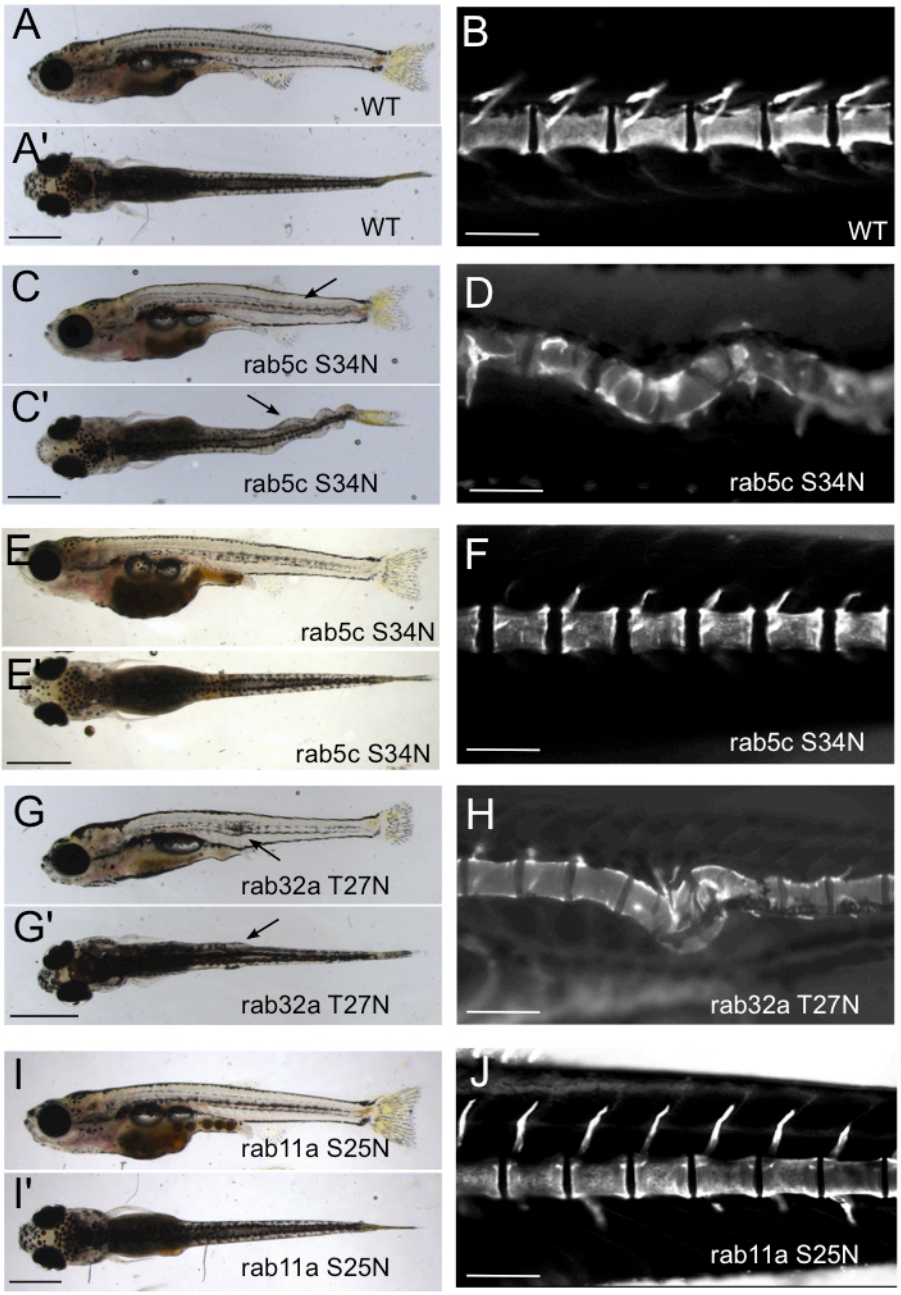


**Figure 23. Notochord vacuoles are necessary for proper spine morphogenesis**

Figure 23**. Notochord vacuoles are necessary for proper spine formation**

(A, A') Whole-mount image of a 21 dpf WT fish. Lateral and dorsal views. (B) Live image of calcein stained 21 dpf WT spine. (C, C') Whole-mount image of a 21 dpf DN-mCherry-Rab5c transgenic fish using the early driver *rcn3*; *Tg(rcn3:gal4); Tg(UAS:mCherry-rab5c-S34N)*. Lateral and dorsal views. Arrows indicate body kinks. (D) Live image of calcein stained 21 dpf spine of a DN mCherry-Rab5c transgenic fish. (E, E') Whole-mount image of a 21 dpf DN mCherry-Rab5 transgenic fish using the later driver *SAG214A*; *Gt(SAGFF214A:gal4); Tg(UAS:mCherry-rab5c-S34N)*. Lateral and dorsal views. (F) Live image of calcein stained spine of a 21 dpf DN mCherry-Rab5 transgenic fish. (G, G') Whole-mount image of a 21 dpf mosaic DN GFP-Rab32a fish; *Tg(rcn3:gal4)* embryos injected with UAS:GFP-rab32a-T27N DNA. Lateral and dorsal views. Arrows indicate body kinks (H) Live image of calcein stained spine of a 21 dpf DN GFP-Rab32a-expressing fish. (I, I') Whole-mount image of a 22 dpf transgenic DN mCherry-Rab11a fish; *Tg(rcn3:gal4); Tg(UAS:mCherry-rab11a-S25N)*. Lateral and dorsal views. (J) Live image of calcein stained spine of a 22 dpf DN mCherry-Rab11a transgenic fish. These data show that notochord vacuoles are important for the process of spine morphogenesis. (A, C, E, G, I) Scale bars = 1 mm. (B, D, F, H, J) Scale bars = 200 μm.

In order to more specifically determine the role of the vacuole in spine morphogenesis, we analyzed fish expressing DN GFP-Rab32a mosaically. *rcn3:gal4* embryos injected with UAS:GFP-rab32a-T27N DNA were raised until 21dpf and then their spines were visualized with the vital dye calcein (Figure 23). These fish also showed body and spine kinks, although less than fish expressing DN mCherry-Rab5c throughout the notochord. Juveniles that expressed DN mCherry-Rab11a, which does not affect the vacuole, showed no body kinks or spine defects (Figure 23), indicating that not all DN rabs affect spine formation. These data indentify a novel role for the notochord vacuoles in spine morphogenesis.

## *4.C. Discussion*

I have shown that notochord vacuoles are important for elongating the embryo along the anterior-posterior axis and that fully inflated vacuoles are critical for straight spine formation. Here I will discuss why the cellular architecture of one vacuole per cell and the tissue architecture of two rows of vacuolated cells seems to be the most efficient ways of elongating the axis and providing a rigid scaffold for bone formation. I will also discuss preliminary data further investigating the role of notochord vacuoles in spine development.

### 4.C.1. Cellular architecture – what makes a single vacuole more efficient than multiple vacuoles

When vacuole formation or maintenance is disrupted, there are many small fragmented vacuoles in a given inner cell and these cells occupy less

volume than neighboring cells with single fully inflated vacuoles. Moreover, multiple small vacuoles also allow for more irregular cell shapes. Thus, the smaller cellular volume and higher deformability allows cells to pack more tightly into the column of the notochord sheath. In notochords where the inner cells are packed more densely and the overall inner cell number stays the same, the resulting embryo is shorter in the anterior-posterior axis.

This can been seen in *vps18* mutants who have fragmented vacuoles in many of the inner cells at 5 dpf (Figure 24). In cross section more inner vacuolated cells are seen in a given plane and the vacuoles are smaller overall. The cells are packed more densely in the notochords of these mutants and the larvae are shorter than wild-type siblings at 5 dpf.

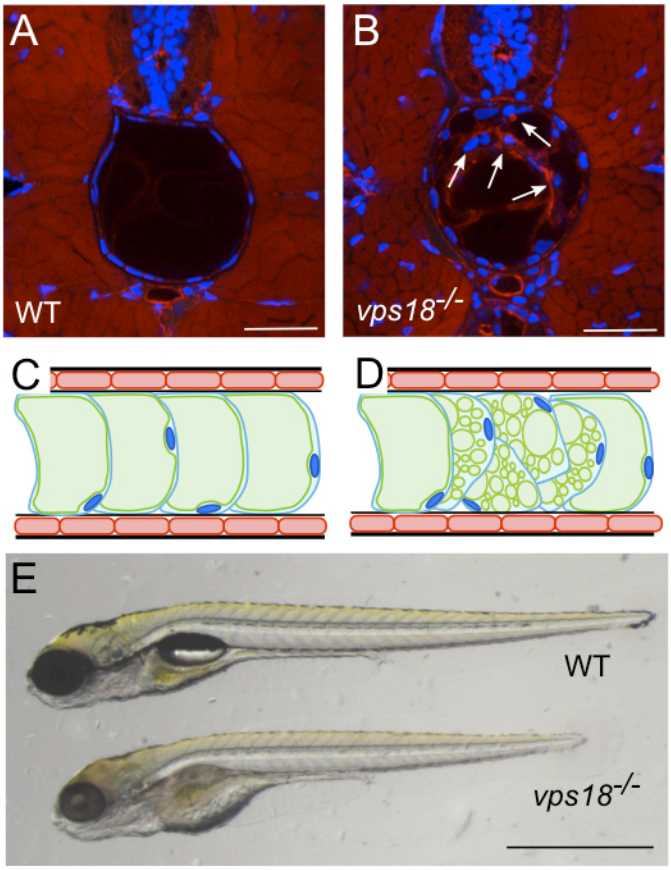


**Figure 24. Fragmented vacuoles leads to cells that are packed more densely, resulting in larvae that are shorter**

A) Confocal image of a cross section of a 5 dpf WT larvae. B) Confocal image of a cross section of a 5 dpf *vps18*$^{hi2499aTg}$ mutant larva. Arrows label the nuclei of multiple inner vacuolated cells. Cross sections were stained with phalloidin in red and DAPI in blue. C) Cartoon depicting normal inner vacuolated cell density. D) Cartoon depicting the cellular deformation and dense packing of inner cells with fragmented vacuoles. E) 5 dpf WT and shortened *vps18*$^{hi2499aTg}$ mutant larvae. Scale bars: (A, B) 50 μm. (E) 1 mm.

Our work has also shown that fragmentation of vacuoles results in a kinking of the spine as it develops. Because the fluid within the vacuoles, water, is incompressible, the fully inflated vacuoles in the notochord provide a stable structure that is able to resist the compressive forces of the vertebrae as they grow concentrically around the notochord during spine formation. This concept can be illustrated by thinking of a bag filled with sand compared to a bag filled with large pebbles. The bag of sand can more readily be deformed because the sand grains are tiny and can move past one another within the bag. The bag full of large pebbles, however, cannot be deformed as much in response to a given load because it is more difficult for the large pebbles to rearrange. When multiple small vacuoles are present, compression from growing vertebrae results in a deformation of the overall notochord shape. This occurs because multiple small vacuoles can be displaced and are able to slide past one another within the inner cells of the notochord while single large vacuoles cannot.

### 4.C.2. Tissue architecture – what determines the organization of two rows of vacuolated cells?

Along the length of the anterior-posterior axis of the notochord, inner vacuolated cells are organized in rows of two. When viewed dorsally, the two rows of inner vacuolated cells are aligned such that two vacuoles are not exactly side-by-side, but are slightly offset, with one row being more anterior than the other.

Two rows of vacuolated cells filling up the notochord allows for the vacuoles to be a manageable size. If there were instead a single row of large vacuolated cells that occupied the width of the notochord, the vacuoles would be nearly 80 μm in diameter. This would require the vacuoles to be 2 times larger in diameter and 8 times larger in volume. With 40 μm in diameter at their widest point, notochord vacuoles are the largest known fluid-filled organelle. Perhaps this is nearing the physiological limit for how large a vacuole can be in terms of membrane stability and capacity to transport osmolytes and water within a short developmental window.

The notochord architecture with two rows of vacuolated cells can also be explained by considering the rate of vacuole inflation and the rate of cellular rearrangement required for notochord expansion. As described previously, the notochord begins as a rod of cells in a line like a stack of coins due to the intercalation of chordamesoderm cells that form the notochord during late gastrulation (Glickman et al., 2003; Sepich et al., 2005). The outer sheath cells then leave the midline of the notochord to fully enclose the vacuolated layer in an epithelial-like sheath while the inner cells rearrange and inflate their characteristic vacuoles. The notochord develops in an anterior to posterior gradient; therefore, inner vacuolated cell rearrangement and rate of vacuole inflation are coupled temporally. That is, the inner vacuolated cells are rearranging and inflating simultaneously in discrete regions of the notochord in a wave that starts anterior and moves posteriorly.

Here I propose three hypothetical notochord arrangements: a hypothetical notochord with a single row of vacuolated cells, the actual zebrafish notochord with two rows of vacuolated cells, and a hypothetical notochord with three rows of vacuolated cells (Figure 25). In the first hypothetical notochord where there is only a single row of vacuolated cells, a low rate of cellular rearrangement is required during vacuole inflation because the inner cells are already present in a single file arrangement. In this notochord the vacuoles must also have a rapid inflation rate, otherwise there would be an opportunity for the vacuolated cells to settle and pack next to one another during inflation. In an actual larval zebrafish notochord there are two rows of vacuolated cells. This organization requires a higher rate of cellular rearrangement than the previous scenario so that two vacuolated cells can move to occupy the same plane in cross-section, but requires a slower inflation rate. Finally, in a hypothetical notochord with three rows of vacuolated cells there must be an even higher rate of cellular rearrangement of inner cells during vacuole inflation to allow for three cells to migrate and occupy the same plane in cross-section. In this type of notochord the vacuoles must also inflate much more slowly in order to allow for the packing of three vacuoles per plane to take place. Therefore, given our three scenarios of notochord structure, the ultimate organization that balances vacuole inflation rate with cellular rearrangement is favored (Figure 25). Future work can test this hypothesis by adjusting the activity of channels on the vacuole membrane and examining the resulting inner vacuolated cell arrangement.

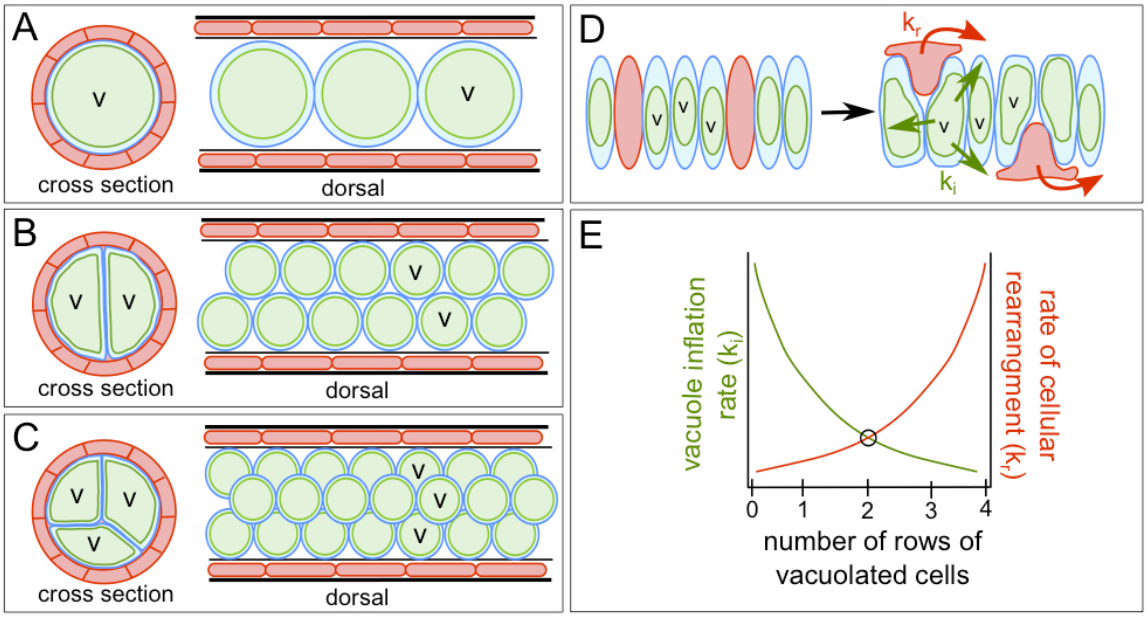


**Figure 25. Proposed model of relationship between rate of vacuole inflation and rate of cellular rearrangement**

A) Cartoons of cross section and dorsal views of a hypothetical notochord consisting of a single row of vacuolated inner cells. B) Cartoons of cross section and dorsal views of a zebrafish notochord consisting of two rows of inner vacuolated cells. C) Cartoons of cross section and dorsal views of a hypothetical notochord consisting of three rows of vacuolated inner cells. D) Cartoon depicting the organization of the notochord before vacuole inflation as a single stack of intercalated sheath and vacuolated cells. During development the sheath cells leave the midline to surround the vacuolated cells at a rate of $k_r$ while the vacuoles inflate simultaneously at a rate of $k_i$. E) Graph of the relationship between the rate of cell rearrangement ($k_r$) and rate of vacuole inflation ($k_i$). We hypothesize a balance between the two rates is seen with an organization of two rows of vacuolated cells.

### 4.C.3. What is the role of the notochord in spine development?

Previously, I hypothesized that a single fluid-filled vacuole per inner cell is the most effective way of resisting the compressive forces of concentrically growing vertebrae. We have shown that fragmented vacuoles or loss of vacuoles leads to kinks or curvatures of the spine, but evidence of a spine kink occurring where a vacuole has been disrupted is still lacking.

In order to directly test if disrupting vacuoles causes local spine kinks, I generated a BAC construct that expresses nitroreductase in the inner cell population. Nitroreductase (NTR) is an enzyme that converts the prodrug metronidazole (Mtz) into a cytotoxic byproduct. Both NTR and Mtz are innocuous to cells on their own, but in combination this system can be used to create tissue specific cell death (Curado et al., 2008). Inner cell-specific NTR was expressed in a mosaic fashion by injecting cyb5r2:mCherry-NTR DNA into a transgenic line expressing soluble GFP in the inner cells and mCherry-NTR in osteoblasts (Figure 26). Mtz was added to the water of larvae before bone formation at either 11 dpf or 14 dpf. 24 hours after Mtz treatment the fish were live imaged using confocal microscopy to verify cell death. In NTR injected fish, mCherry positive inner cells looked sick and their vacuoles had completely deflated compared to non-mCherry expressing inner cells nearby. mCherry-NTR expressing cells in fish not treated with Mtz had fully inflated notochord vacuoles, and control fish treated with just Mtz also had fully inflated notochord vacuoles.

Fish were raised until 3 or 4 weeks of age when vertebrae are fully developed and their spines were imaged using confocal microscopy (Figure 26). Preliminary data shows several fish develop kinks in their spines and surprisingly, vertebral fusions as well. However, at the later timepoints examined, mCherry-NTR positive inner vacuolated cells were seen in several fish with fully inflated vacuoles at 3 and 4 weeks post fertilization. This could be due to an incomplete ablation of cells with Mtz treatment allowing for the cells to recover, or outer cells carrying the BAC divided to give rise to new vacuolated cells after Mtz treatment and only turned on mCherry-NTR expression after transitioning to the inner cell fate. Future work will be directed at ensuring cell death through optimizing the timing and duration of Mtz treatment as well as following individual fish after treatment through the stages of bone formation in order to correlate vacuolated cell death with spine kinks.

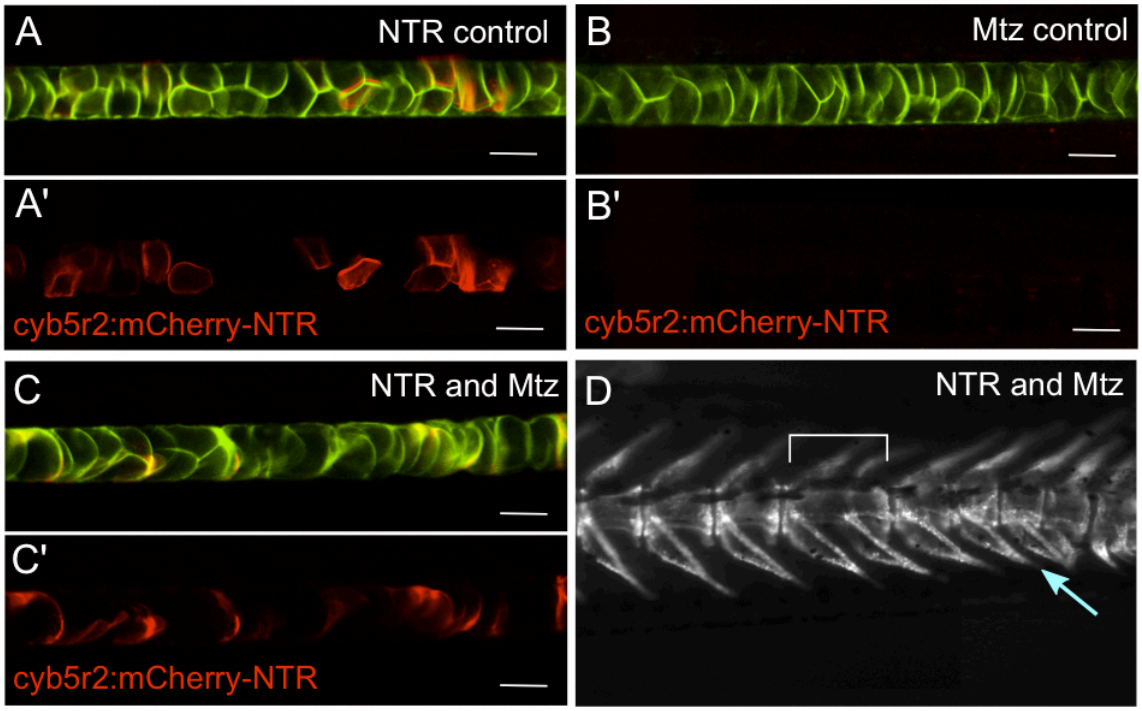


**Figure 26. Genetic ablation of notochord vacuolated cells**

Transgenic embryos expressing soluble GFP in the inner cells were injected with the BAC cyb5r2:mCherry-NTR to mosaically express NTR specifically in the inner cells of the notochord. (A, A') Live confocal image of a 13 dpf control fish injected with cyb5r2:mCherry-NTR. (B,B') Live confocal image of a 13 dpf fish treated with Mtz at 11 dpf. (C,C') Live confocal image of a 13 dpf fish injected with cyb5r2:mCherry-NTR and treated with Mtz at 11 dpf. (A,B,C) merge of inner cell cytosolic GFP and mCherry-NTR. (A', B', C') mCherry-NTR alone. (D) Live confocal image of a 30 dpf fish expressing NTR mosaically in the notochord and treated with Mtz at 11 dpf. Spine visualized using the transgenic marker osx:mCherry-NTR. Bracket indicates vertebral fusion. Arrow indicates slight curvature. Scale bars = 50 μm.

# 5. Discovering new molecular players in vacuole formation

Forward genetic screens are often used to uncover novel molecular components in a particular process. To identify new genes involved in notochord vacuole biogenesis and spine formation, we have obtained mutants with shortened body axis and scoliosis of the spine. Once such mutant, *dwarf*, will be the subject of this chapter. I will characterize the *dwarf* mutant phenotype as well as describe my progress thus far in mapping the mutation.

## *5.A. Introduction*

To carry out a traditional 3-generation forward genetic screen, male zebrafish are mutagenized with ethylnitrosourea (ENU) to randomly causes point mutations in the male's pre-meiotic germ cells. The mutagenized males are then crossed to a wildtype female to generate $F_1$ progeny that are heterozygous for the novel mutation. $F_1$ males are crossed again to wildtype females to generate several $F_2$ families. The $F_2$ families are half heterozygous for the novel mutation and half homozygous wildtype. Lastly, siblings within a single family are randomly crossed together and the $F_3$ progeny are analyzed for a phenotype of interest (Patton and Zon, 2001).

After a phenotype of interest is isolated, the phenotype must then be linked to a region of the genome on a specific chromosome and the mutation mapped to a single locus. This process of mapping is carried out by identifying polymorphisms that are closely linked to the mutant phenotype. In order for the

markers to be useful for this type of mapping, both parents need to be heterozygous for the marker. Physical proximity to the mutant locus is determined by looking at the number of recombination events seen across many single mutant embryos at a given marker or polymorphism. That is, fewer recombinants suggests that the mutation causal for the phenotype is close by. Once an interval of homozygosity is established (a region with zero recombinants for useful markers) candidate genes are picked and analyzed to determine which gene is causal for the mutant phenotype (Leshchiner et al., 2012).

## *5.B. Results*

*dwarf* mutants were isolated from a forward genetic screen because of a shortened body axis and curved vertebral column as adults. Because we have seen shortened axis and spine kinks from notochord vacuole defects, we investigated whether the notochord was the source of these phenotypes in the *dwarf* adult. At 2 dpf DIC imaging shows the vacuoles of *dwarf* mutants appear smaller, more rounded, and sometimes fragmented compared to wildtype siblings (Figure 27). Live imaging with the vital dye MED shows that this phenotype persists and is even more severe at 3 dpf. At 5 dpf *dwarf* mutant ($n = 42$) and wildtype siblings were measured ($n = 35$) from nose to tail and the mutants showed a modest, yet significant, 8.5% decrease in body length ($p < 0.0001$) (Figure 27).

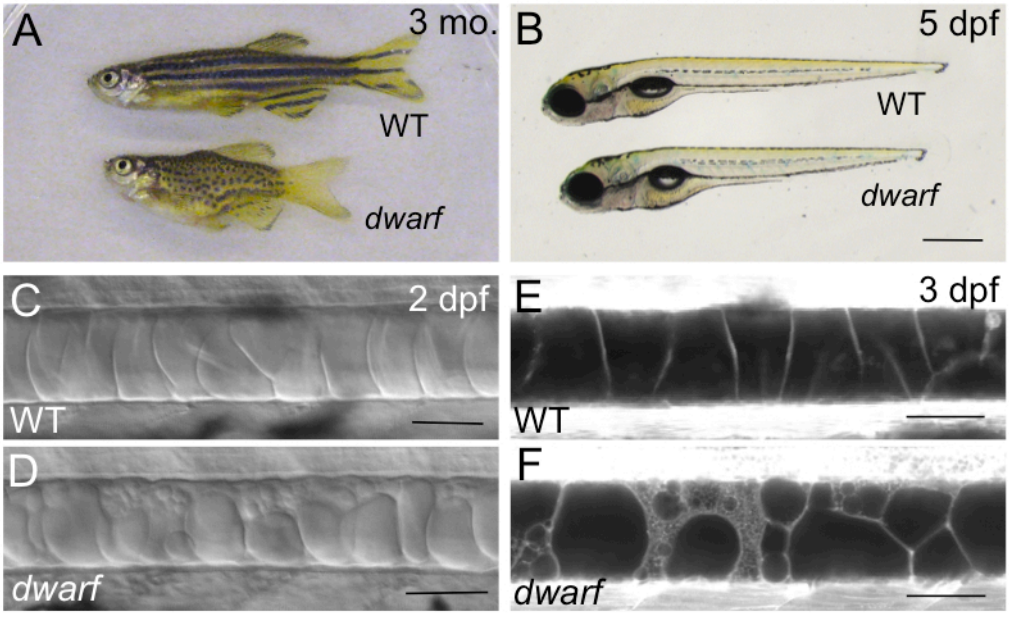


**Figure 27. Dwarf mutants have a shortened body axis and fragmented notochord vacuoles**

(A) Whole mount image of 3 month-old *dwarf* mutant (bottom) and wildtype sibling (top). *dwarf* mutants have scoliosis and are much shorter than wildtype siblings. (B) Whole mount image of 5 dpf, *dwarf* mutant (bottom) and wildtype sibling (top). *dwarf* larvae are 8.5% shorter than wildtype siblings. (C) Live DIC image of a 2 dpf wildtype sibling notochord. (D) Live DIC image of a 2 dpf *dwarf* mutant notochord with fragmented and smaller vacuoles. (E) Live confocal image of a 3 dpf wildtype sibling notochord visualized with MED. (F) Live confocal image of a 3 dpf *dwarf* mutant notochord with fragmented vacuoles visualized with MED. (B) Scale bar = 500 μm. (C – F) Scale bars = 50 μm.

The vertebral columns of juvenile *dwarf* mutants were imaged live using the vital dye calcein. At 21 dpf the spines of *dwarf* mutants showed dramatic dorsal, ventral, and lateral kinks compared to wildtype siblings (Figure 28). As adults these curvatures and kinks become more pronounced as seen using alizarin red in a skeletal prep of 3-month-old mutants and wildtype siblings. Importantly, the notochords of *dwarf* mutant larvae are relatively straight and the kinks do not become apparent until later stages of vertebral bone growth. This data supports the notion that fully inflated notochord vacuoles are important to act as a rigid scaffold during bone deposition to allow for straight spine formation. Interestingly, in adult *dwarf* mutants there were no vertebral fusions seen with any of the other spine defects, suggesting that notochord vacuoles are not responsible for the segmented patterning of vertebrae.

We took a whole exome sequencing approach in order to map the *dwarf* mutation. Genomic DNA was isolated from 30 mutant and 30 wildtype sibling embryos and sequenced using an Illumina HiSeq 2000 platform (Ryan et al., 2013). Linkage analysis was performed using the openly available mapping software SNPTrack in order to find single nucleotide polymorphisms (SNPs) and regions of homozygosity (Leshchiner et al., 2012). The *dwarf* mutation was mapped to a region on chromosome 22. I am currently working to narrow down this region in order to find a small interval of homozygosity so that I can identify candidate genes in the area.

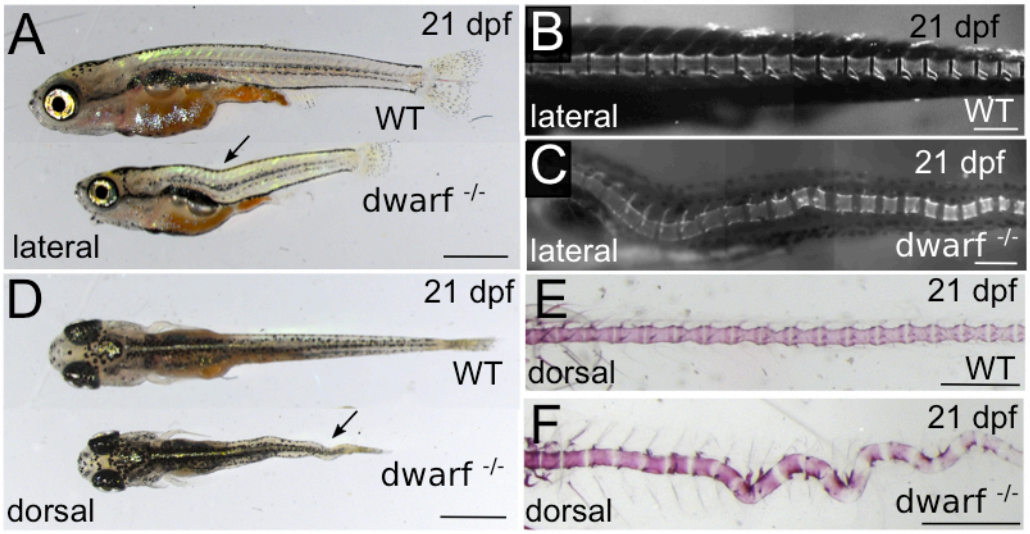


**Figure 28. *dwarf* juveniles have severe scoliosis of the spine**

(A) Whole mount lateral view of a *dwarf* mutant (bottom) and wildtype sibling (top) at 21 dpf. Arrow indicates spine curvature in mutant. (D) Live whole mount confocal lateral view of a wildtype spine at 21 dpf visualized with the vital dye calcein. (E) Live whole mount lateral view of a *dwarf* mutant spine at 21 dpf dyed with calcein. (F) Whole mount dorsal view of a *dwarf* mutant (bottom) and wildtype sibling (top) at 21 dpf. Arrow indicates spine curvature in mutant. (G) Dorsal view of a wildtype spine stained with alizarin red at 21 dpf. (H) Dorsal view of a dwarf mutant spine stained with alizarin red at 21 dpf. (A, B) scale bars = 50 μm. (C, F) scale bars = 1 mm. (D, E) scale bars = 250 μm. (G, H) scale bars = 500 μm.

## *5.C. Discussion*

There are a few candidate genes that fall in the region mapped to chromosome 22 that stand out as potentially being causal for the *dwarf* mutant phenotype.

A splice-site mutation was found in *nuak2*, an AMP-activated protein kinase that has been shown to be a melanomal oncogene. To support this, knockdown of *nuak2* suppresses melanomal growth and migration *in vitro* and *in vivo (*Namiki et al., 2011). Melanoma is a skin cancer that arises from the pigment producing cells of the skin, the melanocytes. *nuak2* is a member of an AMP-activated protein kinase subunit that functions to sense cellular metabolic status and regulate cell proliferation through modulating the cell cycle. However, the exact mechanism by which AMP-activated protein kinases like *nuak2* affect cancer development remains unknown. Melanocytes are rich in LROs that produce pigment for the cell, melanosomes. Because notochord vacuoles are LROs like melanosomes, similar molecular machinery is required for their formation and maintenance. Therefore, it is possible that *nuak2* could function in both melanocytes and the inner vacuolated cells to regulate both of these LROs.

Another exciting candidate is a splice-site mutation affecting *arl8a*. *arl8* is the only known small G protein found on the lysosomal membrane. It is conserved from humans to plants and in some species of yeast. In *C. elegans* mutant for *arl8,* traffic between late endosomes and lysosomes is impaired (Nakae et al., 2010). Also in these mutants vesicles aggregate along axons and

fail to be transported properly to the presynaptic region (Klassen et al., 2010). Over expression of *arl8* in mammalian cells results in the accumulation of lysosomes around the cell's periphery, suggesting an important role for Arl8 in lysosomal motility (Hofmann and Munro, 2006). Recently, Arl8 has been shown to recruit the SifA and kinesin interacting protein (SKIP) in order to link lysosomes to the plus-end directed microtubule motor kinesin (Rosa-Ferreira and Munro, 2011). Arl8 is an interesting candidate for *dwarf* as the multiple small vacuole phenotype observed in *dwarf* mutant embryos could be due to a defect in the trafficking of pre-vacuolar compartments together to allow for fusion into a single vacuole.

Interestingly, Arl8b was shown to bind and recruit Vps41, a member of the HOPS complex, to lysosomes suggesting that HOPS complex members can be effectors of Arl8 (Garg et al., 2011). Preliminary data using synthetic genetic interactions suggests that Dwarf and members of the VPS HOPS complex (Vps11 and Vps18) are interacting at the protein level. Fish that are heterozygous for *vps18* were crossed to fish that are heterozygous for *dwarf* and a small percentage of the clutch showed notochord vacuole fragmentation. While the number of embryos with fragmented vacuoles was much lower than the percentage of the clutch that should have been compound heterozygous, fragmented vacuoles are never seen in embryos heterozygous for either gene. This data suggests that the genetic interaction produced the fragmented vacuole

phenotype and that Dwarf and Vps18 proteins interact in the process of notochord vacuole formation.

Future work will narrow down a homozygosity interval so that candidates within a refined interval can be tested. Morpholinos or CRISPRs can be designed against candidates in an attempt to phenocopy the *dwarf* mutant phenotype. Additionally, mRNA can be injected into one-cell staged embryos in order to test if the candidate gene product can rescue the mutant vacuole phenotype.

# 6. Conclusions and Future Directions

Here I have elucidated the trafficking requirements necessary for vacuole biogenesis and show that post-Golgi trafficking, $H^+$-ATPase-dependent acidification and Rab32a are necessary for formation and maintenance of this specialized structure (Figure 29). Our *in vivo* studies in zebrafish show that the inflating vacuoles act as a morphogenetic force to elongate the embryonic body axis. Previous ex-vivo work had suggested that vacuole inflation could drive both the elongation and straightening of the body axis (Koehl et al., 2000). However, our results show that in vivo vacuole inflation is not required for straightening of the embryonic axis. The expansion of the vacuoles results in the elongation of the embryonic axis longitudinally along the anterior-posterior axis and not radially, due to the rigid ECM surrounding the notochord (Adams et al., 1990; Stemple et al., 1996).

Characterization of the cellular machinery regulating notochord vacuole biogenesis and maintenance uncovered a role for vacuoles in spine morphogenesis. We propose that fully inflated notochord vacuoles are necessary to evenly distribute the compressive force of concentrically growing vertebrae during spine formation and that lack of a hydrostatic scaffold for bone deposition in fish with disrupted notochord vacuoles leads to aberrant spine morphogenesis.

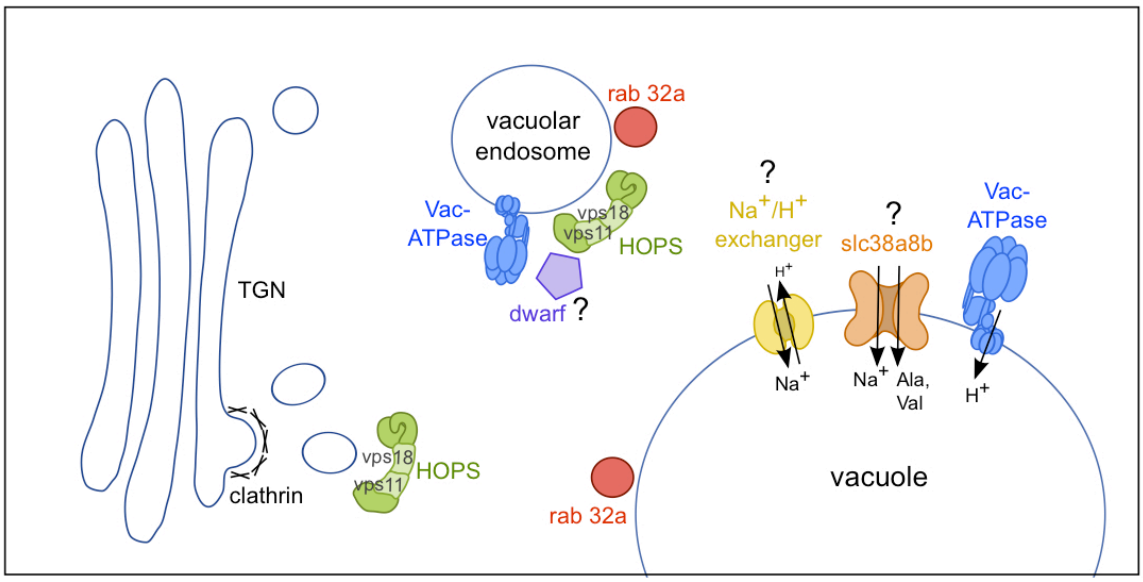


**Figure 29. Model of trafficking requirements for vacuole biogenesis**

Cartoon depicting trafficking requirements and protein complexes shown to be important for vacuole biogenesis and maintenance. Clathrin-dependent biosynthetic trafficking from the TGN is essential for vacuole formation. VPS HOPS complex likely functions at the TGN as well as at vacuolar endosomes to mediate this traffic. V-ATPase-dependent acidification is also necessary for trafficking of membrane and cargo to the vacuole and these proton pumps are likely found on both vacuolar endosomes and the vacuole itself. Rab32a localizes to the vacuole and is an important regulator of cargo delivery from the vacuolar endosome to the vacuole. Dwarf interacts with members of the VPS HOPS complex and likely functions at the vacuolar endosome to mediate homotypic fusion of pre-vacuolar compartments.

Many future directions have been discussed previously in the discussion sections above and several of these experiments are already underway. However, the field of notochord vacuole biology is still in its infancy and several questions remain. Here I will discuss a few areas of future interest that I have divided into two broad categories: A) Notochord vacuole biogenesis and B) The role of the notochord in spine formation.

## *6.A. Notochord vacuole biogenesis*

While the notochord vacuole has been described for decades, technology is just allowing for these structures to be characterized molecularly. Here I will focus on questions pertaining to notochord vacuole biology.

### 6.A.1. Regulation of final vacuole size

An area of future interest is investigating how vacuole expansion and final size are determined. The rigid ECM encasing the notochord ultimately restricts the expansion of the single vacuole within inner cells. This raises the interesting question of whether the vacuole is at an equilibrium where the final volume is obtained when the channels are all at a steady state or if there are mechanisms that down regulate the activity of transporters and channels involved in vacuole inflation to limit its expansion. A candidate mechanosensory element limiting vacuole growth is a member of the transient receptor potential (TRP) family of ion channels, TRPV4. TRPV4 is an osmotically activated calcium ion channel that has been shown to be important for osmoregulation in mice (Liedtke and

Friedman, 2003) and cell volume regulation *in vitro* (Becker et al., 2005). Importantly, TRPV4 is expressed in the notochord of zebrafish at the time of vacuole inflation (Mangos et al., 2007). Future work should investigate the role of this channel in regulating notochord vacuole volume.

### 6.A.2. Using genetic interactions to understand the molecular network involved in vacuole biogenesis

Our work has identified several proteins and protein complexes that are important for vacuole formation and maintenance, such as the vacuolar ATPase, the VPS HOPS complex, Rab32a, Clathrin and Dwarf. However, we don't know exactly where these proteins are acting along the endosomal pathway and to what extent they interact with one another (Figure 29).

One way to determine if proteins are acting in a synergistic manner is to analyze synthetic genetic interactions between members of different protein complexes. These types of studies will allow us to place molecular components necessary for vacuole formation into a pathway or network. To this end, we crossed fish that carried a single mutant allele for a given gene (for example *vps18*$^{+/-}$) to another fish carrying a single mutant allele for a different gene (for example the vacuolar ATPase subunit *atp6v0ca*$^{+/-}$*)* to generate compound heterozygous offspring. We then looked for a fragmented notochord vacuole phenotype in the compound heterozygous offspring and compared the rates of fragmentation in compound heterozygotes to that of single heterozygous offspring. Larvae with fragmented vacuoles were then raised until 21 dpf to see if

the fragmented notochord vacuoles would result in a spine defect. Thus far, we have completed crosses between most of the genes found to be involved in vacuole formation and analyzed at least 200 embryos per combination.

We have found several crosses that generate a higher rate of vacuole fragmentation and therefore suggest an interaction at the protein level. For example, our results suggest that Vps11 and Vps18 members of the HOPS complex interact directly with clathrin, possibly at the TGN where we have seen clathrin to be essential for biosynthetic trafficking to the vacuole. Clathrin and members of the VPS HOPS complex have recently been shown to interact with each other along with the adaptor complex AP-3 in HEK293 cells through co-immunoprecipitation assays. Using a chemical/genetic approach to induce oligomerization of clathrin heavy chains, these studies also showed that acute perturbations of clathrin resulted in an accumulation of enlarged Vps18 positive endosomes at the cellular periphery (Zlatic et al., 2011). Taken together the previous *in vitro* and biochemical analyses along with our *in vivo* data suggest that VPS HOPS complex members are associated with clathrin-coated vesicles en route to the notochord vacuole. An example of these types of synthetic genetic interactions can be seen in Figure 30 between *vps11* and *vps18*, two members of the VPS HOPS complex known to interact at the protein level.

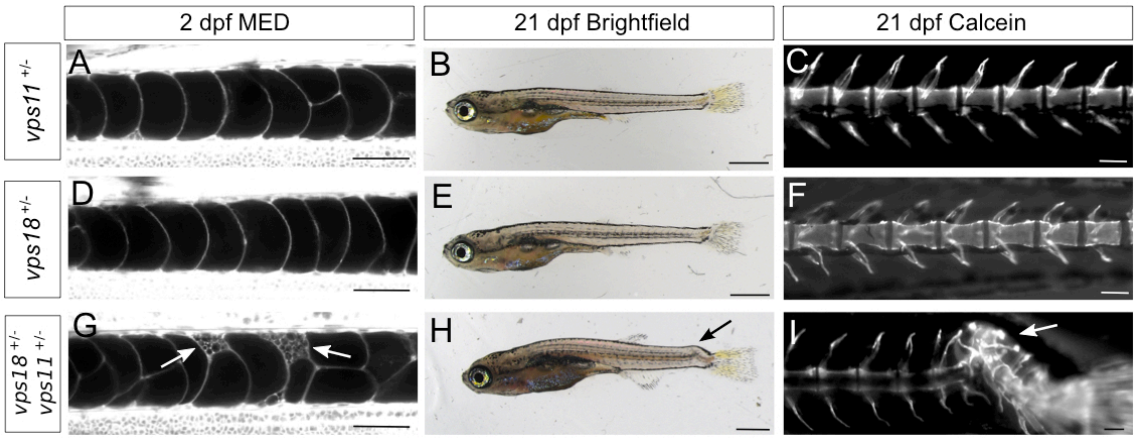


**Figure 30. Compound heterozygotes reveal synthetic genetic interactions**

(A) Live confocal image of a 2 dpf *vps11* $^{+/-}$ embryo visualized with MED. (B) Whole mount image of a 21 dpf *vps11* $^{+/-}$ fish. (C) Live whole mount image of a *vps11* $^{+/-}$ spine at 21 dpf dyed with calcein. (D) Live confocal image of a 2 dpf *vps18* $^{+/-}$ embryo dyed with MED. (E) Whole mount image of a 21 dpf *vps18* $^{+/-}$ fish. (F) Live whole mount image of a *vps18* $^{+/-}$ spine at 21 dpf dyed with calcein. (G) Live confocal image of a 2 dpf *vps11* $^{+/-}$; *vps18* $^{+/-}$ compound heterozygous embryo dyed with MED. Arrows indicate fragmented vacuoles. (H) Whole mount image of a 21 dpf *vps11* $^{+/-}$; *vps18* $^{+/-}$ compound heterozygous fish. Arrow indicates spine kink. (I) Live whole mount image of a *vps11* $^{+/-}$; *vps18* $^{+/-}$ compound heterozygous spine at 21 dpf dyed with calcein. Arrow indicates kink in the spine. (A, D, G) scale bars = 50 μm. (B, E, H) scale bars = 1 mm. (C, F, I) scale bars = 100 μm.

Future work in this area is aimed at completing all of the crosses for mutants we have that are known to have impaired vacuole formation. Control single heterozygous crosses also need to be completed to make sure the phenotypes seen in compound heterozygotes are in fact due to a compound effect of the two different alleles and not an additive effect. Furthermore, more data need to be collected to see if the fragmented vacuole phenotype of compound heterozygotes is sufficient to cause spine kinks or if the vacuoles can recover over time. Also, the type of mutation for each gene will also need to be considered. Some of the mutants we are using contain retroviral insertions and produce a null mutation, whereas others contain point mutations and are likely producing transcripts and partially functional proteins. Therefore, in some mutants the effects we are seeing could be because the proteins being produced are acting as dominant negatives to cause more of a severe phenotype than a null mutation would.

### 6.A.3. Investigating cell turnover in the notochord

Both historical and recent papers have referred to the outer sheath cells as chordoblasts and the inner vacuolated cells as chordocytes (Grotmol et al., 2003). These terms imply that the outer cells are more immature while the inner cells are fully differentiated. However, lineage-tracing experiments have not been performed to definitively show the outer cells giving rise to vacuolated cells.

In our work we have seen that damaged vacuolated cells cause kinks in the spine as it develops. This suggests that there is still a defect in vacuolated

cells at the time of vertebrae formation. We have performing time lapse imaging of *dwarf* mutants and seen that the vacuoles remain fragmented for weeks throughout the process of spine formation and do not recover. It is unclear why some mutants such as *chordostatin*, the intermediate filament discussed previously, are able to recover their vacuolated cells while others such as *dwarf* are not.

Future work should investigate the ability of the inner vacuolated cells to divide after differentiation in normal conditions as well as after damage. Additionally, lineage-tracing experiments are needed in order to determine if the outer cells are a source of new vacuolated cells. In order to genetically lineage trace the outer sheath cells, a fish line using a ubiquitous promoter (like βact) driving a floxed stop codon upstream of a reporter gene (like GFP or *lacZ*) would be crossed to a fish line using an outer cell specific promoter driving Cre recombinase. In this way, only cells that had at one point been under the control of the outer cell specific promoter would turn on the reporter through Cre-mediated recombination and continue to express the reporter even if the cells became inner vacuolated cells. To this end, it can be determined if outer cells give rise to inner vacuolated cells.

### 6.A.4. Sorting to the notochord vacuole

Biosynthetic proteins are differentially sorted within the cell to their final destinations based on sorting signals. The lysosomal protein Lamp2 is sorted to lysosomes while Lamp1 is sorted to the vacuole membrane. What is the sorting

signal on vacuolar membrane proteins or cargo that direct their trafficking to the vacuole?

Future work should identify the sorting motif necessary for sorting to the vacuole. Tyrosine-based lysosomal sorting motifs are found on the C-terminus of lysosomal proteins as discussed previously (Bonifacino and Traub, 2003). Therefore, a good place to start looking for the vacuole-sorting motif is by comparing the C-termini of the differentially sorted Lamp1 and Lamp2. An amino acid sequence specific to the vacuole-targeted Lamp1 could be fused to the C-terminus of soluble GFP or a GFP-tagged transmembrane protein to see if the peptide is sufficient to send GFP to the lumen or membrane of the vacuole.

## *6.B. The role of the notochord in spine formation*

The notochord has been previously under-appreciated for its roles during later development specifically, during spine morphogenesis. Here I will focus on future directions that address the role of the notochord during vertebral column development.

### 6.B.1. The patterning of vertebrae segmentation

We have shown that absence of notochord vacuoles or disrupted vacuoles give rise to kinks and curvatures of the spine as it develops. What remains unknown is how the spine is patterned into regularly spaced vertebrae with intervertebral spaces. There does not seem to be a role for notochord vacuoles in this process, as we have not seen many vertebral fusions in our perturbations of vacuoles or in the *dwarf* mutant. However, the invading osteoblasts must

receive information from either surrounding sclerotome or the notochord directly in order to position themselves correctly to allow for such regular vertebral spacing. Future work should investigate the notochord outer sheath cells as being a source of signals to the osteoblasts.

Work in our lab has identified a promoter that is specific to the outer sheath cells, a regulatory sequence from a collagen gene. Preliminary data using a GFP reporter line shows that the collagen expression turns off in a segmented manner along the length of the notochord before any osteoblasts are present. This segmentation of the notochord appears to be instructive for osteoblast recruitment as osteoblasts are only recruited to GFP negative spaces along the notochord. Collagen GFP expression persists in intervertebral spaces throughout vertebral development. Future work is aimed at isolating cells from GFP-positive and GFP-negative regions of the segmented notochord and performing microarray or RNA Seq analysis. Transcriptional profiles of these two populations of cells will provide insights into what could be regulating notochord segmentation in order to instruct osteoblast localization.

### 6.B.2. Using synthetic genetic interactions to understand the inheritance of congenital scoliosis.

Congenital scoliosis (CS) affects 2-3% of the U.S. population and back pain is the leading cause of pain in the adult population. CS is a curvature of the spine that originates during development and is the result of at least one vertebral malformation. Historically, the etiology of congenital scoliosis has been

focused on irregular somitogenesis, as the somites are the precursors for the cells generating vertebral bone (Hensinger, 2009). However, developmental studies have long shown a role for the notochord in patterning the somites and therefore, CS could be due in part to underlying notochord defects. Our studies have shown that disruption of notochord vacuoles results in juveniles with spine kinks that are similar to those found in human congenital scoliosis (CS) patients. Thus, we are using the zebrafish, a powerful developmental and genetic model, to undercover novel molecular and cellular mechanisms contributing to CS.

The inheritance mode for CS in humans is unclear; therefore it is likely that several genes are contributing to the disease phenotype. Using our synthetic genetic interaction model (described above in section 6.A.2), we will identify combinations of genes that produce higher instances of fragmented notochord vacuoles and spine kinks. We have obtained three samples of CS patient and family DNA and will be performing sequencing for the genes that we have found to be important for notochord vacuole formation in fish such as, *vps11*, *vps18*, *rab32*, and members of the V-ATPase complex. While no single gene has been linked to CS, perhaps combinations of variants in multiple alleles are sufficient to cause CS. Future work is aimed at obtaining more patient DNA and carrying out the sequencing based on the genetic interactions we find using zebrafish.

## *6.C. Concluding remarks*

For many years the vertebrate notochord has been considered an evolutionary relic that only functions in early embryonic development and

degenerates shortly thereafter. However, recent work in several vertebrate species has clearly shown that notochord cells persist within the nucleus pulposus of the intervertebral discs (Hunter et al., 2004). This work establishes a continuous structural role for the notochord from embryogenesis until vertebral column formation.

We have elucidated many molecular players involved in notochord vacuole biogenesis and created numerous tools and techniques to uncover more. Using forward genetics, reverse genetics, and live imaging techniques, we are well poised to fully understand how notochord vacuoles are formed and the role the notochord plays during spine formation.

# References


Adams, D.S., R. Keller, and M.A. Koehl. 1990. The mechanics of notochord elongation, straightening and stiffening in the embryo of Xenopus laevis. *Development*. 110:115-130.

Akitake, C.M., M. Macurak, M.E. Halpern, and M.G. Goll. 2011. Transgenerational analysis of transcriptional silencing in zebrafish. *Developmental biology*. 352:191-201.

Ambrosio, A.L., J.A. Boyle, and S.M. Di Pietro. 2012. Mechanism of platelet dense granule biogenesis: study of cargo transport and function of Rab32 and Rab38 in a model system. *Blood*. 120:4072-4081.

Amsterdam, A., R.M. Nissen, Z. Sun, E.C. Swindell, S. Farrington, and N. Hopkins. 2004. Identification of 315 genes essential for early zebrafish development. *Proceedings of the National Academy of Sciences of the United States of America*. 101:12792-12797.

Anderson, R.G., J.L. Goldstein, and M.S. Brown. 1977. A mutation that impairs the ability of lipoprotein receptors to localise in coated pits on the cell surface of human fibroblasts. *Nature*. 270:695-699.

Arratia, G., H.P. Schultze, and J. Casciotta. 2001. Vertebral column and associated elements in dipnoans and comparison with other fishes: development and homology. *Journal of morphology*. 250:101-172.

Bagnat, M., A. Navis, S. Herbstreith, K. Brand-Arzamendi, S. Curado, S. Gabriel, K. Mostov, J. Huisken, and D.Y. Stainier. 2010. Cse1l is a negative regulator of CFTR-dependent fluid secretion. *Current biology : CB*. 20:1840-1845.

Bancroft, M., and R. Bellairs. 1976. The development of the notochord in the chick embryo, studied by scanning and transmission electron microscopy. *Journal of embryology and experimental morphology*. 35:383-401.

Barlowe, C., L. Orci, T. Yeung, M. Hosobuchi, S. Hamamoto, N. Salama, M.F. Rexach, M. Ravazzola, M. Amherdt, and R. Schekman. 1994. COPII: a membrane coat formed by Sec proteins that drive vesicle budding from the endoplasmic reticulum. *Cell*. 77:895-907.

Becker, D., C. Blase, J. Bereiter-Hahn, and M. Jendrach. 2005. TRPV4 exhibits a functional role in cell-volume regulation. *Journal of cell science*. 118:2435-2440.

Bibby, S.R., and J.P. Urban. 2004. Effect of nutrient deprivation on the viability of intervertebral disc cells. *European spine journal : official publication of the European Spine Society, the European Spinal Deformity Society, and the European Section of the Cervical Spine Research Society*. 13:695-701.

Bocina, I., and M. Saraga-Babic. 2006. The notochordal sheath in amphioxus--an ultrastructural and histochemical study. *Collegium antropologicum*. 30:361-367.

Bonifacino, J.S., and L.M. Traub. 2003. Signals for sorting of transmembrane proteins to endosomes and lysosomes. *Annual review of biochemistry*. 72:395-447.

Bowman, E.J., A. Siebers, and K. Altendorf. 1988. Bafilomycins: a class of inhibitors of membrane ATPases from microorganisms, animal cells, and plant cells. *Proceedings of the National Academy of Sciences of the United States of America*. 85:7972-7976.

Brett, C.L., R.L. Plemel, B.T. Lobingier, M. Vignali, S. Fields, and A.J. Merz. 2008. Efficient termination of vacuolar Rab GTPase signaling requires coordinated action by a GAP and a protein kinase. *The Journal of cell biology*. 182:1141-1151.

Bryant, N.J., and T.H. Stevens. 1998. Vacuole biogenesis in Saccharomyces cerevisiae: protein transport pathways to the yeast vacuole. *Microbiology and molecular biology reviews : MMBR*. 62:230-247.

Cantagrel, V., J.L. Silhavy, S.L. Bielas, D. Swistun, S.E. Marsh, J.Y. Bertrand, S. Audollent, T. Attie-Bitach, K.R. Holden, W.B. Dobyns, D. Traver, L. Al-Gazali, B.R. Ali, T.H. Lindner, T. Caspary, E.A. Otto, F. Hildebrandt, I.A. Glass, C.V. Logan, C.A. Johnson, C. Bennett, F. Brancati, E.M. Valente, C.G. Woods, and J.G. Gleeson. 2008. Mutations in the cilia gene ARL13B lead to the classical form of Joubert syndrome. *American journal of human genetics*. 83:170-179.

Casey, J.R., S. Grinstein, and J. Orlowski. 2010. Sensors and regulators of intracellular pH. *Nature reviews. Molecular cell biology*. 11:50-61.

Chardin, P., and F. McCormick. 1999. Brefeldin A: the advantage of being uncompetitive. *Cell*. 97:153-155.

Chavrier, P., and B. Goud. 1999. The role of ARF and Rab GTPases in membrane transport. *Current opinion in cell biology*. 11:466-475.

Chen, M.S., R.A. Obar, C.C. Schroeder, T.W. Austin, C.A. Poodry, S.C. Wadsworth, and R.B. Vallee. 1991. Multiple forms of dynamin are encoded by shibire, a Drosophila gene involved in endocytosis. *Nature*. 351:583-586.

Choi, K.S., C. Lee, and B.D. Harfe. 2012. Sonic hedgehog in the notochord is sufficient for patterning of the intervertebral discs. *Mechanisms of development*. 129:255-262.

Christiansen, H.E., M.R. Lang, J.M. Pace, and D.M. Parichy. 2009. Critical early roles for col27a1a and col27a1b in zebrafish notochord morphogenesis, vertebral mineralization and post-embryonic axial growth. *PloS one*. 4:e8481.

Clark, B.S., M. Winter, A.R. Cohen, and B.A. Link. 2011. Generation of Rab-based transgenic lines for in vivo studies of endosome biology in zebrafish. *Developmental dynamics : an official publication of the American Association of Anatomists*. 240:2452-2465.

Cleaver, O., and P.A. Krieg. 2001. Notochord patterning of the endoderm. *Developmental biology*. 234:1-12.

Cole, N.B., and J. Lippincott-Schwartz. 1995. Organization of organelles and membrane traffic by microtubules. *Current opinion in cell biology*. 7:55-64.

Cook, T.A., R. Urrutia, and M.A. McNiven. 1994. Identification of dynamin 2, an isoform ubiquitously expressed in rat tissues. *Proceedings of the National Academy of Sciences of the United States of America*. 91:644-648.

Coutinho, P., M.J. Parsons, K.A. Thomas, E.M. Hirst, L. Saude, I. Campos, P.H. Williams, and D.L. Stemple. 2004. Differential requirements for COPI transport during vertebrate early development. *Developmental cell*. 7:547-558.

Curado, S., D.Y. Stainier, and R.M. Anderson. 2008. Nitroreductase-mediated cell/tissue ablation in zebrafish: a spatially and temporally controlled ablation method with applications in developmental and regeneration studies. *Nature protocols*. 3:948-954.

Dale, R.M., and J. Topczewski. 2011. Identification of an evolutionarily conserved regulatory element of the zebrafish col2a1a gene. *Developmental biology*. 357:518-531.

Danos, M.C., and H.J. Yost. 1996. Role of notochord in specification of cardiac left-right orientation in zebrafish and Xenopus. *Developmental biology*. 177:96-103.

Darwen, C.W., and P. John. 1989. Localization of the Enzymes of Fructan Metabolism in Vacuoles Isolated by a Mechanical Method from Tubers of Jerusalem Artichoke (Helianthus tuberosus L.). *Plant physiology*. 89:658-663.

Deborde, S., E. Perret, D. Gravotta, A. Deora, S. Salvarezza, R. Schreiner, and E. Rodriguez-Boulan. 2008. Clathrin is a key regulator of basolateral polarity. *Nature*. 452:719-723.

Denker, E., and D. Jiang. 2012. Ciona intestinalis notochord as a new model to investigate the cellular and molecular mechanisms of tubulogenesis. *Seminars in cell & developmental biology*. 23:308-319.

Dettmer, J., A. Hong-Hermesdorf, Y.D. Stierhof, and K. Schumacher. 2006. Vacuolar H+-ATPase activity is required for endocytic and secretory trafficking in Arabidopsis. *The Plant cell*. 18:715-730.

Donaldson, J.G., D. Finazzi, and R.D. Klausner. 1992. Brefeldin A inhibits Golgi membrane-catalysed exchange of guanine nucleotide onto ARF protein. *Nature*. 360:350-352.

Du, S.J., V. Frenkel, G. Kindschi, and Y. Zohar. 2001. Visualizing normal and defective bone development in zebrafish embryos using the fluorescent chromophore calcein. *Developmental biology*. 238:239-246.

Etxeberria, E., J. Pozueta-Romero, and P. Gonzalez. 2012. In and out of the plant storage vacuole. *Plant science : an international journal of experimental plant biology*. 190:52-61.

Fan, C.M., and M. Tessier-Lavigne. 1994. Patterning of mammalian somites by surface ectoderm and notochord: evidence for sclerotome induction by a hedgehog homolog. *Cell*. 79:1175-1186.

Fouquet, B., B.M. Weinstein, F.C. Serluca, and M.C. Fishman. 1997. Vessel patterning in the embryo of the zebrafish: guidance by notochord. *Developmental biology*. 183:37-48.

Franchi-Gazzola, R., V. Dall'Asta, R. Sala, R. Visigalli, E. Bevilacqua, F. Gaccioli, G.C. Gazzola, and O. Bussolati. 2006. The role of the neutral amino acid transporter SNAT2 in cell volume regulation. *Acta Physiol (Oxf)*. 187:273-283.

Garg, S., M. Sharma, C. Ung, A. Tuli, D.C. Barral, D.L. Hava, N. Veerapen, G.S. Besra, N. Hacohen, and M.B. Brenner. 2011. Lysosomal trafficking, antigen presentation, and microbial killing are controlled by the Arf-like GTPase Arl8b. *Immunity*. 35:182-193.

Glickman, N.S., C.B. Kimmel, M.A. Jones, and R.J. Adams. 2003. Shaping the zebrafish notochord. *Development*. 130:873-887.

Goldstein, A.M., and M.C. Fishman. 1998. Notochord regulates cardiac lineage in zebrafish embryos. *Developmental biology*. 201:247-252.

Granger, B.L., S.A. Green, C.A. Gabel, C.L. Howe, I. Mellman, and A. Helenius. 1990. Characterization and cloning of lgp110, a lysosomal membrane glycoprotein from mouse and rat cells. *The Journal of biological chemistry*. 265:12036-12043.

Gray, R.S., T.P. Wilm, J. Smith, M. Bagnat, R.M. Dale, J. Topczewski, S.L. Johnson, and L. Solnica-Krezel. 2014. Loss of col8a1a function during zebrafish embryogenesis results in congenital vertebral malformations. *Developmental biology*. 386:72-85.

Grosshans, B.L., D. Ortiz, and P. Novick. 2006. Rabs and their effectors: achieving specificity in membrane traffic. *Proceedings of the National Academy of Sciences of the United States of America*. 103:11821-11827.

Grotmol, S., H. Kryvi, K. Nordvik, and G.K. Totland. 2003. Notochord segmentation may lay down the pathway for the development of the vertebral bodies in the Atlantic salmon. *Anatomy and embryology*. 207:263-272.

Hanton, S.L., L.A. Matheson, L. Chatre, M. Rossi, and F. Brandizzi. 2007. Post-Golgi protein traffic in the plant secretory pathway. *Plant cell reports*. 26:1431-1438.

Hara-Nishimura, I., and N. Hatsugai. 2011. The role of vacuole in plant cell death. *Cell death and differentiation*. 18:1298-1304.

Helms, J.B., and J.E. Rothman. 1992. Inhibition by brefeldin A of a Golgi membrane enzyme that catalyses exchange of guanine nucleotide bound to ARF. *Nature*. 360:352-354.

Hensinger, R.N. 2009. Congenital scoliosis: etiology and associations. *Spine*. 34:1745-1750.

Herskovits, J.S., C.C. Burgess, R.A. Obar, and R.B. Vallee. 1993. Effects of mutant rat dynamin on endocytosis. *The Journal of cell biology*. 122:565-578.

Hicke, L., and R. Dunn. 2003. Regulation of membrane protein transport by ubiquitin and ubiquitin-binding proteins. *Annual review of cell and developmental biology*. 19:141-172.

Hinshaw, J.E., and S.L. Schmid. 1995. Dynamin self-assembles into rings suggesting a mechanism for coated vesicle budding. *Nature*. 374:190-192.

Hofmann, I., and S. Munro. 2006. An N-terminally acetylated Arf-like GTPase is localised to lysosomes and affects their motility. *Journal of cell science*. 119:1494-1503.

Hunter, C.J., S. Bianchi, P. Cheng, and K. Muldrew. 2007. Osmoregulatory function of large vacuoles found in notochordal cells of the intervertebral disc. *Molecular and cellular biomechanics*. 4:227-237.

Hunter, C.J., J.R. Matyas, and N.A. Duncan. 2004. Cytomorphology of notochordal and chondrocytic cells from the nucleus pulposus: a species comparison. *Journal of anatomy*. 205:357-362.

Hurbain, I., W.J. Geerts, T. Boudier, S. Marco, A.J. Verkleij, M.S. Marks, and G. Raposo. 2008. Electron tomography of early melanosomes: implications for melanogenesis and the generation of fibrillar amyloid sheets. *Proceedings of the National Academy of Sciences of the United States of America*. 105:19726-19731.

Inohaya, K., Y. Takano, and A. Kudo. 2007. The teleost intervertebral region acts as a growth center of the centrum: in vivo visualization of osteoblasts and their progenitors in transgenic fish. *Developmental dynamics : an official publication of the American Association of Anatomists*. 236:3031-3046.

Jaquinod, M., F. Villiers, S. Kieffer-Jaquinod, V. Hugouvieux, C. Bruley, J. Garin, and J. Bourguignon. 2007. A proteomics dissection of Arabidopsis thaliana vacuoles isolated from cell culture. *Molecular & cellular proteomics : MCP*. 6:394-412.

Johnson, A.E., and M.A. van Waes. 1999. The translocon: a dynamic gateway at the ER membrane. *Annual review of cell and developmental biology*. 15:799-842.

Kajikawa, M., T. Shoji, A. Kato, and T. Hashimoto. 2011. Vacuole-localized berberine bridge enzyme-like proteins are required for a late step of nicotine biosynthesis in tobacco. *Plant physiology*. 155:2010-2022.

Kang, B.H., E. Nielsen, M.L. Preuss, D. Mastronarde, and L.A. Staehelin. 2011. Electron tomography of RabA4b- and PI-4Kbeta1-labeled trans Golgi network compartments in Arabidopsis. *Traffic*. 12:313-329.

Kent, G.C., and R.K. Carr. 2001. Comparative Anatomy of the Vertebrates. McGraw Hill, New York, NY. 524 pp.

Kida, Y.S., T. Sato, K.Y. Miyasaka, A. Suto, and T. Ogura. 2007. Daam1 regulates the endocytosis of EphB during the convergent extension of the zebrafish notochord. *Proceedings of the National Academy of Sciences of the United States of America*. 104:6708-6713.

Kim, S.K., M. Hebrok, and D.A. Melton. 1997. Notochord to endoderm signaling is required for pancreas development. *Development*. 124:4243-4252.

Klassen, M.P., Y.E. Wu, C.I. Maeder, I. Nakae, J.G. Cueva, E.K. Lehrman, M. Tada, K. Gengyo-Ando, G.J. Wang, M. Goodman, S. Mitani, K. Kontani, T. Katada, and K. Shen. 2010. An Arf-like small G protein, ARL-8, promotes the axonal transport of presynaptic cargoes by suppressing vesicle aggregation. *Neuron*. 66:710-723.

Klionsky, D.J., R. Cueva, and D.S. Yaver. 1992. Aminopeptidase I of Saccharomyces cerevisiae is localized to the vacuole independent of the secretory pathway. *The Journal of cell biology*. 119:287-299.

Kobialka, S., N. Beuret, H. Ben-Tekaya, and M. Spiess. 2009. Glycosaminoglycan chains affect exocytic and endocytic protein traffic. *Traffic*. 10:1845-1855.

Koehl, M.A., K.J. Quillin, and C.A. Pell. 2000. Mechanical design of fiber-wound hydraulic skeletons: the stiffening and straightening of embryonic notochords. *American Zoologist*. 40:28-41.

Kornfeld, S., and I. Mellman. 1989. The biogenesis of lysosomes. *Annual review of cell biology*. 5:483-525.

Kreitzer, G., A. Marmorstein, P. Okamoto, R. Vallee, and E. Rodriguez-Boulan. 2000. Kinesin and dynamin are required for post-Golgi transport of a plasma-membrane protein. *Nature cell biology*. 2:125-127.

Kwan, K.M., E. Fujimoto, C. Grabher, B.D. Mangum, M.E. Hardy, D.S. Campbell, J.M. Parant, H.J. Yost, J.P. Kanki, and C.B. Chien. 2007. The Tol2kit: a multisite gateway-based construction kit for Tol2 transposon transgenesis constructs. *Developmental dynamics : an official publication of the American Association of Anatomists*. 236:3088-3099.

Lam, S.K., C.L. Siu, S. Hillmer, S. Jang, G. An, D.G. Robinson, and L. Jiang. 2007. Rice SCAMP1 defines clathrin-coated, trans-golgi-located tubular-vesicular structures as an early endosome in tobacco BY-2 cells. *The Plant cell*. 19:296-319.

Latimer, A.J., and B. Appel. 2006. Notch signaling regulates midline cell specification and proliferation in zebrafish. *Developmental biology*. 298:392-402.

Latterich, M., and M.D. Watson. 1991. Isolation and characterization of osmosensitive vacuolar mutants of Saccharomyces cerevisiae. *Molecular microbiology*. 5:2417-2426.

Lauwers, E., C. Jacob, and B. Andre. 2009. K63-linked ubiquitin chains as a specific signal for protein sorting into the multivesicular body pathway. *The Journal of cell biology*. 185:493-502.

Lee, E., and P. De Camilli. 2002. Dynamin at actin tails. *Proceedings of the National Academy of Sciences of the United States of America*. 99:161-166.

Leeson, T.S., and C.R. Leeson. 1958. Observations on the histochemistry and fine structure of the notochord in rabbit embryos. *Journal of anatomy*. 92:278-285.

Leshchiner, I., K. Alexa, P. Kelsey, I. Adzhubei, C.A. Austin-Tse, J.D. Cooney, H. Anderson, M.J. King, R.W. Stottmann, M.K. Garnaas, S. Ha, I.A. Drummond, B.H. Paw, T.E. North, D.R. Beier, W. Goessling, and S.R. Sunyaev. 2012. Mutation mapping and identification by whole-genome sequencing. *Genome research*. 22:1541-1548.

Liedtke, W., and J.M. Friedman. 2003. Abnormal osmotic regulation in trpv4-/- mice. *Proceedings of the National Academy of Sciences of the United States of America*. 100:13698-13703.

Lohr, J.L., M.C. Danos, and H.J. Yost. 1997. Left-right asymmetry of a nodal-related gene is regulated by dorsoanterior midline structures during Xenopus development. *Development*. 124:1465-1472.

Mackenzie, B., and J.D. Erickson. 2004. Sodium-coupled neutral amino acid (System N/A) transporters of the SLC38 gene family. *Pflugers Archiv : European journal of physiology*. 447:784-795.

Mangos, S., Y. Liu, and I.A. Drummond. 2007. Dynamic expression of the osmosensory channel trpv4 in multiple developing organs in zebrafish. *Gene expression patterns : GEP*. 7:480-484.

Marks, M.S., H.F. Heijnen, and G. Raposo. 2013. Lysosome-related organelles: unusual compartments become mainstream. *Current opinion in cell biology*. 25:495-505.

Martinez-Munoz, G.A., and P. Kane. 2008. Vacuolar and plasma membrane proton pumps collaborate to achieve cytosolic pH homeostasis in yeast. *The Journal of biological chemistry*. 283:20309-20319.

Martoglio, B., and B. Dobberstein. 1998. Signal sequences: more than just greasy peptides. *Trends in cell biology*. 8:410-415.

Marty, F. 1999. Plant vacuoles. *The Plant cell*. 11:587-600.

Mayor, S. 2011. Need tension relief fast? Try caveolae. *Cell*. 144:323-324.

McCann, M.R., O.J. Tamplin, J. Rossant, and C.A. Seguin. 2012. Tracing notochord-derived cells using a Noto-cre mouse: implications for intervertebral disc development. *Disease models & mechanisms*. 5:73-82.

Meachim, G., and M.S. Cornah. 1970. Fine structure of juvenile human nucleus pulposus. *Journal of anatomy*. 107:337-350.

Mellman, I. 1992. The importance of being acid: the role of acidification in intracellular membrane traffic. *The Journal of experimental biology*. 172:39-45.

Mellman, I., R. Fuchs, and A. Helenius. 1986. Acidification of the endocytic and exocytic pathways. *Annual review of biochemistry*. 55:663-700.

Melville, D.B., M. Montero-Balaguer, D.S. Levic, K. Bradley, J.R. Smith, A.K. Hatzopoulos, and E.W. Knapik. 2011. The feelgood mutation in zebrafish dysregulates COPII-dependent secretion of select extracellular matrix proteins in skeletal morphogenesis. *Disease models & mechanisms*. 4:763-776.

Michaux, G., K.B. Abbitt, L.M. Collinson, S.L. Haberichter, K.E. Norman, and D.F. Cutler. 2006. The physiological function of von Willebrand's factor depends on its tubular storage in endothelial Weibel-Palade bodies. *Developmental cell*. 10:223-232.

Miller, J.C., S. Tan, G. Qiao, K.A. Barlow, J. Wang, D.F. Xia, X. Meng, D.E. Paschon, E. Leung, S.J. Hinkley, G.P. Dulay, K.L. Hua, I. Ankoudinova, G.J. Cost, F.D. Urnov, H.S. Zhang, M.C. Holmes, L. Zhang, P.D. Gregory, and E.J. Rebar. 2011. A TALE nuclease architecture for efficient genome editing. *Nature biotechnology*. 29:143-148.

Mimura, T., M. Kura-Hotta, T. Tsujimura, M. Ohnishi, M. Miura, Y. Okazaki, M. Mimura, M. Maeshima, and S. Washitani-Nemoto. 2003. Rapid increase of vacuolar volume in response to salt stress. *Planta*. 216:397-402.

Nakae, I., T. Fujino, T. Kobayashi, A. Sasaki, Y. Kikko, M. Fukuyama, K. Gengyo-Ando, S. Mitani, K. Kontani, and T. Katada. 2010. The arf-like GTPase Arl8 mediates

delivery of endocytosed macromolecules to lysosomes in Caenorhabditis elegans. *Molecular biology of the cell*. 21:2434-2442.

Namiki, T., A. Tanemura, J.C. Valencia, S.G. Coelho, T. Passeron, M. Kawaguchi, W.D. Vieira, M. Ishikawa, W. Nishijima, T. Izumo, Y. Kaneko, I. Katayama, Y. Yamaguchi, L. Yin, E.C. Polley, H. Liu, Y. Kawakami, Y. Eishi, E. Takahashi, H. Yokozeki, and V.J. Hearing. 2011. AMP kinase-related kinase NUAK2 affects tumor growth, migration, and clinical outcome of human melanoma. *Proceedings of the National Academy of Sciences of the United States of America*. 108:6597-6602.

Neuhauss, S.C., L. Solnica-Krezel, A.F. Schier, F. Zwartkruis, D.L. Stemple, J. Malicki, S. Abdelilah, D.Y. Stainier, and W. Driever. 1996. Mutations affecting craniofacial development in zebrafish. *Development*. 123:357-367.

Nickerson, D.P., C.L. Brett, and A.J. Merz. 2009. Vps-C complexes: gatekeepers of endolysosomal traffic. *Current opinion in cell biology*. 21:543-551.

Niemes, S., M. Labs, D. Scheuring, F. Krueger, M. Langhans, B. Jesenofsky, D.G. Robinson, and P. Pimpl. 2010. Sorting of plant vacuolar proteins is initiated in the ER. *The Plant journal : for cell and molecular biology*. 62:601-614.

Nixon, S.J., A. Carter, J. Wegner, C. Ferguson, M. Floetenmeyer, J. Riches, B. Key, M. Westerfield, and R.G. Parton. 2007. Caveolin-1 is required for lateral line neuromast and notochord development. *Journal of cell science*. 120:2151-2161.

Novick, P., and M. Zerial. 1997. The diversity of Rab proteins in vesicle transport. *Current opinion in cell biology*. 9:496-504.

Nuckels, R.J., A. Ng, T. Darland, and J.M. Gross. 2009. The vacuolar-ATPase complex regulates retinoblast proliferation and survival, photoreceptor morphogenesis, and pigmentation in the zebrafish eye. *Investigative ophthalmology & visual science*. 50:893-905.

Otegui, M.S., R. Herder, J. Schulze, R. Jung, and L.A. Staehelin. 2006. The proteolytic processing of seed storage proteins in Arabidopsis embryo cells starts in the multivesicular bodies. *The Plant cell*. 18:2567-2581.

Parodi, A.J. 2000. Role of N-oligosaccharide endoplasmic reticulum processing reactions in glycoprotein folding and degradation. *The Biochemical journal*. 348 Pt 1:1-13.

Parton, R.G., and M.A. del Pozo. 2013. Caveolae as plasma membrane sensors, protectors and organizers. *Nature reviews. Molecular cell biology*. 14:98-112.

Patton, E.E., and L.I. Zon. 2001. The art and design of genetic screens: zebrafish. *Nature reviews. Genetics*. 2:956-966.

Pelham, H.R. 2001. SNAREs and the specificity of membrane fusion. *Trends in cell biology*. 11:99-101.

Peplowska, K., D.F. Markgraf, C.W. Ostrowicz, G. Bange, and C. Ungermann. 2007. The CORVET tethering complex interacts with the yeast Rab5 homolog Vps21 and is involved in endo-lysosomal biogenesis. *Developmental cell*. 12:739-750.

Peters, P.J., J. Borst, V. Oorschot, M. Fukuda, O. Krahenbuhl, J. Tschopp, J.W. Slot, and H.J. Geuze. 1991. Cytotoxic T lymphocyte granules are secretory lysosomes, containing both perforin and granzymes. *The Journal of experimental medicine*. 173:1099-1109.

Peterson, M.R., and S.D. Emr. 2001. The class C Vps complex functions at multiple stages of the vacuolar transport pathway. *Traffic*. 2:476-486.

Pfeffer, S.R. 1994. Rab GTPases: master regulators of membrane trafficking. *Current opinion in cell biology*. 6:522-526.

Piper, R.C., A.A. Cooper, H. Yang, and T.H. Stevens. 1995. VPS27 controls vacuolar and endocytic traffic through a prevacuolar compartment in Saccharomyces cerevisiae. *The Journal of cell biology*. 131:603-617.

Placzek, M., M. Tessier-Lavigne, T. Yamada, T. Jessell, and J. Dodd. 1990. Mesodermal control of neural cell identity: floor plate induction by the notochord. *Science*. 250:985-988.

Purhonen, P., K. Pursiainen, and H. Reunanen. 1997. Effects of brefeldin A on autophagy in cultured rat fibroblasts. *European journal of cell biology*. 74:63-67.

Qi, B.Q., and S.W. Beasley. 1999. Relationship of the notochord to foregut development in the fetal rat model of esophageal atresia. *Journal of pediatric surgery*. 34:1593-1598.

Raposo, G., M.S. Marks, and D.F. Cutler. 2007. Lysosome-related organelles: driving post-Golgi compartments into specialisation. *Current opinion in cell biology*. 19:394-401.

Raymond, C.K., I. Howald-Stevenson, C.A. Vater, and T.H. Stevens. 1992. Morphological classification of the yeast vacuolar protein sorting mutants: evidence for a prevacuolar compartment in class E vps mutants. *Molecular biology of the cell*. 3:1389-1402.

Reyes, F.C., R. Buono, and M.S. Otegui. 2011. Plant endosomal trafficking pathways. *Current opinion in plant biology*. 14:666-673.

Richardson, S.M., J.A. Hoyland, R. Mobasheri, C. Csaki, M. Shakibaei, and A. Mobasheri. 2010. Mesenchymal stem cells in regenerative medicine:

opportunities and challenges for articular cartilage and intervertebral disc tissue engineering. *Journal of cellular physiology*. 222:23-32.

Rieder, S.E., L.M. Banta, K. Kohrer, J.M. McCaffery, and S.D. Emr. 1996. Multilamellar endosome-like compartment accumulates in the yeast vps28 vacuolar protein sorting mutant. *Molecular biology of the cell*. 7:985-999.

Roberts, C.J., S.F. Nothwehr, and T.H. Stevens. 1992. Membrane protein sorting in the yeast secretory pathway: evidence that the vacuole may be the default compartment. *The Journal of cell biology*. 119:69-83.

Rosa-Ferreira, C., and S. Munro. 2011. Arl8 and SKIP act together to link lysosomes to kinesin-1. *Developmental cell*. 21:1171-1178.

Rothman, J.E., and F.T. Wieland. 1996. Protein sorting by transport vesicles. *Science*. 272:227-234.

Ryan, S., J. Willer, L. Marjoram, J. Bagwell, J. Mankiewicz, I. Leshchiner, W. Goessling, M. Bagnat, and N. Katsanis. 2013. Rapid identification of kidney cyst mutations by whole exome sequencing in zebrafish. *Development*. 140:4445-4451.

Sadler, K.C., A. Amsterdam, C. Soroka, J. Boyer, and N. Hopkins. 2005. A genetic screen in zebrafish identifies the mutants vps18, nf2 and foie gras as models of liver disease. *Development*. 132:3561-3572.

Sato, T.K., P. Rehling, M.R. Peterson, and S.D. Emr. 2000. Class C Vps protein complex regulates vacuolar SNARE pairing and is required for vesicle docking/fusion. *Molecular cell*. 6:661-671.

Saude, L., K. Woolley, P. Martin, W. Driever, and D.L. Stemple. 2000. Axis-inducing activities and cell fates of the zebrafish organizer. *Development*. 127:3407-3417.

Scheer, N., and J. Campos-Ortega. 1999. Use of the Gal4-UAS technique for targeted gene expression in the zebrafish. *Mechanisms of development*. 80:153-158.

Schekman, R., and L. Orci. 1996. Coat proteins and vesicle budding. *Science*. 271:1526-1533.

Scott, S.V., A. Hefner-Gravink, K.A. Morano, T. Noda, Y. Ohsumi, and D.J. Klionsky. 1996. Cytoplasm-to-vacuole targeting and autophagy employ the same machinery to deliver proteins to the yeast vacuole. *Proceedings of the National Academy of Sciences of the United States of America*. 93:12304-12308.

Sepich, D.S., C. Calmelet, M. Kiskowski, and L. Solnica-Krezel. 2005. Initiation of convergence and extension movements of lateral mesoderm during zebrafish gastrulation. *Developmental dynamics : an official publication of the American Association of Anatomists*. 234:279-292.

Sherer, N.M., M.J. Lehmann, L.F. Jimenez-Soto, A. Ingmundson, S.M. Horner, G. Cicchetti, P.G. Allen, M. Pypaert, J.M. Cunningham, and W. Mothes. 2003. Visualization of retroviral replication in living cells reveals budding into multivesicular bodies. *Traffic*. 4:785-801.

Shestopalov, I.A., C.L. Pitt, and J.K. Chen. 2012. Spatiotemporal resolution of the Ntla transcriptome in axial mesoderm development. *Nature chemical biology*. 8:270-276.

Shih, J., and S.E. Fraser. 1996. Characterizing the zebrafish organizer: microsurgical analysis at the early-shield stage. *Development*. 122:1313-1322.

Spoorendonk, K.M., J. Peterson-Maduro, J. Renn, T. Trowe, S. Kranenbarg, C. Winkler, and S. Schulte-Merker. 2008. Retinoic acid and Cyp26b1 are critical regulators of osteogenesis in the axial skeleton. *Development*. 135:3765-3774.

Stemple, D.L., L. Solnica-Krezel, F. Zwartkruis, S.C. Neuhauss, A.F. Schier, J. Malicki, D.Y. Stainier, S. Abdelilah, Z. Rangini, E. Mountcastle-Shah, and W. Driever. 1996. Mutations affecting development of the notochord in zebrafish. *Development*. 123:117-128.

Sumoy, L., J.B. Keasey, T.D. Dittman, and D. Kimelman. 1997. A role for notochord in axial vascular development revealed by analysis of phenotype and the expression of VEGR-2 in zebrafish flh and ntl mutant embryos. *Mechanisms of development*. 63:15-27.

Takeshige, K., M. Baba, S. Tsuboi, T. Noda, and Y. Ohsumi. 1992. Autophagy in yeast demonstrated with proteinase-deficient mutants and conditions for its induction. *The Journal of cell biology*. 119:301-311.

Thisse, B., S. Pfumio, M. Furthauer, B. Loppin, V. Heyer, A. Degrave, R. Woehl, A. Lux, T. Steffan, X.Q. Charbonnier, and C. Thisse. 2001. Expression of the zebrafish genome during embryogenesis. *ZFIN on-line publication*.

Thomas, J.L., T.S. Vihtelic, A.D. denDekker, G. Willer, X. Luo, T.R. Murphy, R.G. Gregg, D.R. Hyde, and R. Thummel. 2011. The loss of vacuolar protein sorting 11 (vps11) causes retinal pathogenesis in a vertebrate model of syndromic albinism. *Investigative ophthalmology & visual science*. 52:3119-3128.

Tong, X., Z. Xia, Y. Zu, H. Telfer, J. Hu, J. Yu, H. Liu, Q. Zhang, Sodmergen, S. Lin, and B. Zhang. 2013. ngs (notochord granular surface) gene encodes a novel type of intermediate filament family protein essential for notochord maintenance in zebrafish. *The Journal of biological chemistry*. 288:2711-2720.

Toyooka, K., Y. Goto, S. Asatsuma, M. Koizumi, T. Mitsui, and K. Matsuoka. 2009. A mobile secretory vesicle cluster involved in mass transport from the Golgi to the plant cell exterior. *The Plant cell*. 21:1212-1229.

Urban, J.P., and S. Roberts. 2003. Degeneration of the intervertebral disc. *Arthritis research & therapy*. 5:120-130.

Vaccari, T., H. Lu, R. Kanwar, M.E. Fortini, and D. Bilder. 2008. Endosomal entry regulates Notch receptor activation in Drosophila melanogaster. *The Journal of cell biology*. 180:755-762.

van Nispen tot Pannerden, H., F. de Haas, W. Geerts, G. Posthuma, S. van Dijk, and H.F. Heijnen. 2010. The platelet interior revisited: electron tomography reveals tubular alpha-granule subtypes. *Blood*. 116:1147-1156.

Viotti, C., J. Bubeck, Y.D. Stierhof, M. Krebs, M. Langhans, W. van den Berg, W. van Dongen, S. Richter, N. Geldner, J. Takano, G. Jurgens, S.C. de Vries, D.G. Robinson, and K. Schumacher. 2010. Endocytic and secretory traffic in Arabidopsis merge in the trans-Golgi network/early endosome, an independent and highly dynamic organelle. *The Plant cell*. 22:1344-1357.

von Heijne, G. 1995. Membrane protein assembly: rules of the game. *BioEssays : news and reviews in molecular, cellular and developmental biology*. 17:25-30.

Waddington, C.H., Perry, F.R.S. and Margaret M. 1962. The ultrastructure of the developing urodele notochord. *Proceedings of the Royal Society of London. Series B, Biological Sciences*. 156:459-482.

Walmsley, R. 1953. The development and growth of the intervertebral disc. *Edinburgh medical journal*. 60:341-364.

Walter, P., and A.E. Johnson. 1994. Signal sequence recognition and protein targeting to the endoplasmic reticulum membrane. *Annual review of cell biology*. 10:87-119.

Wang, S., H. Kryvi, S. Grotmol, A. Wargelius, C. Krossoy, M. Epple, F. Neues, T. Furmanek, and G.K. Totland. 2013. Mineralization of the vertebral bodies in Atlantic salmon (Salmo salar L.) is initiated segmentally in the form of hydroxyapatite crystal accretions in the notochord sheath. *Journal of anatomy*. 223:159-170.

Wasmeier, C., M. Romao, L. Plowright, D.C. Bennett, G. Raposo, and M.C. Seabra. 2006. Rab38 and Rab32 control post-Golgi trafficking of melanogenic enzymes. *The Journal of cell biology*. 175:271-281.

Wei, A.H., and W. Li. 2013. Hermansky-Pudlak syndrome: pigmentary and non-pigmentary defects and their pathogenesis. *Pigment cell & melanoma research*. 26:176-192.

Weisman, L.S. 2006. Organelles on the move: insights from yeast vacuole inheritance. *Nature reviews. Molecular cell biology*. 7:243-252.

Westerfield, M. 2000. The Zebrafish Book. A guide for the laboratory use of zebrafish (Danio rerio). University of Oregon Press, Eugene, OR.

Wiemken, A., and M. Durr. 1974. Characterization of amino acid pools in the vacuolar compartment of Saccharomyces cerevisiae. *Archives of microbiology*. 101:45-57.

Wilcox, C.A., K. Redding, R. Wright, and R.S. Fuller. 1992. Mutation of a tyrosine localization signal in the cytosolic tail of yeast Kex2 protease disrupts Golgi retention and results in default transport to the vacuole. *Molecular biology of the cell*. 3:1353-1371.

Wu, M.M., J. Llopis, S. Adams, J.M. McCaffery, M.S. Kulomaa, T.E. Machen, H.P. Moore, and R.Y. Tsien. 2000. Organelle pH studies using targeted avidin and fluorescein-biotin. *Chemistry & biology*. 7:197-209.

Wurmser, A.E., T.K. Sato, and S.D. Emr. 2000. New component of the vacuolar class C-Vps complex couples nucleotide exchange on the Ypt7 GTPase to SNARE-dependent docking and fusion. *The Journal of cell biology*. 151:551-562.

Yamada, T., S.L. Pfaff, T. Edlund, and T.M. Jessell. 1993. Control of cell pattern in the neural tube: motor neuron induction by diffusible factors from notochord and floor plate. *Cell*. 73:673-686.

Yamamoto, M., R. Morita, T. Mizoguchi, H. Matsuo, M. Isoda, T. Ishitani, A.B. Chitnis, K. Matsumoto, J.G. Crump, K. Hozumi, S. Yonemura, K. Kawakami, and M. Itoh. 2010. Mib-Jag1-Notch signalling regulates patterning and structural roles of the notochord by controlling cell-fate decisions. *Development*. 137:2527-2537.

Yoshimori, T., A. Yamamoto, Y. Moriyama, M. Futai, and Y. Tashiro. 1991. Bafilomycin A1, a specific inhibitor of vacuolar-type H(+)-ATPase, inhibits acidification and protein degradation in lysosomes of cultured cells. *The Journal of biological chemistry*. 266:17707-17712.

Zhang, L., K. Yu, K.W. Robert, K.M. DeBolt, N. Hong, J.Q. Tao, M. Fukuda, A.B. Fisher, and S. Huang. 2011. Rab38 targets to lamellar bodies and normalizes their sizes in lung alveolar type II epithelial cells. *American journal of physiology. Lung cellular and molecular physiology*. 301:L461-477.

Zlatic, S.A., K. Tornieri, S.W. L'Hernault, and V. Faundez. 2011. Clathrin-dependent mechanisms modulate the subcellular distribution of class C Vps/HOPS tether subunits in polarized and nonpolarized cells. *Molecular biology of the cell*. 22:1699-1715.

## Biography

Kathryn Leigh Ellis was born and raised in Raleigh, North Carolina on August 31, 1987. She attended East Carolina University where she graduated *summa cum laude* and received her Bachelor of Science in biology in December of 2008. In college, Kathryn was elected into the honors society *Phi Betta Kappa* and received the Michael C. Bunting academic merit scholarship. From college, she attended Duke University for graduate studies after being accepted to the Developmental and Stem Cell Biology training program. During her graduate career, Kathryn published in the Journal of Cell Biology, “Notochord vacuoles are lysosome-related organelles that function in axis and spine morphogenesis,” where her article was featured on the cover and in the In Focus section of that issue. Kathryn is a member of the Society for Developmental Biology and Genetics Society of America professional societies.